Title: Molecular pathways in heart development and disease

By

Eunjin Cho

Doctor of Philosophy

(Molecular and Cellular Pharmacology)

at the

UNIVERSITY OF WISCONSIN-MADISON

2018

Date of Final Oral Examination: August 20, 2018

This Dissertation is approved by the following members of the Final Oral Committee:

Youngsook Lee, Associate Professor, Cell and Regenerative Biology

John Svaren, Professor, Comparative Biosciences

Thimothy Kamp, Professor, Cardiovascular medicine

Rupa Sridharan, Assistant Professor, Cell and Regenerative Biology

Chad Vezina, Associate Professor, Pharmacology

Acknowledgements

I would like to thank everyone who has contributed to my completion of this dissertation. I would like to express my sincere gratitude to my advisor Professor Youngsook Lee for her guidance, support, and patience. I would also like to thank all of my committee members, Dr. John Svaren, Dr. Timothy Kamp, Dr. Rupa Sridharan, Dr. Chad Vezina, and Dr. Xin Sun for insightful comments and guidance. I give thanks to all of the members of the Lee lab who helped my research project, including Jia Bin Tan, Amanda Perez, Erin Kaufmann, Riley Groh, Anjali Iyengar, Dr. Matthew Brody and Dr. Matthew Mysliwiec. I am grateful to all my Korean friends in UW-Madison. I can complete my dissertation because of your help, suggestion and kindness. Finally, I would like to thank my parents.

Abstract

Jarid2 (Jumonji A/T-rich interaction domain 2) is an essential factor for normal heart development. Deletion of *Jarid2* in mice results in cardiac malformations recapitulating human congenital cardiac disease, and dysregulation of gene expression during development. However, the cardiac-specific developmental function and the precise epigenetic regulation of gene expression by Jarid2 remain to be elucidated. Here I demonstrate that cardiac-specific deletion of *Jarid2* in the developmental or postnatal myocardium causes cardiac malformations and functional defects. I employed three different cardiac-expressing Cre transgenic mice. Deletion of *Jarid2* by *Nkx2.5*-Cre (*Jarid2*^{Nkx}) caused cardiac malformations including ventricular septal defects, thin myocardium, hypertrabeculation, increased cardiac jelly and neonatal lethality. In contrast, later deletion of *Jarid2* in mice with *cTnt*-Cre or *αMHC*-Cre transgenic lines did not cause gross abnormalities in development. By employing combinatorial genome-wide approaches and molecular analyses, I show that Jarid2 is required for PRC2 occupancy and H3K27me3 on the *Isl1* locus, leading to proper repression of the target gene expression during cardiac development. Jarid2 represses neural gene expression, cardiac jelly, and several important factors such as Isl1 and Bmp10, all of which are crucial for normal ventricular development. Thus, early deletion of *Jarid2* in the myocardium results in dysregulation of gene expression and developmental defects later in development.

Interestingly, deletion of *Jarid2* by *αMHC*-Cre (*Jarid2*^{αMHC}) resulted in complete lethality by 9 months of age with dilated cardiomyopathy. *Jarid2*^{αMHC} mice showed an

increase in fetal gene expression, such as *Tnni1* and *Acta2* at neonatal stages. By performing RNA-seq and pathway analyses on *Jarid2*$^{\alpha MHC}$ postnatal hearts, we discovered that *Jarid2*$^{\alpha MHC}$ hearts showed marked changes in heart failure associated with genes and metabolism. Further, a set of genes such as heart failure related genes were already dysregulated in neonatal *Jarid2*$^{\alpha MHC}$ hearts, which may be causal for heart failure later. Therefore, Jarid2 is also required for myocardial maturation and maintaining cardiac function in adult stages.

These studies reveal critical roles of Jarid2 in the myocardial development. Jarid2 is necessary to establish correct epigenetics on the target genomic loci during a narrow developmental window, which is prior to differentiation of cardiac progenitors into cardiomyocytes and maturation of cardiomyocytes.

Table of contents

List of Figures

List of Tables

Chapter 1

Introduction

Heart development

The heart is the first developed organ during embryo genesis [1]. During gastrulation at embryonic day (E) 6.5-E7.0 in mice, cardiac precursor cells, which are originated from the mesodermal layer, migrate laterally and anteriorly to locate in the anteroposterior region of the primitive streak and develop cardiogenic crescent (Fig. 1-1). The myocardial progenitor cells are divided into the first and second heart fields. The second heart field (SHF) lies medially to the first heart field (FHF). These cardiac precursor cells migrate into the ventral midline and fuse to a develop linear tube. At this stage, the cells are destined to form the conus and ventricles. Two cell types are constituted, the outer myocardium and the inner endocardium facing the lumen with extracellular matrix, cardiac jelly in between [2]. The linear tube undergoes rightward looping by expansion of portions of the tube, whereas the outflow tract and the atrioventricular canal grow less and remain tubular at E9.0-E10.0. This is the first overt sign of braking left-right symmetry. The proepicardial cells from the extracardiac mesoderm, termed the third heart field, migrate and envelop the surface of the myocardium at this stage to create the epicardial layer [2]. A subset of epicardial cells undergo epithelial-mesenchymal transition (EMT, transition to a mesenchymal phenotype) and penetrate the matrix-rich subepicardium to differentiate into fibroblasts and coronary vascular smooth muscle cells and endothelial cells. Cardiac neural crest cells migrate to the looping heart and contribute to smooth muscle cells of the aorta and branchial arch arteries, valves and conduction tissue, and the parasympathetic innervation of the heart. The four-chambered heart is formed by septation, myocardial trabeculation and

thickening, and endocardial cushion formation in mammalian [3]. As the tube forms, the SHF comes to lie behind the cardiac tube, as well as extending more anteriorly and posteriorly. SHF cells contribute to right ventricle and outflow tract, while FHF cells give rise to the left ventricle, the atrioventricular canal and parts of the atria.

During chamber development in the ventricle, the myocardium differentiates into two different layers, a trabecular layer facing the endocardium and a compact layer, for contractility and conductivity and establishment of the coronary circulation system (Fig. 1-2) [4]. The endocardial cells invaginate, and the inner myocardial cells in specific regions form sheet-like protrusions into the lumen to give rise to trabeculae. The outer myocardial cells proliferate and become the compact layer. Trabeculation is important for oxygen and nutrient exchange and ventricular contractility in developing embryos [5, 6]. Signaling networks between the endocardium and myocardium are essential for the formation of the trabeculae and thickening of the ventricular wall. Notch1 pathway and its direct target, EphrinB2 activate Neuregulin1 (Nrg1) in the endocardium, and secreted Nrg1 activates the ErbB2 and ErbB4 receptors in the myocardium to regulate the maturation of trabeculae. Bone morphogenic protein 10 (Bmp10), expressed transiently in the trabecular myocardium, regulates cell proliferation by inhibiting $p57^{kip2}$, a cyclin-dependent kinase inhibitor. Thickening of the ventricular wall is accompanied by decreased cell proliferation in the trabecular layer at late midgestational stage, after E14.5 in mice. The trabeculae collapse toward the myocardium and contribute to form a thick compact ventricular wall [7]. Ventricular septation occurs by aggregation and protrusion of trabeculae into the ventricular cavity at the specific site in the myocardium. The interventricular septum is formed by outgrowth of two adjacent trabeculae in the left and

right ventricles. Cardiac jelly is the extracellular matrix components which is abundant between the endocardium and myocardium during early cardiac tube [8]. Cardiac jelly is important for cell migration, proliferation and signal transmission between the endocardium and myocardium. The critical cardiac factors during ventricular development are listed in Table 1-1.

The embryonic heart undergoes dramatic molecular and physiological changes after birth because of the environmental changes. In mice, these dramatic changes occur within one to two weeks after birth [9, 10]. The sarcomere genes' isoforms switch from fetal to adult forms, which are involved in contractility, calcium handling and energy utilization [11]. The cardiac cells in embryonic stages actively proliferate to generate a thick ventricular wall. However, the cardiomyocytes lose the proliferative capacity, and undergo hypertrophic growth and binucleation within postnatal day (P) 5 to P10 [10]. Expression of metabolic genes responsible for glycolytic process is decreased whereas oxidative and fatty acid metabolisms are induced in the postnatal heart. The metabolic shift is to support a high-energy demand due to increased cardiac output. Mitochondrial density increases as the metabolic rate increases [10].

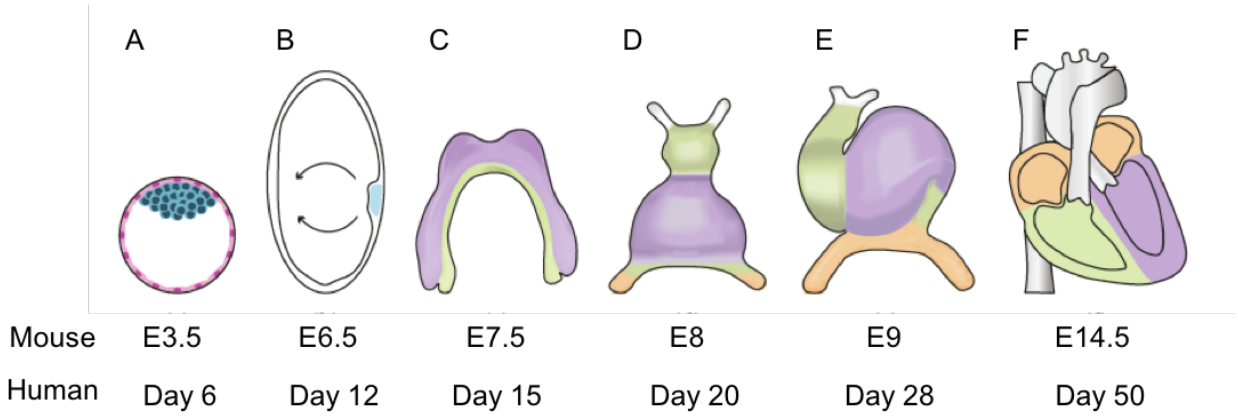

Figure 1-1. Diagram of mammalian heart development.

A, Preimplantation blastocyst stage showing pluripotent inner cell mass. B, Gastrulating embryo showing mesoderm migration (arrows). C, Cardiac crescent. (FHF, purple; SHF, green). D, Early cardiac tube (atria, orange). E, Looping heart. F, Four-chambered heart. [2]

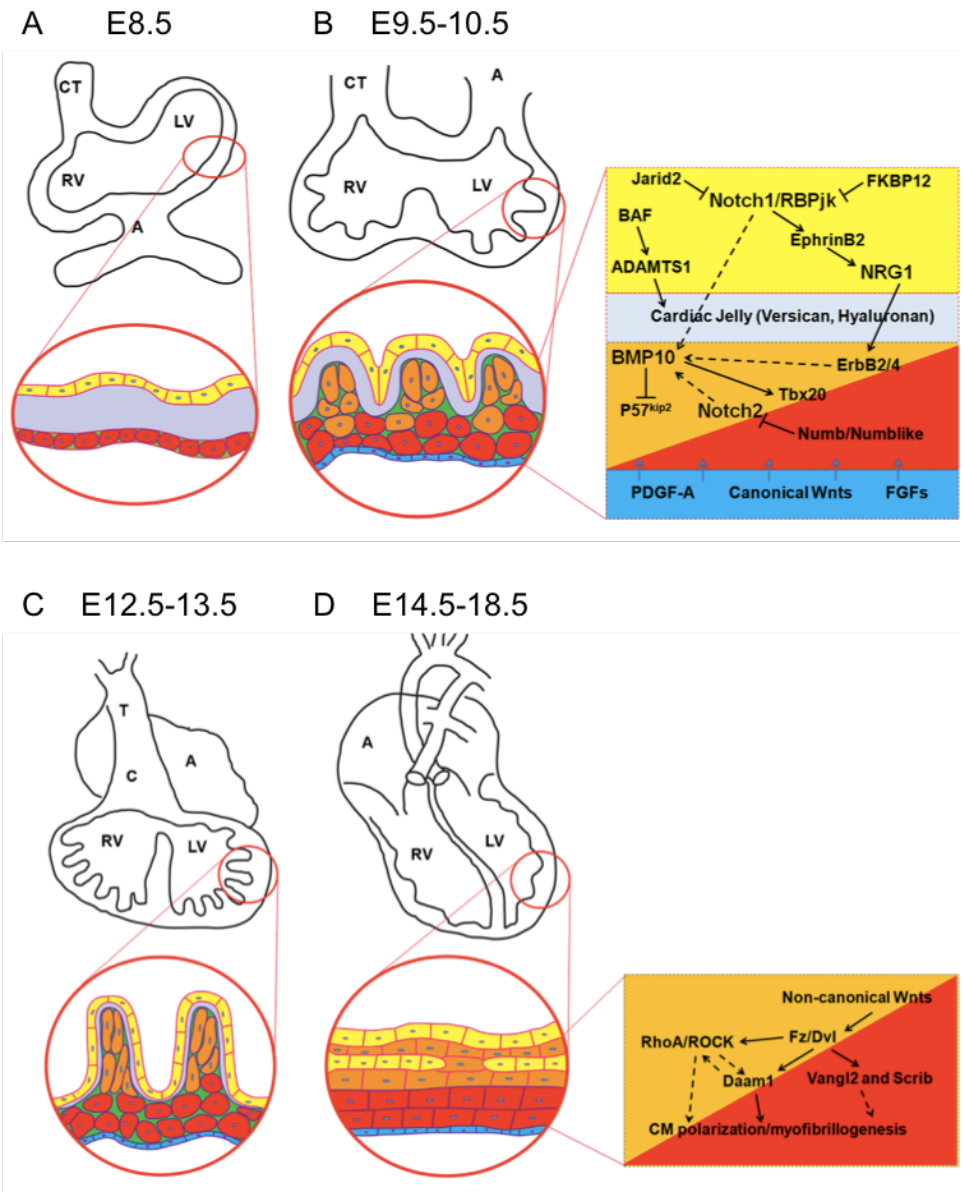

Figure 1-2. Ventricular wall development.

A, Growth of clonal cluster of myocardia cells. B, Invagination of endocardial cells and formation of trabecular myocardium. C, Elongation and myofibrillogenesis of trabecular cardiomyocytes. D, Compaction and maturation. The interactive regulation of growth factors and signaling networks are critical to the ventricular wall growth and maturation. Endocardial cells, yellow; Cardiomyocytes in the trabecular zone, orange; Cardiomyocytes in the compact zone, red; Epicardial cells, blue. [4]

Table 1-1. Cardiac factors in the developing ventricles.

Embryonic stage	Cardiac factors
E7.5- E10.5	Mesp1/2, GATA4, Nkx2.5, Mef2C, Hand1/2, ANF Tbx5 (FHF) Isl1, Tbx2, Pitx2 (SHF) Tbx3, Pax3 (Neural crest cells) NfatC1, Notch1 (Endocardium) Wt1 and Tbx18 (Epicardium)
E14.5	GATA4, Nxk2.5, Tbx5, Mef2C, Hand1/2, Pax3, Bmp10 (Trabecular layer) Hey2 and Tbx20 (Compact layer)
E17	GATA4, Nxk2.5, Tbx5, Mef2C, Hand1/2, Pax3, Mlc2v

Mesp1/2, Mesoderm posterior 1/2; GATA4, GATA-binding protein 4; Nkx2.5, Nk2 homeobox 5; Mef2C, Myocyte enhancer factor 2C; Hand1/2, Heart and neural crest derivatives expressed transcript 1/2; ANF, Atrial natriuretic factor; Isl1, Islet 1; Tbx, T-box; Pitx2, Pituitary homeobox 2; Pax3, Paired box 3; NfatC1, Nuclear factor of activated T cell cytoplasmic 1; Wt1, Wilms' tumor 1; Bmp10, Bone morphogenic protein 10; Hey2, Hairy and enhancer of Split-related with YRPW motif 2; Mlc2, Myosin light chain 2

Function of Jarid2 in the heart

The JmjC domain-containing proteins are a family of redox enzyme that can catalyze a wide variety of oxidative reaction with two cofactors Fe(II) and α-ketoglutarate [12]. Jumonji AT-rich interactive domain2 (Jarid2, Jumonji) was first discovered by Takeuchi *et al*. (1995) using Gene trapped technology [13], which randomly inserts an alternative gene to disrupt targeted gene's function. At first, Jarid2 is emphasized in neural tube and cerebellum development. In 1997, Jarid2 is identified in ES cell-derived cardiomyocytes by Baker et al. using the same gene trap method [14]. In cancer, Jarid2 expression is reported in rhabdomyosarcomas and leukemia, and Jarid2 contributes to metastatic mechanisms by EMT in lung and colon cancer [15-17].

Jarid2 is an essential factor in the heart. Jarid2 expresses in the ventricular myocardium from E8.0, specifically in the trabeculae (E10.5) during heart development [18, 19]. *Jarid2* knockout (*Jarid2* KO) mice die perinatally and exhibit cardiac defects mimicking human congenital cardiac defects, including ventricular septal defect (VSD), double-outlet right ventricle (DORV), thin myocardium and hypertrabeculation (Fig. 1-3). Jarid2 inhibits cell proliferation mediated by inhibition of cyclin D1 expression at E10.5 in C3H/He background mice [20]. Indeed, Jarid2 interacts with the retinoblastoma protein (Rb) and modulates the repressive function of Rb on E2F activation in Svj/B6 background mice [21]. Therefore, Jarid2 functions to repress cell proliferation in the myocardium for normal ventricular development. Jarid2 also expresses in the endocardial cells to regulate Notch1 expression in the mid-gestation [22]. Notch1 and Nrg1 signaling pathways activate trabeculation in the myocardium, leading to hypertrabecular phenotype in the

absence of *Jarid2* in the endocardium.

Jarid2 has a transcriptional repressor domain and a nuclear localization signal domain, and thus can function as a transcriptional repressor (Fig. 1-4). Jarid2 interacts with and represses the cardiac transcription factors, Nkx2.5 and GATA4, which activate *Anf* gene expression [23]. α-Cardiac myosin heavy chain (αMHC) is a contractile protein whose expression is synergistically activated by myocyte enhancer factor 2 (Mef2). Jarid2 represses the transcriptional activity of Mef2, resulting in the inhibition of *αMHC* expression [24].

Jarid2 expresses in the postnatal heart although the expression level is reduced compared to that of the embryonic heart (See chapter 3). Jarid2 expression is reduced in human heart failure [25]. Jarid2 is necessary to inhibit fetal genes' transcriptional expression, such as *Anf* and *Mlc2a*. JARID2 mutations in human have been linked to congenital heart abnormalities, and haploinsufficiency of JARID2 leads to intellectual disability and brain dysfunction such as schizophrenia [26].

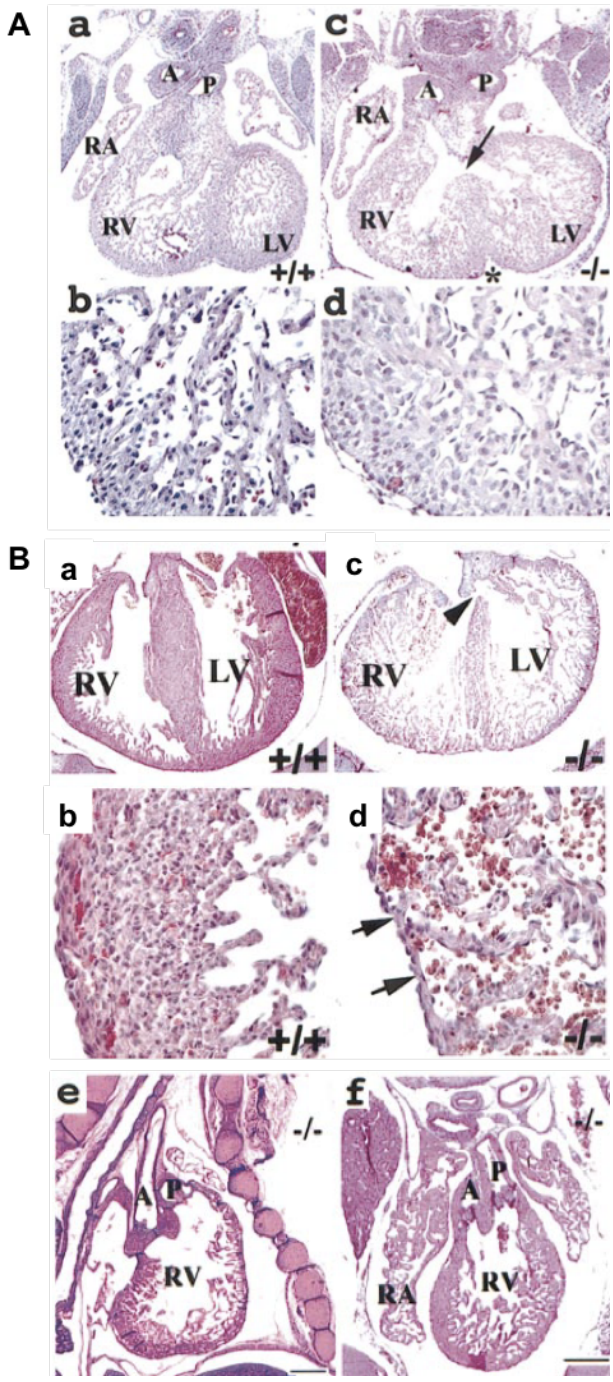

Figure 1-3. Cardiac defects in the Jarid2 KO heart.

A, E13, mutant hearts (c and d) have DORV and VSD (arrows) compared with wild type (a and b). An asterisk (c) indicates an abnormally deep interventricular groove. B, At E16,

compared with wild type (a and b), mutants (c and d) exhibit a thin trabeculated wall and VSD (arrowhead). Arrows (d) indicate outer compact zone. DORV is observed in mutants (e and f) at E19. Bar, 5400 mm. RV right ventricle; LV, left ventricle; RA, right atria; A, aorta; P, pulmonary trunk. [18]

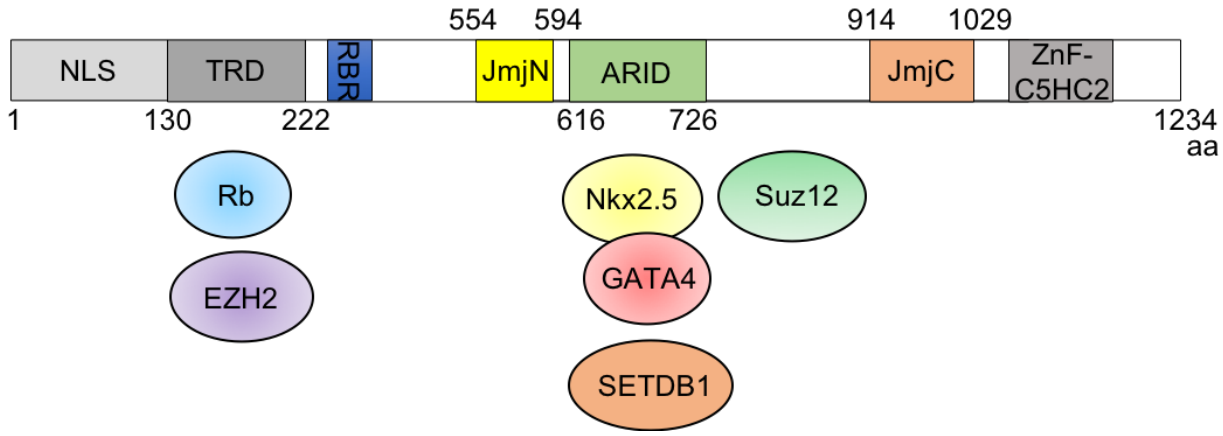

Figure 1-4. Diagram of Jarid2 and its interacting proteins.

NLS, Nuclear localization signal; TRD, Transcriptional repression domain; RBR, RNA binding region; ARID, AT-rich interaction domain; ZnF-C5HC2, Zinc finger domain.

Epigenetic regulation by Jarid2

Regulation of the developing heart and its transcription factors greatly rely on epigenetic regulation by chromatin remodeling and histone modifications. Chromatin is the stage in which DNA is packaged within the nucleus of eukaryotic organisms. Nucleosome is the fundamental unit of chromatin, containing nucleic acids and histones [27]. Two copies of the four core histones, H2A, H2B, H3 and H4 are wrapped by 147 base pairs of DNAs. Transcription is activated or repressed by chromatin structure via modification of the N-termini (trail) of the histone, including acetylation, phosphorylation, sumoylation, ubiquitination and methylation. Dysregulation of histone modifications has been implicated in cancer and developmental defects [28, 29]. Histone modification is specific, depending on amino acid substrates, and many modifications are reversible by interacting enzymatic proteins.

Histone methylation is the most well studied modification by identifying histone-modifying enzymes, methyltransferases and demethylases. Histone methylation targets arginine (R) and lysine (K) residues in three distinct states (mono-, di-, or trimethylation) [30]. Methylation at histone H3 lysine 9 (H3K9), H3K27, or H4K20 is associated with gene repression, while methylation at H3K4, H3K36, or H3K79 is correlated with gene activation.

Jarid2 is a founding member of the histone demethylase family [12]. Jarid2 has a DNA binding domain called ARID (AT-rich interaction domain) and JmjN and JmjC domains which are catalytic domains and extensive homology with Jarid1 proteins [31]. However, Jarid2 is enzymatically inactive because of amino acid substitution on JmjC

domain. Jarid2 interacts with other methyltransferase proteins to activate or repress their function. During embryonic stem (ES) cell differentiation, Jarid2 is an associated member of polycomb repressive complex 2 (PRC2) [32-34]. The trimethylation of H3K27 (H3K27me3) is laid down by the PRC2, which comprises core subunits: Suppressor of Zeste 12 (Suz12), Enhancer of Zeste 2 (Ezh2) and Embryonic ectoderm development (Eed), and additional subunits: Jarid2 and Aebp2. Ezh2, the catalytic histone methyltransferase, is an essential component for normal heart development such that a deletion in mice leads to defective cardiac morphogenesis or to cardiac enlargement after birth [35, 36]. The association of Jarid2 and PRC2 complex activates or represses the methylation of H3K27 for normal differentiation of ES cells [32, 34]. Interestingly, PRC2 directly methylates Jarid2 on R116 [37]. Jarid2 interacts with Non-coding RNAs, including Xist, Meg3 and Hotair to recruit PRC2 at target genes in ES cells or X chromosome inactivation [38, 39]. Jarid2 deficiency in neonatal epidermis reveals reduced H3K27me3 and Suz12 accumulation on epidermal differentiation genes [40]. In the developing heart, Jarid2 recruits PRC2 on islet 1 (Isl1) promoter to regulate proper repression of Isl1 expression in midgestation (See chapter 2).

Jarid2 guides histone methyltransferases such as G9a and GLP to cyclin D1 promoter and represses cyclin D1 expression via the modification of H3K9 methylation [41]. Additionally, Jarid2 represses cyclin D1 promoter mediated by H3K27me3 in leukemia cells [16]. Jarid2 interacts with Setdb1 by depositing H3K9me3 epigenetic marks during heart and immune cell development [42, 43].

References

1 Paige SL, Plonowska K, Xu A, Wu SM: Molecular regulation of cardiomyocyte differentiation. Circ Res 2015;116:341-353.

2 Aguilar-Sanchez C, Michael M, Pennings S: Cardiac Stem Cells in the Postnatal Heart: Lessons from Development. Stem Cells Int 2018;1247857.

3 Lindsey SE, Butcher JT, Yalcin HC: Mechanical regulation of cardiac development. Front Physiol 2014;5:318.

4 Zhang W, Chen H, Qu X, Chang CP, Shou W: Molecular mechanism of ventricular trabeculation/compaction and the pathogenesis of the left ventricular noncompaction cardiomyopathy (LVNC). Am J Med Genet C Semin Med Genet 2013;163C:144-156.

5 Paun B, Bijnens B, Butakoff C: Relationship between the left ventricular size and the amount of trabeculations. Int J Numer Method Biomed Eng 2018;34

6 Sedmera D, Pexieder T, Vuillemin M, Thompson RP, Anderson RH: Developmental patterning of the myocardium. Anat Rec 2000;258:319-337.

7 Samsa LA, Yang B, Liu J: Embryonic cardiac chamber maturation: Trabeculation, conduction, and cardiomyocyte proliferation. Am J Med Genet C Semin Med Genet 2013;163C:157-168.

8 Nandadasa S, Foulcer S, Apte SS: The multiple, complex roles of versican and its proteolytic turnover by ADAMTS proteases during embryogenesis. Matrix Biol 2014;35:34-41.

9 Taegtmeyer H, Sen S, Vela D: Return to the fetal gene program: a suggested metabolic link to gene expression in the heart. Ann N Y Acad Sci 2010;1188:191-198.

10 Naqvi N, Li M, Calvert JW, Tejada T, Lambert JP, Wu J, Kesteven SH, Holman SR, Matsuda T, Lovelock JD, Howard WW, Iismaa SE, Chan AY, Crawford BH, Wagner MB, Martin DI, Lefer DJ, Graham RM, Husain A: A proliferative burst during preadolescence establishes the final cardiomyocyte number. Cell 2014;157:795-807.

11 Yin Z, Ren J, Guo W: Sarcomeric protein isoform transitions in cardiac muscle: a journey to heart failure. Biochim Biophys Acta 2015;1852:47-52.

12 Accari SL, Fisher PR: Emerging Roles of JmjC Domain-Containing Proteins. Int Rev Cell Mol Biol 2015;319:165-220.

13 Takeuchi T, Yamazaki Y, Katoh-Fukui Y, Tsuchiya R, Kondo S, Motoyama J, Higashinakagawa T: Gene trap capture of a novel mouse gene, jumonji, required for neural tube formation. Genes Dev 1995;9:1211-1222.

14 Baker RK, Haendel MA, Swanson BJ, Shambaugh JC, Micales BK, Lyons GE: In vitro preselection of gene-trapped embryonic stem cell clones for characterizing novel developmentally regulated genes in the mouse. Dev Biol 1997;185:201-214.

15 Walters ZS, Villarejo-Balcells B, Olmos D, Buist TW, Missiaglia E, Allen R, Al-Lazikani B, Garrett MD, Blagg J, Shipley J: JARID2 is a direct target of the PAX3-FOXO1 fusion protein and inhibits myogenic differentiation of rhabdomyosarcoma cells. Oncogene 2014;33:1148-1157.

16 Su CL, Deng TR, Shang Z, Xiao Y: JARID2 inhibits leukemia cell proliferation by regulating CCND1 expression. Int J Hematol 2015;102:76-85.

17 Tange S, Oktyabri D, Terashima M, Ishimura A, Suzuki T: JARID2 is involved in transforming growth factor-beta-induced epithelial-mesenchymal transition of lung and colon cancer cell lines. PLoS One 2014;9:e115684.

18 Lee Y, Song AJ, Baker R, Micales B, Conway SJ, Lyons GE: Jumonji, a nuclear protein that is necessary for normal heart development. Circ Res 2000;86:932-938.

19 Takeuchi T, Kojima M, Nakajima K, Kondo S: jumonji gene is essential for the neurulation and cardiac development of mouse embryos with a C3H/He background. Mech Dev 1999;86:29-38.

20 Toyoda M, Shirato H, Nakajima K, Kojima M, Takahashi M, Kubota M, Suzuki-Migishima R, Motegi Y, Yokoyama M, Takeuchi T: jumonji downregulates cardiac cell proliferation by repressing cyclin D1 expression. Dev Cell 2003;5:85-97.

21 Jung J, Kim TG, Lyons GE, Kim HR, Lee Y: Jumonji regulates cardiomyocyte proliferation via interaction with retinoblastoma protein. J Biol Chem 2005;280:30916-30923.

22 Mysliwiec MR, Bresnick EH, Lee Y: Endothelial Jarid2/Jumonji is required for normal cardiac development and proper Notch1 expression. J Biol Chem 2011;286:17193-17204.

23 Kim TG, Chen J, Sadoshima J, Lee Y: Jumonji represses atrial natriuretic factor gene expression by inhibiting transcriptional activities of cardiac transcription factors. Mol Cell Biol 2004;24:10151-10160.

24 Kim TG, Jung J, Mysliwiec MR, Kang S, Lee Y: Jumonji represses alpha-cardiac myosin heavy chain expression via inhibiting MEF2 activity. Biochem Biophys Res Commun 2005;329:544-553.

25 Bovill E, Westaby S, Reji S, Sayeed R, Crisp A, Shaw T: Induction by left ventricular overload and left ventricular failure of the human Jumonji gene (JARID2) encoding a protein that regulates transcription and reexpression of a protective fetal program. J Thorac Cardiovasc Surg 2008;136:709-716.

26 Landeira D, Bagci H, Malinowski AR, Brown KE, Soza-Ried J, Feytout A, Webster Z, Ndjetehe E, Cantone I, Asenjo HG, Brockdorff N, Carroll T, Merkenschlager M, Fisher AG: Jarid2 Coordinates Nanog Expression and PCP/Wnt Signaling Required for Efficient ESC Differentiation and Early Embryo Development. Cell Rep 2015;12:573-586.

27 Zhang T, Cooper S, Brockdorff N: The interplay of histone modifications - writers that read. EMBO Rep 2015;16:1467-1481.

28 Zaidi S, Choi M, Wakimoto H, Ma L, Jiang J, Overton JD, Romano-Adesman A, Bjornson RD, Breitbart RE, Brown KK, Carriero NJ, Cheung YH, Deanfield J, DePalma S, Fakhro KA, Glessner J, Hakonarson H, Italia MJ, Kaltman JR, Kaski J, Kim R, Kline JK, Lee T, Leipzig J, Lopez A, Mane SM, Mitchell LE, Newburger JW, Parfenov M, Pe'er I, Porter G, Roberts AE, Sachidanandam R, Sanders SJ, Seiden HS, State MW, Subramanian S, Tikhonova IR, Wang W, Warburton D, White PS, Williams IA, Zhao H, Seidman JG, Brueckner M, Chung WK, Gelb BD, Goldmuntz E, Seidman CE, Lifton RP: De novo mutations in histone-modifying genes in congenital heart disease. Nature 2013;498:220-223.

29 Johansson C, Tumber A, Che K, Cain P, Nowak R, Gileadi C, Oppermann U: The roles of Jumonji-type oxygenases in human disease. Epigenomics 2014;6:89-120.

30 Zhang QJ, Liu ZP: Histone methylations in heart development, congenital and adult heart diseases. Epigenomics 2015;7:321-330.

31 Landeira D, Fisher AG: Inactive yet indispensable: the tale of Jarid2. Trends Cell Biol 2011;21:74-80.

32 Peng JC, Valouev A, Swigut T, Zhang J, Zhao Y, Sidow A, Wysocka J: Jarid2/Jumonji coordinates control of PRC2 enzymatic activity and target gene occupancy in pluripotent cells. Cell 2009;139:1290-1302.

33 Landeira D, Sauer S, Poot R, Dvorkina M, Mazzarella L, Jørgensen HF, Pereira CF, Leleu M, Piccolo FM, Spivakov M, Brookes E, Pombo A, Fisher C, Skarnes WC, Snoek T, Bezstarosti K, Demmers J, Klose RJ, Casanova M, Tavares L, Brockdorff N, Merkenschlager M, Fisher AG: Jarid2 is a PRC2 component in embryonic stem cells required for multi-lineage differentiation and recruitment of

PRC1 and RNA Polymerase II to developmental regulators. Nat Cell Biol 2010;12:618-624.

34 Pasini D, Cloos PA, Walfridsson J, Olsson L, Bukowski JP, Johansen JV, Bak M, Tommerup N, Rappsilber J, Helin K: JARID2 regulates binding of the Polycomb repressive complex 2 to target genes in ES cells. Nature 2010;464:306-310.

35 He A, Ma Q, Cao J, von Gise A, Zhou P, Xie H, Zhang B, Hsing M, Christodoulou DC, Cahan P, Daley GQ, Kong SW, Orkin SH, Seidman CE, Seidman JG, Pu WT: Polycomb repressive complex 2 regulates normal development of the mouse heart. Circ Res 2012;110:406-415.

36 Delgado-Olguín P, Huang Y, Li X, Christodoulou D, Seidman CE, Seidman JG, Tarakhovsky A, Bruneau BG: Epigenetic repression of cardiac progenitor gene expression by Ezh2 is required for postnatal cardiac homeostasis. Nat Genet 2012;44:343-347.

37 Sanulli S, Justin N, Teissandier A, Ancelin K, Portoso M, Caron M, Michaud A, Lombard B, da Rocha ST, Offer J, Loew D, Servant N, Wassef M, Burlina F, Gamblin SJ, Heard E, Margueron R: Jarid2 Methylation via the PRC2 Complex Regulates H3K27me3 Deposition during Cell Differentiation. Mol Cell 2015;57:769-783.

38 da Rocha ST, Boeva V, Escamilla-Del-Arenal M, Ancelin K, Granier C, Matias NR, Sanulli S, Chow J, Schulz E, Picard C, Kaneko S, Helin K, Reinberg D, Stewart AF, Wutz A, Margueron R, Heard E: Jarid2 Is Implicated in the Initial Xist-Induced Targeting of PRC2 to the Inactive X Chromosome. Mol Cell 2014;53:301-316.

39 Kaneko S, Bonasio R, Saldaña-Meyer R, Yoshida T, Son J, Nishino K, Umezawa A, Reinberg D: Interactions between JARID2 and noncoding RNAs regulate PRC2 recruitment to chromatin. Mol Cell 2014;53:290-300.

40 Mejetta S, Morey L, Pascual G, Kuebler B, Mysliwiec MR, Lee Y, Shiekhattar R, Di Croce L, Benitah SA: Jarid2 regulates mouse epidermal stem cell activation and differentiation. EMBO J 2011;30:3635-3646.

41 Shirato H, Ogawa S, Nakajima K, Inagawa M, Kojima M, Tachibana M, Shinkai Y, Takeuchi T: A jumonji (Jarid2) protein complex represses cyclin D1 expression by methylation of histone H3-K9. J Biol Chem 2009;284:733-739.

42 Mysliwiec MR, Carlson CD, Tietjen J, Hung H, Ansari AZ, Lee Y: Jarid2 (Jumonji, AT rich interactive domain 2) regulates NOTCH1 expression via histone modification in the developing heart. J Biol Chem 2012;287:1235-1241.

43 Pereira RM, Martinez GJ, Engel I, Cruz-Guilloty F, Barboza BA, Tsagaratou A, Lio CW, Berg LJ, Lee Y, Kronenberg M, Bandukwala HS, Rao A: Jarid2 is induced by

TCR signalling and controls iNKT cell maturation. Nat Commun 2014;5:4540.

Chapter 2

Cardiac-specific developmental and epigenetic functions of Jarid2 during embryonic development

Adapted from

Eunjin Cho, Matthew R. Mysliwiec, Clayton D. Carlson, Aseem Ansari, Robert J. Schwartz, and Youngsook Lee, 2018. *J Biol Chem* 293(30):11659-11673.

Abstract

Epigenetic regulation is critical in normal cardiac development. We have demonstrated that the deletion of *Jarid2* (Jumonji (Jmj) A/T-rich interaction domain 2) in mice results in cardiac malformations recapitulating human congenital cardiac disease and dysregulation of gene expression. However, the precise developmental and epigenetic functions of Jarid2 within the developing heart remain to be elucidated. Here, we determined the cardiac-specific functions of Jarid2 and the genetic networks regulated by Jarid2. *Jarid2* was deleted using different cardiac-specific Cre mice. The deletion of *Jarid2* by *Nkx2.5*-Cre mice (*Jarid2*^{Nkx}) caused cardiac malformations including ventricular septal defects, thin myocardium, hypertrabeculation, and neonatal lethality. *Jarid2*^{Nkx} mice exhibited elevated expression of neural genes, cardiac jelly, and other key factors including Isl1 and Bmp10 in the developing heart. By employing combinatorial genome-wide approaches and molecular analyses, we showed that Jarid2 in the myocardium regulates a subset of Jarid2 target gene expression and H3K27me3 enrichment during heart development. Specifically, Jarid2 was required for PRC2 occupancy and H3K27me3 at the *Isl1* promoter locus, leading to the proper repression of *Isl1* expression. In contrast, *Jarid2* deletion in differentiated cardiomyocytes by *cTnt*-Cre mice caused no gross morphological defects or neonatal lethality. Thus, the early deletion of *Jarid2* in cardiac progenitors, prior to the differentiation of cardiac progenitors into cardiomyocytes, results in morphogenetic defects manifested later in development. Our studies reveal that there is a critical window during early cardiac progenitor differentiation when Jarid2 is crucial to establish the epigenetic landscape at later stages of development.

Introduction

Human congenital cardiac defects are one of the most common forms of birth defects [1]. Normal cardiovascular development requires precise control of gene expression in a spatial and temporal-dependent manner. Eukaryotic gene transcription is regulated by chromatin structure partly via modifications of histone tails. Due to a groundbreaking discovery of histone demethylases such as Jumonji (Jmj) family factors, histone methylation is now considered a reversible epigenetic mark. Methylated histone tails are recognized as a marker for transcriptional activation or repression. In general, methylation at histone H3 lysine 9 (H3K9), H3K27, or H4K20 is associated with gene repression, while methylation at H3K4, H3K36, or H3K79 is correlated with gene activation [2, 3]. However, the regulatory roles of histone methylation status in gene expression are not fully understood. Histone lysine demethylases show exquisite substrate specificity and participate in diverse biological processes. Mutations or deregulation of histone demethylases are often linked to human diseases [4, 5].

Jarid2 (JMJ) is a nuclear factor critical for mouse embryonic development [6]. Jarid2 is the founding member of the Jmj family that functions as histone lysine demethylases. However, Jarid2 is enzymatically inactive due to amino acid substitutions in the JmjC domain that is a catalytic domain [7, 8]. Nonetheless, Jarid2 is essential for embryonic development in the heart, liver, and hematopoietic tissues [6]. *Jarid2* knockout (*Jarid2* KO) mice die perinatally and exhibit cardiac defects mimicking human congenital cardiac defects including ventricular septal defect (VSD), double-outlet right ventricle (DORV), thin myocardium and hypertrabeculation [9, 10]. Left ventricular noncompaction

(LVNC) in humans is characterized by a spongy ventricular myocardium with excessive trabeculations and deep trabecular recesses in the left ventricle leading to a thin ventricular wall [11], which is manifested in *Jarid2* KO hearts [9]. The American Heart Association formally classified LVNC as a distinct cardiomyopathy [11]. The genesis of LVNC has been speculated to represent an arrest of the final stage of myocardial morphogenesis, which is often referred to as 'myocardial compaction' for a lack of better terminology. The etiology of LVNC remains unclear partly because the genetic causes of LVNC are heterogeneous, and there is insufficient knowledge on the molecular control of normal trabeculation and compaction during ventricular myocardial wall development.

During mammalian heart development, the ventricles undergo complex morphogenetic events [12]. The initial step is the formation of a single cell layer of myocardium at an early developmental stage, followed by the formation of a trabecular and compact myocardium at early midgestation stage. The final step involves the myocardial compaction to give rise to the thickened ventricular wall with the reduced trabecular layer at late midgestation stage, but molecular events leading to the mature ventricular wall remain poorly understood. In mouse models, noncompaction cardiomyopathy has been used to describe the thin compact layer with normal or excessive trabeculations, leading to the thin ventricular myocardial wall at mid- to late stages of cardiac development [13]. Notch pathways, Neuregulin1, and bone morphogenic protein 10 (Bmp10) expression are critical for initiation and expansion of the trabecular layer, which in turn affect the ventricular wall thickness [12]. Cardiac jelly between the endocardium and the underlying trabecular layer is also essential for initiation and growth of the trabecular layer [12, 14]. Interestingly, all of the above signals

in the heart are significantly reduced in later developmental stages, which coincides with the cessation of trabeculation as well as compaction of the ventricular myocardium.

Jarid2 functions as a major component of the transcriptional networks that balance pluripotency and differentiation in embryonic stem (ES) cells. Jarid2 is associated with the Polycomb repressive complex 2 (PRC2) in ES cells and is required for an efficient accumulation of PRC2 on the chromatin [7, 15, 16]. Major components of PRC2 consist of SET domain containing histone methylases, EZH1/EZH2 and SUZ12, and EED, which specifically methylate at H3K27. Trimethylation of H3K27 (H3K27me3) is associated with repressed chromatin states, and widely distributed among genes encoding developmental regulators. However, it is debated whether Jarid2 loss in ES cells causes increases or decreases in H3K27me3 levels. PRC2 and H3K27me3 occupy a set of genes controlling differentiation and prevent full expression of these genes until lineage commitment in ES cells [17, 18]. Although loss of Jarid2 or PRC2 function results in defective ES cell differentiation, the epigenetic role of Jarid2 remains unclear during heart development. We have demonstrated that the endothelial deletion of *Jarid2* partially recapitulates cardiac defects observed in *Jarid2* KO mice [19]. In the endocardial layer, Jarid2 represses *Notch1* expression by interacting with Setdb1 via H3K9me3 enrichment at the *Notch1* locus [8]. This seems crucial for termination of trabeculation and initiation of compaction of the ventricular myocardial wall. As a major epigenetic marker, H3K9 methylation is known as a ‘histone code’ for gene silencing. Conditional deletion of *Ezh2*, a catalytic subunit of PRC2, using *Nkx2.5*-Cre mice results in cardiac developmental defects such as hypertrabeculation, thinning of the compact myocardium, and VSD, which are similar to the defects observed in *Jarid2* KO mice [9, 20]. However, it remains

unknown whether Jarid2 cooperates with PRC2 during heart development.

In this study, we demonstrate that cardiac-specific deletion of *Jarid2* in cardiac progenitors and their progeny causes neonatal lethality and cardiac malformations including VSD, hypertrabeculation, and thin compact layer. In contrast, *Jarid2* deletion in differentiated cardiomyocytes did not result in overt cardiac malformation. These data indicate that there is a critical window during early cardiac progenitor differentiation when Jarid2 is crucial to establish the epigenetic landscape at later stages of development. We provide evidence that Jarid2 cooperates with PRC2 for H3K27me3 accumulation on a subset of Jarid2 target genes in the developing heart, which contributes to repress differentiation of other lineages such as neural differentiation, and to guide normal myocardial development.

RESULTS

Cardiac-specific deletions of Jarid2

Jarid2 deletion in mice causes congenital heart defects and death right after birth [9]. However, the precise developmental and molecular functions of Jarid2 remain to be elucidated within the early developing heart. Thus, we set out to determine the cardiac-specific function of Jarid2 by deleting *Jarid2* in cardiac progenitors and their progeny using *Nkx2.5*-Cre KI mice (*Jarid2*^{Nkx}) [21]. We first analyzed Mendelian ratios from embryonic day (E) 9.5 through postnatal day (P) 10 (Table 2-1). The Mendelian ratios for *Jarid2*^{Nkx} mutants (*Nkx2.5*-Cre*/+;Jarid2f/f*) were normal until birth, but all mutants succumbed to death within one day after birth. Heterozygous mutant mice (*Nkx2.5*-Cre*/+;Jarid2f/+*) were present at the expected Mendelian ratio. We further examined roles of Jarid2 within the myocardium after cardiac cells had differentiated to cardiomyocytes. Cardiomyocyte-specific deletion of *Jarid2* using *αMHC*-Cre mice causes neither gross cardiac malformation nor perinatal lethality [19]. It is plausible that Jarid2 plays a critical role earlier than expected. *cTnt*-Cre mice express Cre from E7.5 onwards, while *αMHC*-Cre mice express Cre at E8.5 [22, 23]. Thus *Jarid2* deletion mice using *cTnt*-Cre mice, *cTnt*-Cre*/+;Jarid2f/f* (*Jarid2*^{cTnt}), were generated. *Jarid2*^{cTnt} mice were born at the expected Mendelian ratio without overt cardiac defects (data not shown) and survived to adulthood (Table 2-1). These results suggest that Jarid2 in differentiated cardiomyocytes is dispensable for cardiac morphogenesis, supporting the critical roles of Jarid2 early in cardiac progenitors.

We first confirmed that *Jarid2* was efficiently deleted in the heart. PCR data on

isolated genomic DNAs showed that the floxed exon 3 of *Jarid2* was deleted only in the heart, but not in the tail or the brain of *Jarid2*^{Nkx} embryos (Fig. 2-1*A*). Jarid2 transcripts and protein levels were significantly decreased in *Jarid2*^{Nkx} vs. control embryonic hearts (Fig. 2-1*B* and 1*C*). *Jarid2f/f* mice were used as the control (Ctrl) throughout this study.

Cardiac progenitors can contribute to different cardiac cell types such as endocardium. Conflicting reports exist that *Nkx2.5*-Cre mice delete a floxed allele only in the myocardium or both in the myocardium and endocardium due to an early expression of Cre in cardiac progenitors [20, 21, 24]. To determine whether Jarid2 is deleted only in the myocardium or also in the endocardium, co-immunostaining was performed using antibodies against Jarid2 and MF20, a cardiomyocyte marker (Fig. 2-1*D*). Jarid2 was detected in the control myocardium but was not detectable in the *Jarid2*^{Nkx} myocardium (arrowheads). In contrast, Jarid2 was detected in the endocardium of the *Jarid2*^{Nkx} heart similar to the control endocardium as indicated by arrows. When primary cultured cells isolated from *Jarid2*^{Nkx} hearts were co-immunostained using Jarid2 and MF20 or PECAM antibodies, Jarid2 expression was detected in PECAM positive cells, whereas it was not detectable in MF20 positive cells (Fig. A1-1*A* and 1*B*). These data suggest that Jarid2 was deleted in cardiomyocytes but not in endothelial/endocardial cells. We have previously demonstrated that Jarid2 plays important roles in the endocardium by repressing Notch1-Neuregulin1 (Nrg1) signaling pathways to the underlying myocardium [8]. Since we cannot exclude a possibility that *Jarid2* may be deleted in a subpopulation of endocardial cells in *Jarid2*^{Nkx} hearts, we examined whether endocardial signaling pathways are altered in *Jarid2*^{Nkx} hearts. qRT-PCR data showed that Notch1-Nrg1 pathways were not increased in *Jarid2*^{Nkx} vs. control hearts (Fig. A1-1*C*). Further, none of

the Jarid2 mutants generated by other cardiac Cre drivers including αMHC-, MLC2v-, and Nkx2.5-transgenic (Tg) Cre showed cardiac malformations or perinatal lethality [19]. These data support that Jarid2 functions normally in the endocardial cells of *Jarid2*^{Nkx} hearts.

Jarid2^{Nkx} mice exhibit cardiac developmental defects

Next, we examined cardiac defects in mutant hearts during development by H&E staining of transverse sections (Fig. 2-2). At E12.5, *Jarid2*^{Nkx} hearts showed the grossly normal trabecular and compact layers in the ventricle as compared to the control hearts (Fig. 2-2*A*, a and b). However, an increased space between the endocardium and the myocardium was observed in *Jarid2*^{Nkx} vs. control hearts as indicated by arrow (Fig. 2-2*A*, c and d). Around E14, the interventricular septum in the control heart fused to the endocardial cushion and separated the right and left ventricles (Fig. 2-2*A*, e). In contrast, *Jarid2*^{Nkx} hearts showed defective interventricular septation leading to VSD as indicated by a star (Fig. 2-2*A*, f). Due to decreased cardiac jelly in the normal heart around E14, the endocardium is in direct contact with the myocardium for termination of trabeculation and compaction of trabeculae into the compact layer, leading to the development of a thick ventricular wall [14]. However, *Jarid2*^{Nkx} ventricles at E14 showed an increased subendocardial space (arrow), a thin compact layer (Fig. 2-2*A*, h), and hypertrabeculae (arrowhead, Fig. 2-2*A*, f) as compared to controls (Fig. 2-2*A*, e and g). At E15.5, the mutants continued to show VSDs (star), thin myocardium, and hypertrabeculation (arrowhead, Fig. 2-2*A*, j and l) compared to controls (Fig. 2-2*A*, i and k), which persisted in *Jarid2*^{Nkx} mutant hearts at P1 (Fig. 2-2*A*, n). Ventricular wall thickness and a distribution

of trabeculae were quantitated at E15.5, indicating a decrease in compact layer thickness mainly in the left ventricle, and an increase in trabeculation in the ventricle of *Jarid2*^{Nkx} hearts (Fig. 2-2*B*). *Jarid2*^{Nkx} hearts exhibited partially penetrant cardiac defects as summarized in Table 2-2 (see details in Table A2-1). Some *Jarid2* heterozygous mutant mice (*Nkx2.5-Cre/+;Jarid2f/+*) showed cardiac defects, while either *Nkx2.5-Cre* alone (*Nkx2.5-Cre/+;Jarid2+/+*, Table 2-2 and Fig. A1-2) or *Jarid2* whole body heterozygous mutants [9] did not show any ventricular defects or lethality. Since *Nkx2.5*-Cre mice contain a deletion of *Nkx2.5* in one allele, these results suggest that Nkx2.5 and Jarid2 may cooperate functionally or genetically during development. In summary, *Jarid2*^{Nkx} mutants exhibit ventricular defects including increased subendocardial space, VSD, hypertrabeculation, and the thin compact layer of the ventricular wall.

Increased subendocardial space in *Jarid2*^{Nkx} hearts is indicative of increased cardiac jelly. The cardiac jelly in the ventricle is critical for ventricular wall development and required for the initiation and growth of trabeculation between E9.5-13.5 [14]. Cardiac jelly components are mainly produced by the myocardium in the ventricle during the early stages of cardiac development until E12, and then the amounts of cardiac jelly begin to diminish at E12.5. The cardiac jelly is degraded by matrix metalloproteinases that are generated by the endocardium, which signals termination of trabecular growth. Thus, the heart sections were stained with Alcian Blue to detect the presence of mucopolysaccharides, components of the cardiac jelly (Fig. 2-2*C*). Alcian Blue staining was increased in the mutant vs. control ventricle at E12. At E15.5, the mutant heart showed cardiac jelly between the endocardium and the trabecular myocardium, while the control heart did not show any staining. The thin compact layer is evident in the mutant

ventricle compared to the control.

Since cardiac jelly was increased in *Jarid2*^{Nkx} hearts, we analyzed the expression levels of cardiac jelly components that play important roles in heart development. Our previous gene expression profile showed that Fibronectin 1 (Fn1), Cartilage link protein 1 (Crtl1, Hapln1), and Versican (Vcan) are highly elevated in *Jarid2* KO hearts [8]. Fn1 is critical for cardiac development [25]. It is produced by the myocardium and endocardium, and secreted into the cardiac jelly [26]. Crtl1 is mainly expressed in the endocardial lining of the heart and in the atrioventricular junction. At later stages, it becomes restricted to endocardially-derived mesenchyme. Crtl1 functions to stabilize the interaction between hyaluronan and proteoglycan such as Vcan [27]. Vcan, a chondroitin sulfate proteoglycan produced by the myocardium, is normally decreased at E12.5. Vcan is proteolyzed by the ADAMTS (a disintegrin and metalloproteinase with thrombospondin motif) family for myocardial compaction [28]. Our qRT-PCR data showed that only *Fn1* was significantly increased in *Jarid2*^{Nkx} vs. control hearts (Fig. 2-2*D*). *Collagen2a1* (*Col2a1*) was not increased, and collagen staining of heart sections using Masson's trichrome stain also indicated no increase in collagen in *Jarid2*^{Nkx} vs. control ventricles at E13.5 (data not shown). Vitronectin (Vtn) is a component of the extracellular matrix, and functions in cell attachment by interacting with other components or receptors [29]. *Vtn* expression was not altered in *Jarid2*^{Nkx} hearts vs controls. Adamts1 is a metalloproteinase that breaks down the cardiac jelly and contributes to the termination of trabeculation [14]. *Adamts1* expression was not altered, implying normal degradation of the cardiac jelly in *Jarid2*^{Nkx} hearts. These data suggest that Jarid2 in the myocardium inhibits the production of the cardiac jelly but may not affect the degradation of cardiac jelly.

To determine whether the cardiac defects in *Jarid2*^{Nkx} mice are due to altered cell proliferation in the ventricle, we analyzed cell proliferation rates. The number of phospho-Histone H3 (p-H3) or Ki67 positive cardiomyocytes in mutant heart sections was similar to control sections at E13.5 and 15.5 (Fig. A1-3*A* and 3*B*). Both control and mutant hearts showed very low levels of cleaved-caspase3 expression, indicating no significant changes in apoptosis in *Jarid2*^{Nkx} vs. control hearts (Fig. A1-3*C*). Our previous study also indicates no significant change in apoptosis in *Jarid2* KO vs. wild type hearts [30].

Determination of the genetic network regulated by Jarid2

Analyses of our gene expression profile data indicated that 3606 genes were down-regulated, and 3810 genes were up-regulated in *Jarid2* KO vs. wild type embryonic hearts (Fig. 2-3*A*, fold-change cutoff of >1.2) [8]. The dysregulated genes were involved mainly in heart development and vasculature development by gene ontology (GO) analysis of biological pathways using DAVID functional analysis software (www.david.ncifcrt.gov) (GO/DAVID) (Fig. 2-3*A*). Among the dysregulated genes, up-regulated genes were involved in response to wounding, whereas down-regulated genes represented a generation of precursor metabolites and energy by GO/DAVID analyses. Jarid2 has been shown to occupy the promoter regions to regulate target gene expression [31]. We have identified genome-wide Jarid2 occupancy on the promoters in the developing heart using the RefSeq promoter arrays [8]. To investigate the genetic network regulated by Jarid2, we overlapped the dysregulated genes in *Jarid2* KO hearts with the genes whose promoters were occupied by Jarid2. Our results revealed that of 3898 promoters that were occupied by Jarid2, 1292 genes were dysregulated in *Jarid2* KO

hearts, of which 706 genes were up-regulated, and 586 genes were down-regulated. The overlapping genes were mainly involved in intracellular signaling cascade, blood vessel development, transcription, and skeletal system and heart development by GO/DAVID analyses.

Although Jarid2 can regulate H3K27 methylation [7], it remains unknown whether Jarid2 is involved in H3K27 methylation during heart development. To identify the promoters where H3K27me3 is enriched, we performed ChIP-chip on embryonic hearts using H3K27me3 antibodies, yielding 1,132 promoters (Fig. 2-3*B*). When Jarid2 ChIP data were overlapped with H3K27me3, 605 promoters were identified, which mainly represented multicellular organism development and transcription pathways by GO/David analyses (Fig. 2-3*D*). Of those, 102 genes were up-regulated, and 64 genes were down-regulated in *Jarid2* KO hearts (Fig. 2-3*C*), indicating a subset of Jarid2 target promoters show H3K27me3 accumulation and simultaneously dysregulated in the absence of Jarid2. These analyses also indicate that Jarid2 regulates target genes by other pathways.

To determine potential targets of Jarid2 that are co-occupied by the PRC2 complex, we overlapped Jarid2 targets with the published PRC2 targets in embryonic hearts [20], yielding 263 potential target genes (Fig. A1-4). To determine targets of both Jarid2 and PRC2, which concomitantly show H3K27me3 accumulation, we overlapped the three ChIP data sets. A total of 224 genes among 263 genes showed H3K27me3 accumulation, indicating that a remarkably high percentage (85.2%) of the targets occupied by both Jarid2 and Ezh2 show H3K27me3 accumulation, while only 15.5% (605/3898) of Jarid2 targets showed H3K27me3 accumulation. These results strongly suggest that Jarid2 forms a functional complex with PRC2 to increase or maintain H3K27me3 levels on the

specific promoters in the developing heart. Next, we investigated the transcriptional network regulated by the Jarid2-PRC2-H3K27me3 axis. We performed GO/DAVID analyses with 224 genes. The top two significant pathways were regulation of RNA metabolic process and regulation of transcription. Of the 224 genes, 67 genes (29.9%) were dysregulated in *Jarid2* KO hearts. Among those dysregulated genes, 39 genes were up-regulated, whereas 28 genes were down-regulated (Table A2-2 and A2-3, respectively). Interestingly, among the up-regulated genes, 12 genes were involved in neuron differentiation (*Ngfr*, *Sall1*, *Lhx1*, *Sall3*, *Emx1*, *Barhl2*, *Neurod2*, and *Isl1*) or function (*Npas3*, *Syt6*, *Left1* and *Drd4*). These results imply that Jarid2 together with PRC2 inhibits neuronal pathways via H3K27me3 enrichment on specific promoter loci within the developing heart.

Among the down-regulated genes in *Jarid2* KO hearts, 586 genes were occupied by Jarid2 (Fig. 2-3*A*), which represent generation of precursor metabolites and energy, and regulation of transcription pathways by GO/DAVID. Among the 586 genes, 36 genes were co-occupied by PRC2, and of the 36 genes, 28 genes also showed H3K27me3 accumulation (Table A2-3). These 36 or 28 genes represent embryonic organ development, and multicellular organismal processes, respectively. It is unknown how these genes are down-regulated in *Jarid2* KO hearts. Since only the promoter occupancy was analyzed in this study, it is plausible that other enhancer regions of these genes may elicit dominant roles, which warrants further investigation.

We then analyzed gene expression levels in *Jarid2*^{Nkx} hearts, which are selected among the 67 dysregulated genes (Fig. 2-3*E*). Neural developmental genes, including *Isl1*, *Sall1*, *Sall3* and *Pax6* were up-regulated in *Jarid2*^{Nkx} hearts, suggesting that Jarid2

with PRC2 represses these genes via H3K27me3 accumulation. In contrast, expression levels of some genes involved in neural differentiation, including *Barhl2*, *Neurod2* and *Lef1* showed no significant difference, implying that certain potential targets are not actively repressed by myocardial Jarid2 at E13.5. The genes involved in heart development (*Nkx2.5*, *Nfatc1,* and *Msx1*) were not significantly changed in *Jarid2*^{Nkx} hearts vs. controls. Interestingly, *Isl1* was significantly up-regulated. Isl1 is a critical transcription factor for the development of the secondary heart field and is highly expressed until E10 in the ventricle [32]. *Lef1* and *Sall1* were not included in heart developmental genes by GO/DAVID analyses. However, Tcf/Lef1 mediated Wnt signaling regulates the transcription of cardiac factors, such as *Isl1*, *Mesp1*, and *Anf*, and cardiac development [33-35]. In addition, mutations of *Sall1* cause Townes-Brocks syndrome in humans with heart anomalies, and Sall1 expresses in the undifferentiated cardiac progenitor cell [36, 37]. *Sall1* expression was significantly increased in *Jarid2*^{Nkx} hearts. Our data suggest that neural developmental pathways are suppressed by myocardial Jarid2 in the developing heart. Jarid2 elicits fine transcriptional regulatory function during ventricular myocardial differentiation partly by depositing H3K27me3 via PRC2 on specific promoter loci.

The transcriptional network regulated by Jarid2

To identify transcriptional networks governed by Jarid2 in cardiac development, we have selected up-regulated genes that show more than a 1.7-fold increase in *Jarid2* KO hearts [8], yielding 586 genes. An average fold increase of all the up-regulated genes was 1.7 in our gene expression profile data. Among these, we analyzed expression levels of

important genes in cardiac development, such as *Bmp10*, *Isl1*, *Igf1*, *Igfbp2*, and *Fn1* in *Jarid2*^{Nkx} hearts. qRT-PCR indicated that *Bmp10*, *Isl1* and *Igfbp2* were significantly elevated in *Jarid2*^{Nkx} vs. control hearts at E13.5, and E16.5 (Fig. 2-4*A* and 4*B*). *Igf1* and *Fn1* were transiently up-regulated in *Jarid2*^{Nkx} at E13.5. To confirm the protein levels, Western blotting was performed using antibodies against phosphorylated Smad1/5/8, and Isl1. P-Smad1/5/8 levels were significantly elevated in *Jarid2*^{Nkx} hearts at E13.5, and Isl1 expression was increased at E13.5 and 15.5 compared to control hearts (Fig. 2-4*C* and 4*D*). P-Smad1/5/8 is used as a marker for Bmp10 signaling. When a Bmp10 signal is activated, Smad1/5/8 is phosphorylated and activated [38]. *Bmp10* expression and P-Smad1/5/8 were elevated in *Jarid2*^{Nkx} hearts, which correlates well with hyper-trabecular defects or ventricular myocardial maturation defects. Isl1 is expressed in conduction cells during heart development, and its expression persists in a subset of cardiac cells after birth such as in nodal cells or cardiac progenitors [39]. Our gene expression profile data showed up-regulation of *Bmp2*, *Tbx2* and *Gjd3* in *Jarid2* KO hearts, which are expressed in conduction cells [8, 40]. Hcn4 is a marker of the sinoatrial node with co-expression of Isl1 [41]. All four genes seem increased in *Jarid2*^{Nkx} hearts at E13.5 although only *Gjd3* showed statistical significance (Fig. A1-5). Thus, up-regulation of Isl1 appears to correlate with an increased expression of the conduction system genes in *Jarid2*^{Nkx} hearts.

Ventricular wall maturation requires the precise regulation of gene expression in the trabecular and compact layer. We examined whether the trabecular vs. compact layer fate decision is defective in *Jarid2*^{Nkx} hearts. Bmp10 is critical for trabecular formation and expressed only in the trabecular myocardium between E9-13.5 [38]. *In situ* hybridization analyses showed that *Bmp10* expression was expanded deep into the compact layer in

Jarid2^{Nkx} ventricles at E13.5 (Fig. A1-6). *Anf* is a trabecular-specific gene in the embryonic ventricle, and its expression decreases as the heart develops [9]. *Anf* expressing cardiomyocytes are detected deep into the compact layer in *Jarid2* KO embryonic hearts compared to controls. In contrast, the *Hey2* expression level, a compact layer-specific gene, is not altered in *Jarid2* KO hearts by qRT-PCR [19], and it was detected only in the compact layer of the *Jarid2*^{Nkx} ventricle by *in situ* hybridization (data not shown). Thus, in *Jarid2*^{Nkx} hearts, the trabecular layer appears to be expanded into the compact layer, but the expression pattern of the compact layer-specific gene has not been altered. These data imply that the fate determination of the trabecular vs. compact layer is normal.

***Epigenetic mechanisms of Jarid2 in regulation of Isl1 expressio*n**

Our data indicate that Isl1 is a putative direct target of Jarid2, and one of the most up-regulated genes in the absence of *Jarid2* during heart development. To determine the precise regulatory mechanism of Isl1 expression by Jarid2, we analyzed genomic occupancy of the *Isl1* locus by qChIP assays. We performed VISTA alignments to identify conserved regions at the *Isl1* locus (Fig. 2-5*A*). The conserved regions from 5 kilobases (Kb) upstream and downstream of the *Isl1* transcription start site were selected for qChIP assays using a Jarid2 antibody on E14.5 hearts when Isl1 is normally reduced [32]. In control hearts, the high level of Jarid2 occupancy was detected at -0.5 Kb relative to the transcriptional start site, which was significantly reduced in *Jarid2*^{Nkx} hearts (Fig. 2-5*B*). Our data indicate that Jarid2 accumulates at the *Isl1* promoter region in the developing myocardium.

PRC2 is necessary for normal cardiac development, and Isl1 expression is also

elevated in *PRC2* KO hearts [20]. However, it remains unknown whether Jarid2 cooperates with PRC2 to regulate Isl1 expression in the developing heart. We hypothesize that Jarid2 is essential for recruiting PRC2 to the *Isl1* genomic locus and for histone modifications of H3K27. To test this, qChIP assays were performed to analyze Ezh2, a PRC2 component, and H3K27me3 accumulation in *Jarid2*^{Nkx} vs. control hearts at E14.5. Both Ezh2 and H3K27me3 were enriched at the -0.5 Kb promoter region in control hearts, but significantly reduced in *Jarid2*^{Nkx} hearts (Fig. 2-5*C*). These results suggest that the *Isl1* promoter locus is occupied by Jarid2, and the same region is enriched with Ezh2 and H3K27me3 in a Jarid2-dependent manner. Although the physical interaction between Jarid2 and Ezh2 in the PRC2 complex has been well demonstrated [7, 15], their interaction has not been shown in the heart. Our co-immunoprecipitation showed the physical interaction between Jarid2 and Ezh2 in embryonic heart extracts *in vivo* (Fig. A1-7*A*). To determine whether H3K4 methylation, a transcriptional activation marker, is altered, we measured H3K4me3 enrichment at the *Isl1* promoter locus. H3K4me3 was increased at the -0.5Kb region of the *Isl1* locus in *Jarid2*^{Nkx} vs. control hearts, which correlates well with the active transcriptional status of *Isl1* in *Jarid2*^{Nkx} hearts. Thus, early cardiac-specific deletion of *Jarid2* by *Nkx2.5-Cre* causes a decreased PRC2 and H3K27me3 accumulation on the *Isl1* promoter locus, which correlates well with a failure of Isl1 suppression in *Jarid2*^{Nkx} hearts during development.

Jarid2 suppresses transcriptional activity of Isl1

To investigate whether Jarid2 represses *Isl1* transcription, we constructed two reporter plasmids containing the Isl1 promoter with or without the -0.5Kb region, which is

the site of Jarid2 occupancy. The reporter containing the -0.5Kb region showed a decrease in luciferase levels when co-transfected with Jarid2 in a dose-dependent manner (Fig. 2-6*A*). However, the reporter without the -0.5Kb region or pGL3 basal vector did not show any changes in luciferase levels by Jarid2. These results indicate that the -0.5 Kb region is critical for repression of *Isl1* transcription by Jarid2.

To determine which domain of Jarid2 is required to repress Isl1 transcriptional activity, various Jarid2 mutant plasmids [42] were co-transfected with the Isl1 reporter (Fig. 2-6*B*). Jarid2 mutants, the N-term (aa1-528) or TR (aa1-222) showed about 30-40% decreases in Isl1 reporter activity. These constructs also contain the EZH2 interaction site [31]. In contrast, the C-term (aa 529-1234, cytoplasmic protein) or NLS/C-term (aa1-130/529-1234, nuclear protein) displayed no repressive activity. Since Jarid2 contains NLS in the N-terminal region (aa1-130), the C-term protein without NLS does not localize in the nucleus. The mutant containing NLS fused to the C-term localizes in the nucleus [42]. These data indicate that the TR and EZH2 interacting domain of Jarid2 is required to repress Isl1 reporter activities. Next, we determined whether PRC2 components, EZH2 and EED, regulate Isl1 transcriptional activity in cooperation with Jarid2. Jarid2 or EZH2 alone at a low dose did not repress Isl1 reporter, but EED showed a 10% reduction (Fig. 2-6*C*). Co-transfection of Jarid2 with either EZH2 or EED showed about a 30% reduction whereas Jarid2 together with both EZH2 and EED resulted in a 50% reduction. Therefore, we tested whether the TR domain of Jarid2 is sufficient to repress Isl1 by interacting with PRC2 (Fig. 2-6*D*). Although a low dose of TR domain did not display a significant repression of Isl1, it showed a synergistic repression of about 30-40% with EED or EZH2. Additionally, a combination of EED and EZH2 with TR domain showed about a 50%

repression similar to the full length Jarid2. Jarid2 together with EED and EZH2 significantly repressed the reporter activity as compared to EED and EZH2 without Jarid2 (Fig. 2-6*C* and 6*D*). Altogether, our data indicate that Jarid2 and PRC2 cooperate to significantly inhibit *Isl1* transcription, and that the TR domain of Jarid2 mediates PRC2-dependent inhibition of *Isl1* transcription.

In summary, our working model depicts the mechanism of Jarid2 function within the developing myocardium (Fig. 2-7). There is a critical window during early cardiac progenitor differentiation when Jarid2 is required for normal cardiac development. In contrast, Jarid2 in differentiated cardiomyocytes is dispensable for cardiac morphogenesis. Our finding indicates that Jarid2 is necessary to recruit PRC2 to the promoter region of a subset of Jarid2 target genes and to establish proper histone methyl code such as methylation of H3K27, which leads to transcriptional repression of the target genes in the developing heart. This process is instrumental for normal myocardial differentiation, in part by repressing non-cardiac lineage developmental pathways and regulating cardiac jelly components.

Table 2-1. Mendelian ratios of embryonic or postnatal mice.

Cre mouse	Age	No. of litters	No. of live mice	Genotype of live mice				Dead
				+/+;f/f	***+/+;f/+***	***C/+;f/+***	***C/+;f/f***	
Nkx2.5	E9.5-14.5	41	344	79 (23.0%)	90 (26.2%)	88 (25.6%)	87 (25.3%)	4*
	E15-19.5	27	192	46 (24.0%)	48 (25.0%)	52 (27.1%)	46 (24.0%)	1**
	P1-10	24	107	37 (34.6%)	35 (32.7%)	35 (32.7%)	0 (0%)	8#
cTnt	P21	8	56	16 (28.6%)	13 (23.2%)	14 (25.0%)	13 (23.2%)	

Embryonic (E) or postnatal (P) mice were examined to determine Mendelian ratios.

*, Two were not possible for genotyping because of necrosis, and the other two were +/+;*f*/+; **, One was *C*/+;*f/f*; #, Five dead mice were *C*/+;*f/f* , two were +/+;*f/f* and one was *C*/+;*f/*+. All eight dead mice were observed at P1.

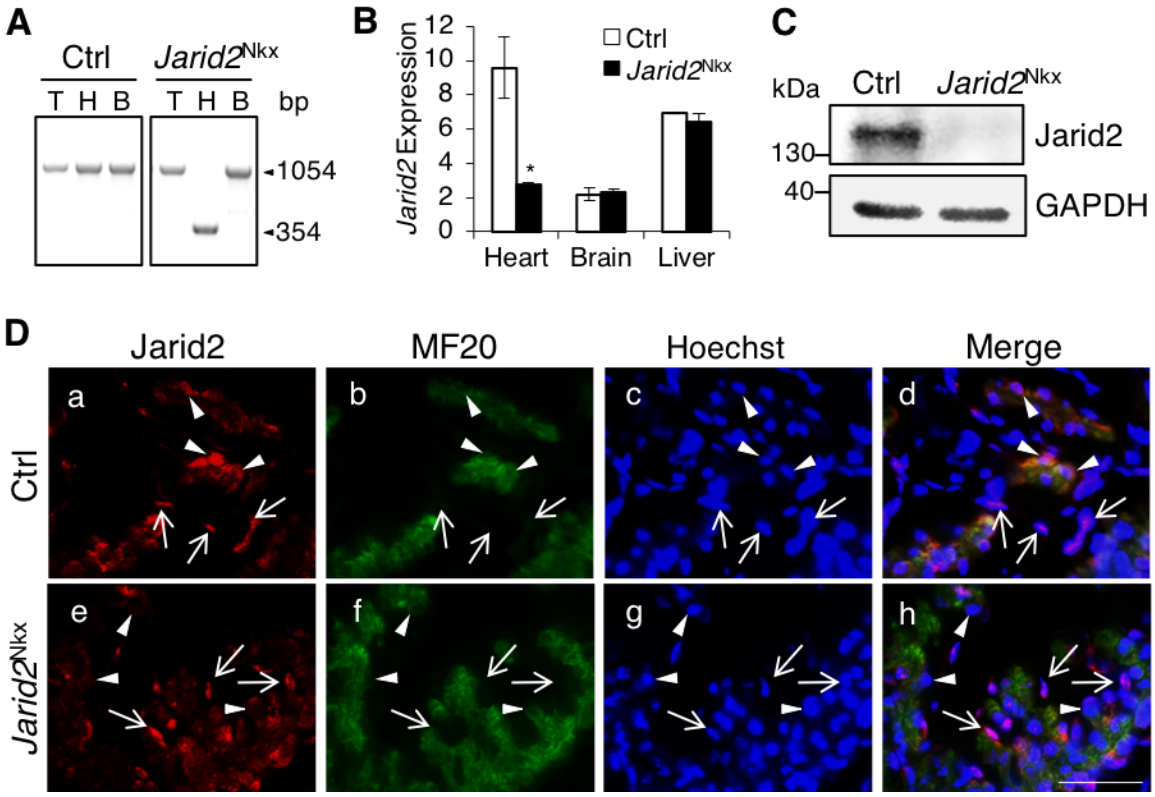

Figure 2-1. Cardiac-specific deletion of *Jarid2* using *Jarid2*^{Nkx} mice.

A, Genomic DNAs were isolated from the tail (T), heart (H), and brain (B) at E18.5. PCR was performed using primers located outside two loxP sites containing exon3 of *Jarid2* (61), yielding floxed allele (1054bp) or floxed out allele (354bp). B, *Jarid2* mRNA levels were detected by qRT-PCR relative to 18S RNA on the control or *Jarid2*^{Nkx} heart, brain or liver at E18.5, n=3. C, Western blotting was performed with Jarid2 antibody on control or *Jarid2*^{Nkx} hearts at E13.5. GAPDH is a loading control. D, Immunostaining analysis was performed on comparable transverse heart sections from E10.5 control (a-d) or *Jarid2*^{Nkx} (e-h) embryos using Jarid2 (Red) and MF20 (Green) antibodies. Arrows indicate the endocardium and arrowheads indicate the myocardium. Scale bar, 50μm.

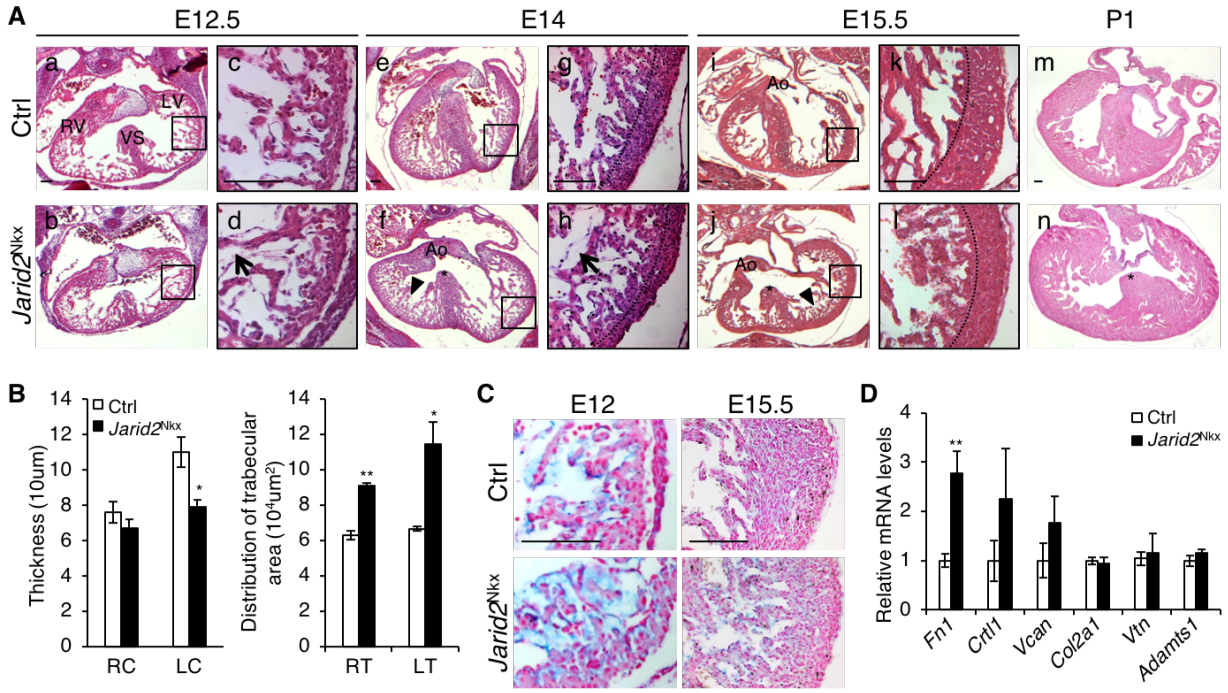

Figure 2-2. Cardiac defects were observed in *Jarid2*^{Nkx} embryos.

A, H&E staining was performed on transverse sections at E12.5 (a-d), E14 (e-h), E15.5 (i-l), and P1 (m and n) of *Jarid2*^{Nkx} (b, d, f, h, j, l and n) vs. control (a, c, e, g, i, k and m) mice. The boxed regions of a, b, e, f, i and j are magnified in c, d, g, h, k and l, respectively. Representative images of *Jarid2*^{Nkx} embryos show VSD (*, f, j and n), thin myocardium (dashed line, h, and l), and disorganized hypertrabeculae (arrow heads, f and j). Arrows (d and h) indicate the increased distance between the endocardium and myocardium in *Jarid2*^{Nkx}. The dotted lines separate the compact and trabecular layers. Scale bar, 100μm. B, Compact layer thickness was measured by drawing lines, and distribution of trabecular area was measured using NIH Image J software on the right (R) or left (L) compact layer (C) and trabecular layer (T) at E15.5. Three slides per heart were measured, n=4. C, Alcian Blue staining showed increased mucopolysaccharides in *Jarid2*^{Nkx} at E12 and

E15.5. The sections were counterstained with nuclear fast red. Scale bar, 100 μm. D, qRT-PCR was performed to determine the expression levels of extracellular matrix components and, a metalloproteinase, *Adamts1* on control or *Jarid2*^{Nkx} hearts at E13.5. The expression levels were normalized to the control. n=3.

Table 2-2. Cardiac phenotypic defects observed in *Jarid2*^{Nkx} mice.

Stages	Genotype	No. of mice	VSD	Hyper-trabeculation	Thin myocardium
E15.5 - E19.5	Control (*+/+;f/f*)	10	0	0	0
	Jarid2^{Nkx} (*C/+;f/f*)	11	10 (91%)	9 (82%)	8 (73%)
	Nkx2.5-Cre (*C/+;+/+*)	7	0	0	0
	Heterozygous (*C/+;f/+*)	7	1 (14%)	1 (14%)	1 (14%)

Mice at various stages were examined by H&E staining on transverse sections. *Jarid2*^{Nkx} mice exhibited cardiac defects including VSD, thin myocardium and hypertrabeculation.

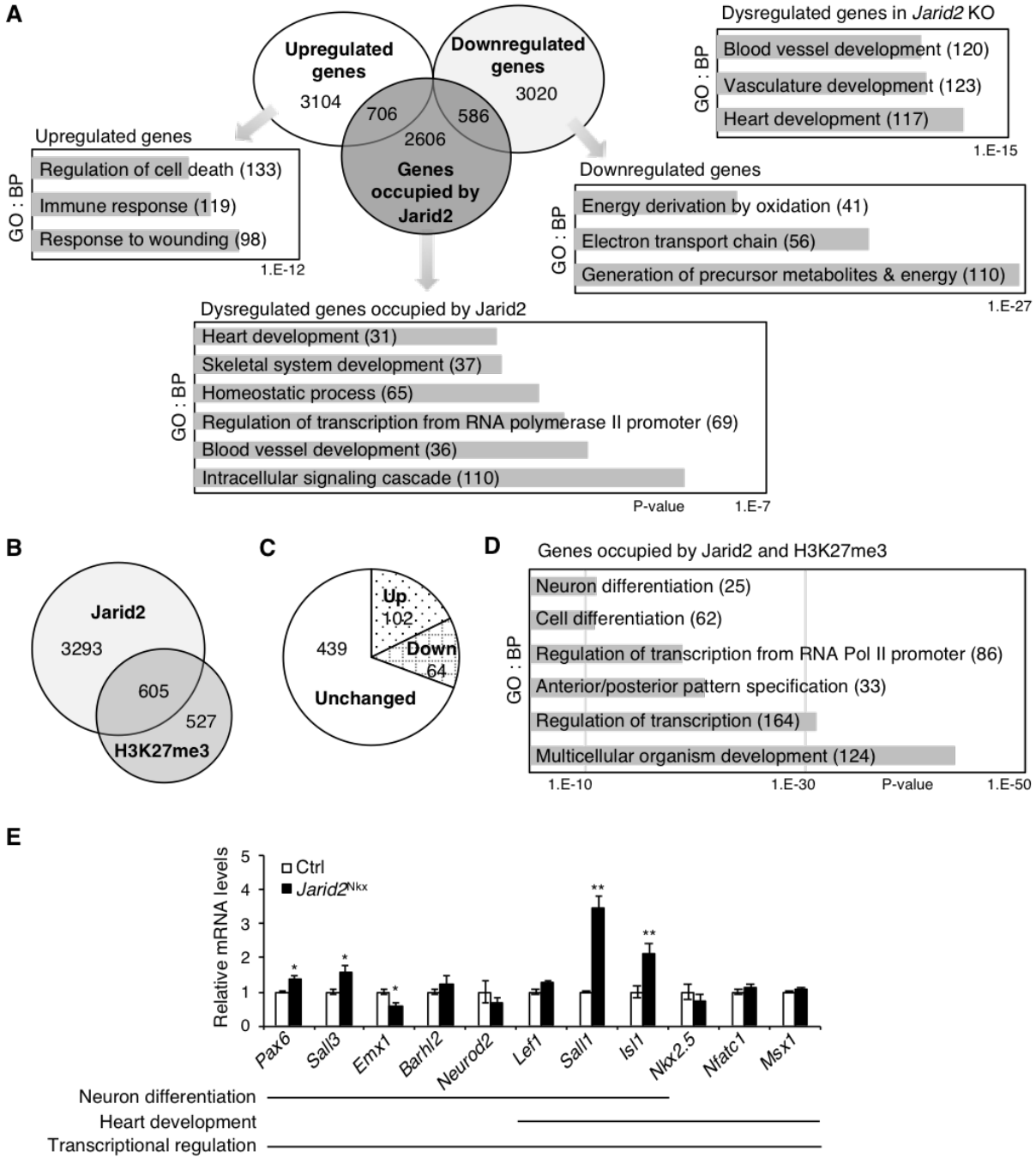

Figure 2-3. Gene expression profile analyses on the promoter occupancy by Jarid2 or H3K27me3.

A, Venn diagram demonstrated the overlap of up- or down-regulated genes in *Jarid2* KO

hearts by microarray analyses and the genes occupied by Jarid2 from ChIP-chip (8). Highly significant biological pathways (BPs) for dysregulated genes, up- or down-regulated genes or overlapping genes with Jarid2 ChIP-chip data were determined by GO/DAVID analyses. Numbers indicate the number of genes in each category. The X axis represents the *p* values. B, Venn diagram demonstrates the overlap of genome-wide occupancy of Jarid2 or H3K27me3 by ChIP-chip. C, 605 overlapping genes in (B) were overlaid with the microarray data. The pie chart shows the number of dysregulated genes in *Jarid2* KO. D, Highly significant BPs for the 605 overlapping genes were determined by GO/DAVID. E, Expression levels of dysregulated genes, occupied by Jarid2, Ezh2 and H3K27me3 (Fig. A1-4), were examined by qRT-PCR on control or *Jarid2*^{Nkx} hearts at E13.5 and normalized to the control, n=3-4.

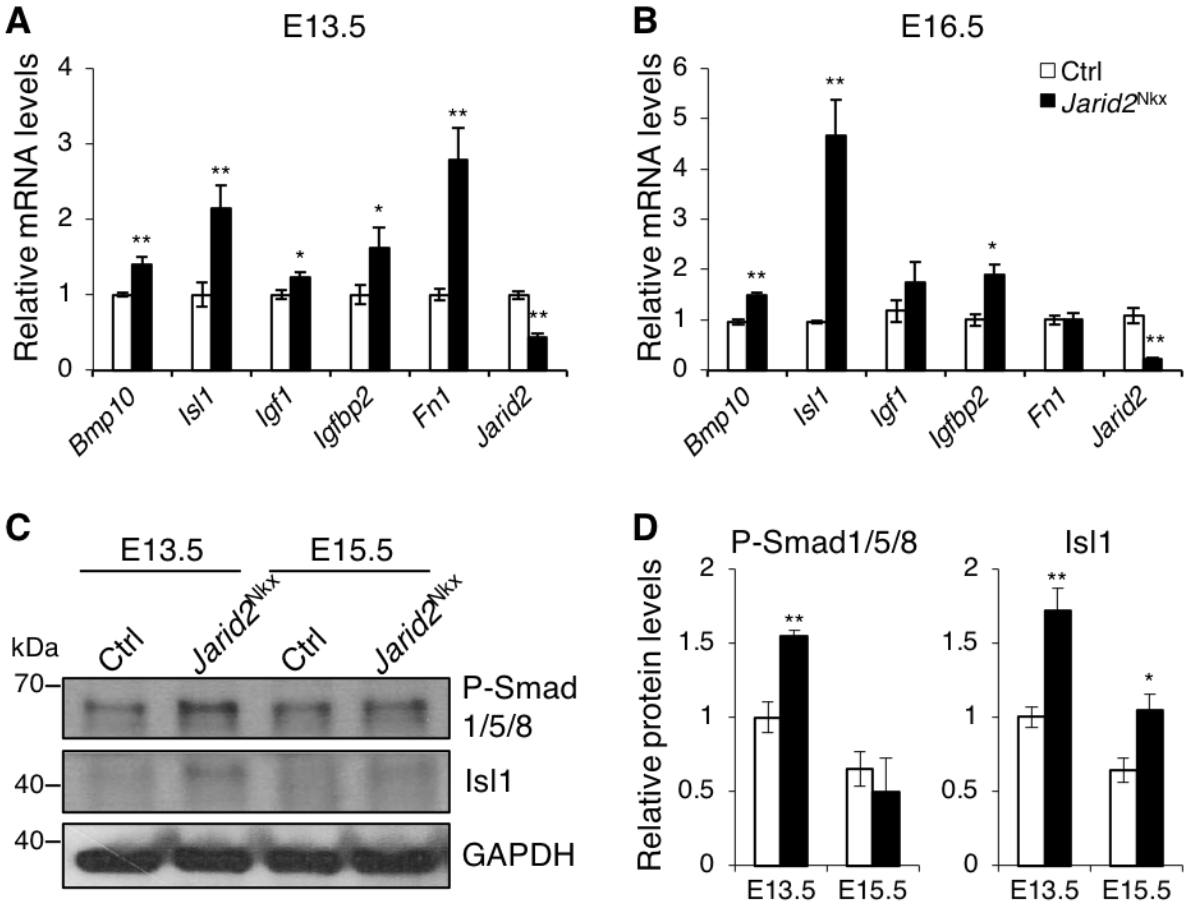

Figure 2-4. Identification of dysregulated genes in *Jarid2*^{Nkx} mice.

qRT-PCR was performed on control or *Jarid2*^{Nkx} hearts at E13.5 (A) and E16.5 (B). The expression levels were normalized to the control, n=3-5. C, Western blotting was performed on E13.5 and E15.5 control or *Jarid2*^{Nkx} hearts with phospho-Smad1/5/8 or Isl1 antibody. GAPDH is a loading control. D, The graph shows the protein levels of phospho-Smad1/5/8 and Isl1 that were standardized to GAPDH and normalized to the control heart at E13.5, n=4.

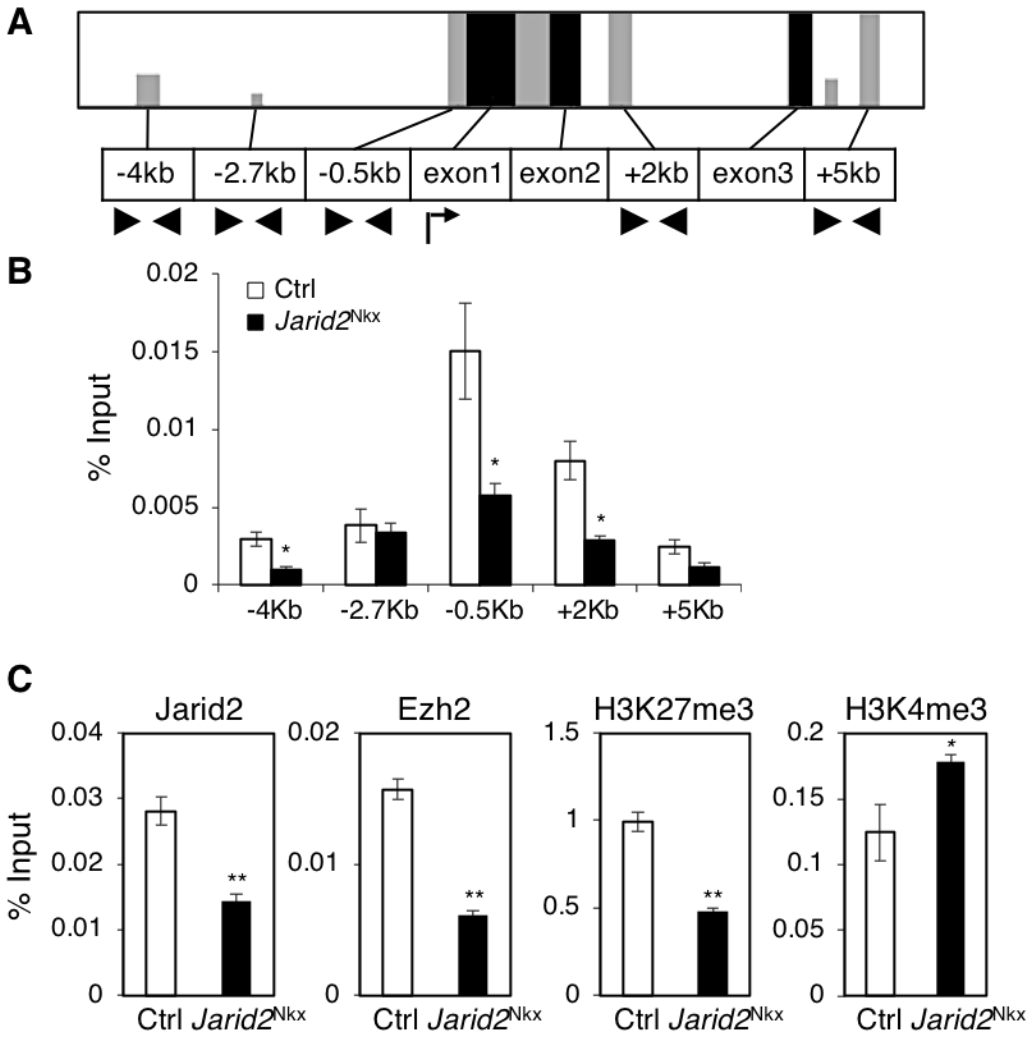

Figure 2-5. Jarid2 occupies a specific region at the *Isl1* locus.

A, VISTA alignment was performed at the *Isl1* genomic locus spanning about 70 Kb for mouse, monkey, human and rat to determine conserved regions. Here, the promoter region around 10 Kb region near the transcription start site (arrow) was analyzed. Grey bars indicate regions with greater than 75% conservation, and black bars indicate exons. Arrowheads indicate primer sites. B, Jarid2 occupancy at the conserved regions was measured by qChIP assays on *Jarid2*^{Nkx} or control hearts using Jarid2 antibody. The bars

show enrichment compared to each input. C, qChIP assays were performed on control or *Jarid2*^{Nkx} hearts at the -0.5Kb region of *Isl1* using Jarid2, Ezh2, H3K27me3 or H3K4me3 antibody, n=3.

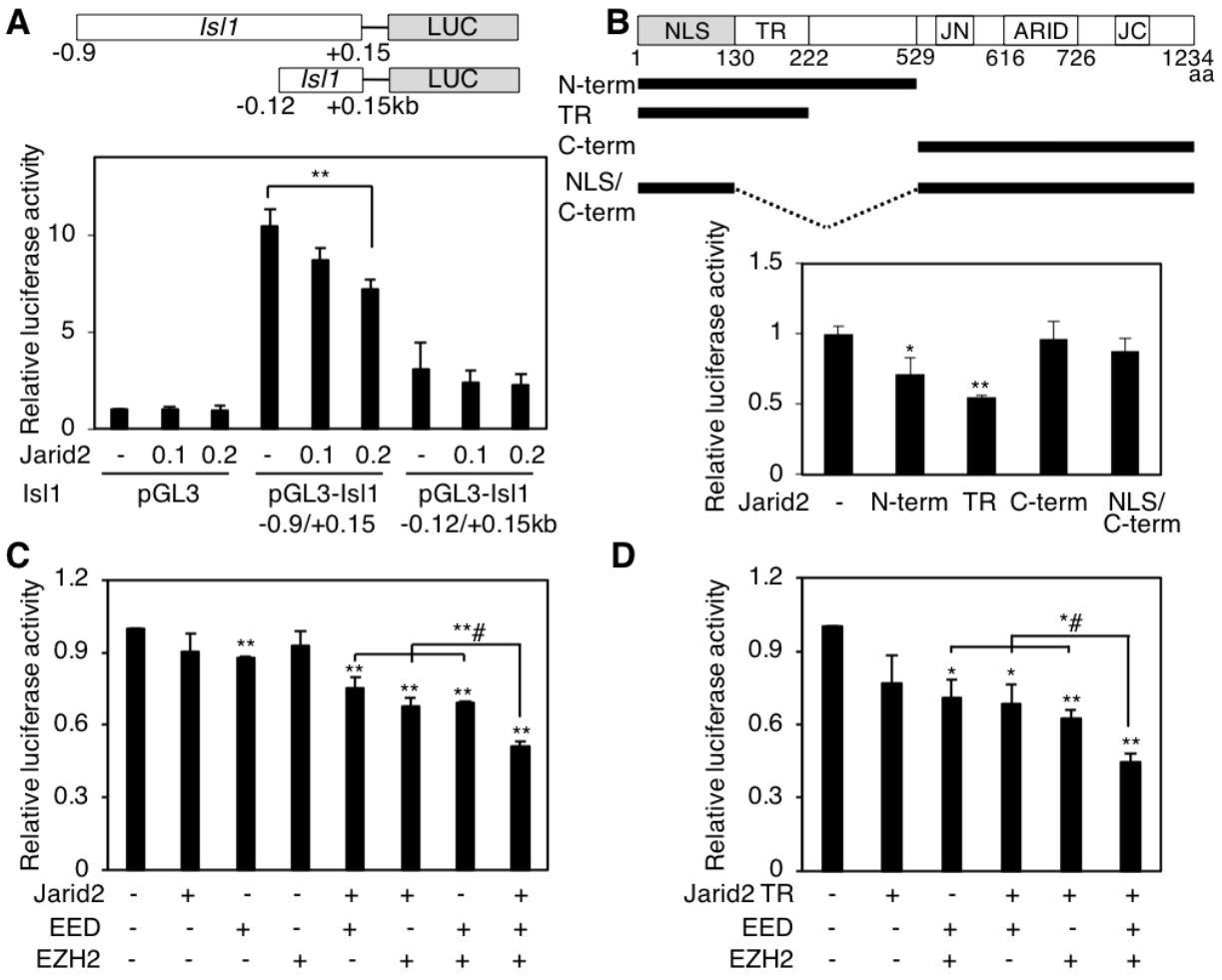

Figure 2-6. Jarid2 represses Isl1 reporter gene.

A, pGL3, pGL3-Isl1 including the -0.5Kb region (-0.9/+0.15Kb) or without the -0.5kb region (-0.12/+0.15Kb) was transfected into 10T1/2 cells with increasing amounts of Jarid2 (μg). B, A schematic diagram shows Jarid2, and Jarid2 mutants (N-term,1-528aa; TR, 1-222aa; C-term, 529-1234aa; NLS/C-term, 1-130/529-1234aa). Jarid2 (0.2 μg) was transfected into 10T1/2 cells with pGL3-Isl1 (-0.9/+0.15Kb) reporter. NLS, nuclear localization signal; TR, transcription repression domain; JN, Jumonji N domain; JC, Jumonji C domain; ARID, AT-rich interaction domain. C, pGL3-Isl1 (-0.9/+0.15kb) reporter was transfected into

10T1/2 cells with Jarid2, EED and/or EZH2 at a low dose (50 ng). D, TR domain of Jarid2 (1-222aa, 25ng) was transfected into 10T1/2 cells with or without EED and/or EZH2 (50 ng) for luciferase activity assays of pGL3-Isl1 (-0.9/+0.15kb). Luciferase activity was normalized to reporter gene alone. Asterisks indicate a significant difference compared to reporter gene alone, n=3. Number signs indicate a significant difference between a combination of any two factors and all three factors together.

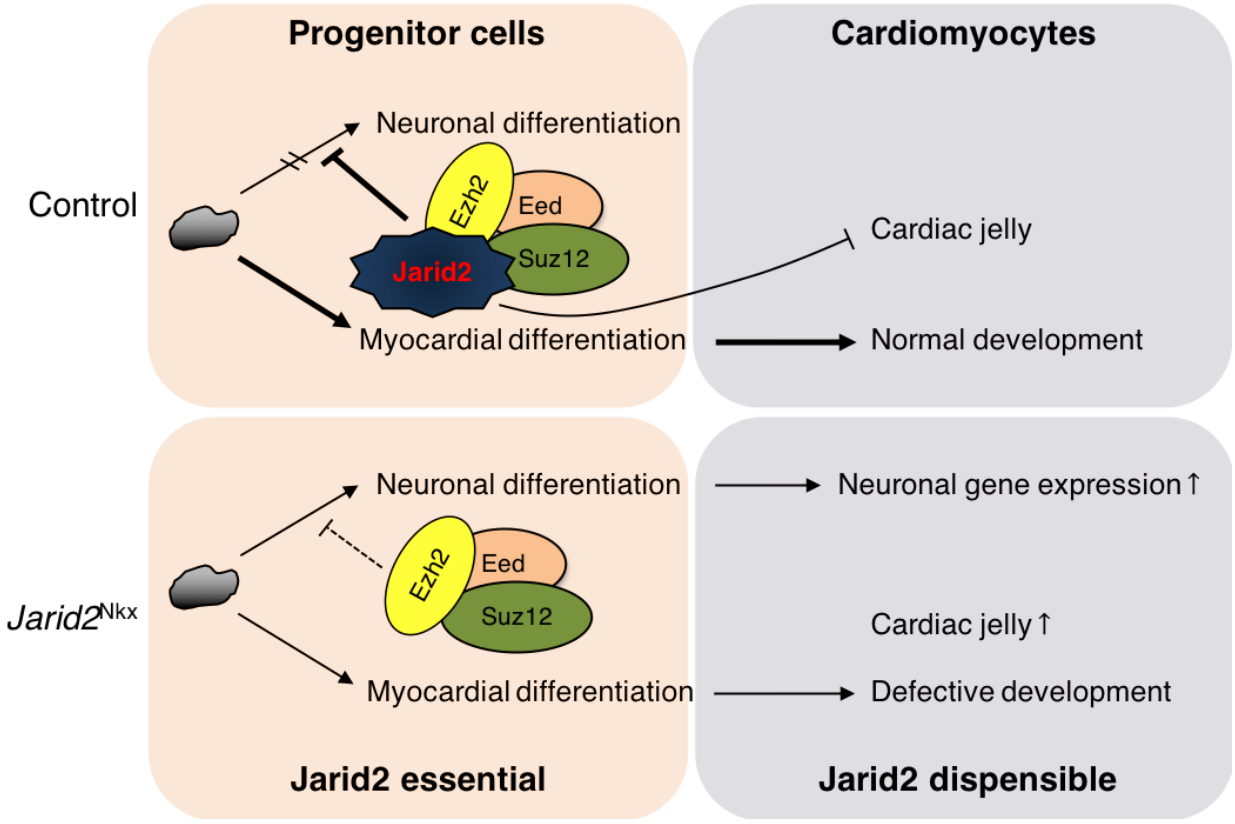

Figure 2-7. Jarid2-mediated gene repression is required for normal cardiomyocyte differentiation.

Jarid2 and PRC2 complex repress neuronal gene expression by deposition of H3K27me3 epigenetic marks in early cardiac cells. However, *Jarid2* deficiency in cardiac cells relieves the suppressive function of PRC2 complex on neuronal genes, and increases cardiac jelly production, all of which contribute to abnormal cardiac differentiation.

Discussion

Jarid2 is essential for embryonic development and is a recognized component of pluripotency networks [5-7]. The present study demonstrates that cardiac-specific deletion of *Jarid2* using *Nkx2.5*-Cre mice causes neonatal lethality and ventricular defects including VSD, hypertrabeculation, and the thin compact layer leading to the thin ventricular myocardial wall. The genes whose promoters are occupied by Jarid2, PRC2, and H2K27me3 showed dysregulated biological pathways in *Jarid2* deficient hearts such as neuronal differentiation pathways. Of note, cardiac-specific deletion of *PRC2* results in cardiac developmental defects, which are remarkably similar to those observed in *Jarid2* KO mice [9, 20]. In contrast, cardiomyocyte-specific deletion of *Jarid2* by *cTnT*-Cre mice did not cause gross cardiac malformations or perinatal lethality, indicating that Jarid2 in differentiated cardiomyocytes is dispensable for cardiac morphogenesis.

To determine roles of Jarid2 in differentiated cardiomyocytes, *Jarid2* floxed mice have been crossed with different myocardial-specific Cre mice, including *αMHC*-Cre, *Nkx2.5*-Cre Tg [19]. These mutant mice show grossly normal hearts and survive to adulthood, which might be due to the late expression of Cre. *Nkx2.5*-Cre Tg mice show Cre activity at E8.0 in the myocardium and a subset of endocardial cells [43]. Since *αMHC*-Cre mice activate Cre from E8.5 in the myocardium [23], we employed *cTnT*-Cre mice that express Cre early from E7.5 [22]. However, *Jarid2* deletion by *cTnT*-Cre mice did not cause cardiac developmental defects or perinatal lethality. Although *Nkx2.5*-Cre and *cTnt*-Cre mice start to express Cre recombinase from E7.5 in the heart, a complete recombination in the cardiogenic fields is observed at E8.0 and E8.5, respectively [44]. In

addition, cTnt-Cre expression starts later in the secondary heart field. These may have caused a lack of cardiac developmental defects in *Jarid2*^{cTnt}. Thus, our results indicate that Jarid2 is necessary in early cardiac progenitors for normal heart development at later stages. Perturbation of this early process may contribute to cardiac malformations manifested later in development. It would be interesting to investigate the impact of *Jarid2* deletion on adult heart pathophysiology using *αMHC*-Cre mice.

Nkx2.5 is a cardiac-specific transcription factor and expressed in the cardiac mesoderm from E7.5 to adult cardiomyocytes. It is believed that endocardial cells are also derived from Nkx2.5 positive cardiac progenitors in the cardiac mesoderm [21, 24]. When the progenitor cells differentiate into endocardial cells around E7.5-8.0, they lose Nkx2.5 expression, while myocardial cells continue to express Nkx2.5. Since the *Nkx2.5*-Cre mice employed in this study express Cre from E7.5 in cardiac progenitors, other lineages such as endocardial cells may have expressed Cre [21]. However, our analyses indicate a myocardial-specific deletion of *Jarid2* in *Jarid2*^{Nkx} hearts (Fig. 2-1, and Fig. A1-1). Thus, the cardiac defects observed in *Jarid2*^{Nkx} hearts are mainly caused by myocardial deletion of *Jarid2*, although we cannot exclude a possibility that *Jarid2* may be deleted in a subset of endocardial cells. *Nkx2.5*-Cre mice are haploinsufficient for *Nkx2.5,* and *Nkx2.5* haploinsufficiency is associated with atrial septal defects, VSD, and conduction system abnormalities albeit at a low rate in mouse models [45, 46]. Thus, we examined *Nkx2.5*-Cre (*Nkx2.5-Cre/+;Jarid2+/+*) and heterozygous (*Nkx2.5-Cre/+;Jarid2f/+*) mice for possible cardiac defects. All *Nkx2.5*-Cre embryos (Table 2-2) or *Jarid2* heterozygous KO embryos [9] showed normal ventricular structure in our genetic background. *Nkx2.5-Cre/+;Jarid2f/+* compound heterozygous mice showed cardiac defects with low

penetrance, suggesting putative functional and/or genetic interactions between Jarid2 and Nkx2.5. Additional mice with *Nkx2.5-Cre/+;Jarid2f/+* need to be examined to determine possible interactions between Jarid2 and Nkx2.5. However, the Mendelian ratio of *Nkx2.5-Cre/+;Jarid2f/+* mice was normal (Table 2-1). Moreover, *Nkx2.5* transcript levels appear unchanged in *Jarid2*^{Nkx} hearts vs. controls (Fig. 2-3*E*), implying that *Nkx2.5* haploinsufficiency may not have contributed significantly to cardiac defects or lethality observed in *Jarid2*^{Nkx} mice. *Jarid2*^{Nkx} embryos exhibited partial penetrance (Table 2-2). It may be due to a limitation of Cre-loxP technology, an incomplete Cre-mediated deletion of the *Jarid2* floxed allele in a subset of cells. However, it should be noted that each mutant showed at least one or more cardiac defects (Table A2-1).

Regulation of the cardiac jelly is crucial for normal trabeculation in the ventricle wall, which requires crosstalk between the endocardium and myocardium [14]. Increased cardiac jelly in the *Jarid2*^{Nkx} ventricle may have contributed to hypertrabeculation and thin myocardium, likely due to the failure of repressing trabeculation and compacting the ventricular wall. Intriguingly, both *Jarid2* KO and endothelial deletion cause increased subendocardial space [9, 19], which indicate that complex regulatory mechanisms exist to regulate the cardiac jelly expression involving both the myocardium and endocardium. In our data, *Fn1* was significantly increased at E13.5 in *Jarid2*^{Nkx} hearts. Deletion of the *Fn1* gene in mice causes embryonic lethality due to severe cardiac defects [25]. Thus, it would be interesting to determine the mechanism by which Jarid2 regulates *Fn1* expression during heart development.

Various mouse models have been generated and studied for ventricular wall morphogenesis or noncompaction cardiomyopathy. Some models exhibit reduced cell

proliferation in the developing heart. These include cardiac-specific *PRC2* deletion mice exhibiting hypertrabeculation and thin compact layer [20], and *Bmp10* deletion mice showing decreased trabeculation and thin myocardium leading to the hypoplastic ventricle [47]. To the contrary, some mouse models show increased cell proliferation mainly in the trabecular layer. For example, *Jarid2* KO, *Fkbp1a* deletion, or cardiac-specific deletion of *Mib1* in mice result in hypertrabeculation and thin compact layer leading to the thin ventricular myocardium [9, 48, 49]. In some mouse models, cell proliferation was not altered. For example, *Daam1*-deficient hearts show hypertrabeculation and noncompaction phenotype [50], and the endothelial deletion of *Brg1* causes reduced cardiac jelly, reduced trabeculae and thin compact layer [14]. Our *Jarid2*^{Nkx} mice also showed no significant changes in cell proliferation at E13.5 and E15 when ventricular defects were obvious. Thus, although cell proliferation is critically involved in the formation of trabecular and compact layers, other processes such as planar cell polarity, cell adhesion and alignment, and proper myocardial differentiation are also important. There has been no direct evidence that the trabecular layer contributes to the thickened ventricular wall at late stages. Interestingly, recent studies using lineage-tracing experiments indicate that both trabecular and compact myocardium contribute to generating the middle hybrid myocardial zone of the ventricular myocardium, although the myocytes from the compact layer contribute more than the trabecular cardiomyocytes [51]. Some coronary vessels in the myocardium seem to arise from an endocardial lineage, suggesting endocardial cells are trapped during trabecular coalescence [52].

Isl1, an important early cardiac transcription factor, was identified as one of the direct target genes of Jarid2 and up-regulated in *Jarid2*^{Nkx} hearts. *Isl1* expression is also

up-regulated in *Nkx2.5-Cre* mediated *PRC2* KO hearts [20], supporting functional cooperation between Jarid2 with PRC2 within the developing heart. *Isl1*-null mice are embryonic lethal at E10.5 with severe abnormalities in the heart [32]. However, the effect of *Isl1* overexpression within the heart remains unknown although *Isl1* overexpression enhances differentiation of ES cells into cardiac progenitors [53]. Isl1 is a marker of secondary heart field, but the recent studies indicate that Isl1 also expresses in the primary heart field [24, 53]. Although Isl1 expression is reduced around E10.5 during normal heart development, Isl1-positive cells have been reported as cardiac progenitors or nodal cells in embryonic and adult hearts [39]. Therefore, the overexpression of Isl1 in *Jarid2*^{Nkx} hearts may be indicative of myocardial differentiation defects or increased progenitor populations in the *Jarid2*^{Nkx} heart. Persistent expression of Isl1 may contribute to a failure of neuronal gene repression and/or an increase in conduction system-specific gene expression, rendering defective ventricular maturation. Although Bmp10 expression was increased in *Jarid2*^{Nkx} hearts, *Bmp10* promoter loci were not identified as Jarid2 targets by ChIP-chip, suggesting indirect regulation of *Bmp10* expression by Jarid2. Interestingly, *Bmp10* is also induced in *PRC2* KO hearts, but not directly regulated by PRC2 [20]. Since Bmp10 expression is restricted to the trabecular layer in the normal heart and critical for trabecular formation [38], it would be interesting to identify the regulatory mechanism of *Bmp10* expression.

In this study, we used whole heart extracts. The heart contains heterogeneous cell populations including fibroblasts and endothelial cells, but cardiomyocytes are a major cell type in the embryonic heart. Jarid2 expresses at a higher level in cardiomyocytes compared to other cell types in the embryonic heart [30], and the fibroblasts express very

low levels of Jarid2 [54]. As shown in Fig. 1, Jarid2 expression levels are significantly reduced in *Jarid2*^{Nkx} vs. control hearts. Thus, major molecular changes in *Jarid2*^{Nkx} hearts are likely to be detected using whole heart extracts.

In undifferentiated ES cells, many genes that are required for subsequent states of development are enriched with histones modified simultaneously for active transcription (H3K4me2/3) and PRC2-mediated repression (H3K27me3), which is referred to as being 'bivalent' [17]. This serves to prime undifferentiated cells to respond rapidly to lineage-dependent induction.

Histone methylation is tightly regulated in part by balancing functions of Jmj histone demethylases and SET domain containing histone methylases [3]. Moreover, the methylation status of H3K27 impacts on H3K4 methylation and vice versa [55, 56]. These cross talks are important for fine regulation of the histone methyl code, and developmental gene expression. Jarid2 may mediate H3K4 methylation as shown in Fig. 5*C*. It would be interesting to determine whether Jarid2 facilitates demethylation of H3K4 or inhibits methylation of H3K4. Jarid1B, a H3K4 demethylase, regulates mouse development by protecting developmental genes from inappropriate H3K4me3 accumulation such as neural master regulators [57]. Recently, de novo mutations identified in congenital heart disease patients are mainly in histone modifying genes [4]. In particular, five genes encode proteins that regulate H3K4me3 including Jarid1B, highlighting the importance of H3K4 methylation status during heart development.

Deletion of *Ezh2* in the secondary heart field causes postnatal myocardial pathology and destabilizes cardiac gene expression with the activation of Six1 [58]. This work suggests that epigenetic dysregulation in embryonic progenitor cells is a

predisposing factor for adult disease and dysregulated stress responses. Since our data indicate that Jarid2 regulates only a subset of targets through PRC2 in the developing heart, other target genes of Jarid2 should be regulated by different mechanisms. Indeed, Jarid2 regulates other target gene expression via interaction with Setdb1 by depositing H3K9me3 epigenetic marks during heart and immune cell development [8, 59]. Jarid2 also interacts with long non-coding RNAs (lncRNAs) such as MEG3 for proper recruitment of PRC2 at target genes in pluripotent stem cells or with Xist lncRNA for X chromosome inactivation [60]. Thus, complex epigenetic regulatory mechanisms exist to confer distinct roles of Jarid2 in different developmental processes. Together, our results indicate that Jarid2 is necessary during a narrow developmental window to establish correct epigenetics on the target genomic loci, which is prior to differentiation of cardiac progenitors into cardiomyocytes. Once cardiac progenitors are differentiated to cardiomyocytes, Jarid2 appears dispensable for cardiac morphogenesis. It would be interesting to determine whether the cardiac progenitors at early stages around E7.5 already show an elevated neuronal profile in the *Jarid2*^{Nkx} mice.

Materials and Methods

Animal husbandry and genotyping

All the mice were housed at the animal facility in accordance with University of Wisconsin Research Animal Resource Center policies and the National Institutes of Health (NIH) *Guide for the Care and Use of Laboratory Animals*. All animal research has been reviewed and approved by an Institutional Animal Care and Use Committee (protocol M005971). All mice were littermate or age-matched control and mutants. Studies were not blinded. Herein, *Jarid2* conditional deletion mice using *Nkx2.5*-Cre Knock in mice [21], *Nkx2.5-Cre/+;Jarid2f/f*, are designated as *Jarid2*^{Nkx}. To generate *Jarid2*^{Nkx} mice, females with floxed *Jarid2* alleles (*Jarid2f/f*) [61] were mated with *Nkx2.5-Cre/+;Jarid2f/+* males. *cTnt*-Cre mice (Jackson lab) were employed to delete *Jarid2* in differentiated cardiomyocytes (*cTnt-Cre/+;Jarid2f/f*), designated as *Jarid2*^{cTnt}. Embryos were isolated from timed-mated females at E9.5-19.5 days postcoitum. All mice employed in this study were bred to a mixed 129/Svj and C57BL/6 genetic background, and genotyping was performed as described previously [61].

Western blotting, coimmunoprecipitation and primary cultures of cardiomyocytes

To determine the protein levels, Western blotting was performed using embryonic heart extracts, as described previously [19]. The primary antibodies used were anti-Jarid2 peptide antibodies [19], anti-Isl1 (DSHB), anti-Phospho-Smad 1/5/8 (CST), or anti-GAPDH (EMD) followed by HRP conjugated secondary antibodies (Santa Cruz). Protein bands were detected by chemiluminescence (Thermo Fisher) and quantitated with NIH

Image J. Coimmunoprecipitation was performed as described [8]. Briefly, precleared nuclear extracts from E15.5 hearts were immunoprecipitated with nonspecific rabbit IgG or Jarid2 antibody, followed by incubation with protein A/G agarose beads (Santa Cruz), SDS-PAGE, and Western blotting with Ezh2 antibody (CST). Primary cultures of embryonic hearts at E15.5 were prepared as described [62], yielding about 70 % cardiomyocytes under our culture conditions. The cells on coverslips were subjected to co-immunostaining using Jarid2 with PECAM (BD) or MF20 (DSHB) antibodies.

In situ hybridization, histology, and immunohistochemistry

In situ hybridization was performed to examine the expression pattern of *Bmp10* mRNA in mouse embryonic hearts. Section *in situ* at E13.5 was carried out using digoxigenin-UTP-labeled antisense cRNA probes (Roche) as described [19]. Bmp10-C1/pSK(+) plasmid was obtained from Dr. W. Shou [20].

Hematoxylin and eosin (H&E) staining was performed as described [9]. Immunohistochemistry was performed on paraffin-embedded sections as described [19]. Briefly, tissue sections were incubated with primary antibodies, anti-Jarid2, anti-MF20, anti-Ki67(Abcam), or anti-P-H3 (EMD). Alexa dye-conjugated secondary antibodies (Thermo Fisher) or Biotin (Sigma)/Streptavidin-HRP (Thermo Fisher) systems with DAB substrate kit (Vector Laboratories) were used for visualization. Hoechst dye was used for the counter-staining of nuclei. Images were taken using a Zeiss Axiovert 200 microscope and an AxoiCam HRc camera. Alcian blue staining for cardiac jelly and Masson's trichrome staining for collagen were performed as described [9, 63].

Quantitative chromatin immunoprecipitation (qChIP) and ChIP-chip assays

qChIP experiments were performed as described previously [8]. All the experiments were repeated in duplicate at least three times on E14.5 control and *Jaird2*^{Nkx} hearts with pre-immune serum, Jarid2, Ezh2 (CST), H3K27me3 (EMD) or H3K4me3 (EMD) antibody. For the amplification of the *Isl1* locus, the following primers were used: -4Kb F, 5'-caaagattccggagaaaggaatg-3'; -4Kb R, 5'-gagttcaggtggttgtttctgtcat-3'; -2.7Kb F, 5'-gaagtccaattttgacaggagagtgt-3'; -2.7Kb R, 5'-cctcttg-tgttcaatgagggatt-3'; -0.5Kb F, 5'-gttccaagtgccccccttt-3'; -0.5Kb R, 5'-agtagctggtgggtaggtccttc-3'; +2Kb F, 5'-gaattagacagagcagatcaaattgc-3'; +2Kb R, 5'-ccaattgttcgcagacagatga-3'; +5Kb F, 5'-ttttaaaaaggagcctgcctctt-3'; and +5Kb R, 5'-caccaaatcacgtagaatgaatgg-3'.

ChIP-chip for H3K27me3 was performed as we described [8, 64]. Briefly, sonicated chromatin from 20 pooled E17.5 fixed hearts was immunoprecipitated using H3K27me3 antibody, followed by the reversal of cross-linking and DNA purification. Immuno-enriched DNA targets were amplified by whole genome amplification and fluorescently labeled, which were then hybridized onto the Roche NimbleGen 3X720K RefSeq promoter arrays and scanned with an Axon 4000B. After the arrays were extracted using Nimblescan (Roche), global and local normalization and data smoothing in R was performed, and peaks were detected using ChIPOIte [64] and in-house algorithms. Peaks with a *p* value less than 10^{-14} were used for analyses.

Reporter gene assays, and quantitative real time PCR (qRT-PCR)

Reporter gene assays were performed as described previously [19]. An Isl1 reporter plasmid containing the Jarid2 occupied region (-0.5Kb region) was

constructed by subcloning the *Isl1* locus from -0.9Kb to +0.15Kb of the transcriptional start site into the pGL3 basic vector (Promega). A reporter plasmid lacking the Jarid2 occupied region was constructed by subcloning a region from -0.12Kb to +0.15Kb into the pGL3 basic vector. The reporter vector (100 ng) was transfected into 10T1/2 cells in a 24-well plate. Jarid2 or Jarid2 mutants in pcDNA3.1-HisB-Xpress [42] were co-transfected with or without EED/pCDH, or EZH2/pCDH (from Dr. P. Lewis) using Lipofectamine 2000 (Thermo Fisher). Luciferase assays were performed two days after transfection using the luciferase assay system (Promega). A ß-galactosidase-CMV vector was used for normalizing the luciferase activity. The Jarid2 mutant constructs have been characterized in detail [42, 65], and they were expressed equally well when transfected as previously reported (Fig. A1-7*B*). Thus, differences in their transcriptional activities are not caused by different expression levels of the mutants.

qRT-PCR was performed as we described [19]. Briefly, mRNAs extracted from embryonic hearts were reverse transcribed to cDNA followed by qRT-PCR using FastStart SYBR Green Master (Roche) on a BioRad iCycler. The appropriate primers for each gene are listed in Table A2-7. All primers were thoroughly evaluated by melt curve analysis to ensure the amplification of a single, desired amplicon. All samples were assayed in duplicate with nearly identical replicate values. Data were generated using the standard curve method and normalized to 18S expression. qRT-PCR data were analyzed by the RQ analysis algorithm (BioRad).

Statistical analysis

Data represent the average of 3 to 5 replicates and standard error of the mean.

The replicate numbers are indicated in the text. Significance was tested by the student's *t*-test for 2 groups, *, p≤0.05; **, p≤0.01.

Acknowledgments: We thank Drs. Weinian Shou, Peter Lewis for generously providing Bmp10 *in situ* probe, and EZH2 and EED in expression vector, respectively. We thank Dr. Chad Vezina for technical assistance for *in situ* hybridization.

References

1 Benjamin EJ, Blaha MJ, Chiuve SE, Cushman M, Das SR, Deo R, de Ferranti SD, Floyd J, Fornage M, Gillespie C, Isasi CR, Jimenez MC, Jordan LC, Judd SE, Lackland D, Lichtman JH, Lisabeth L, Liu S, Longenecker CT, Mackey RH, Matsushita K, Mozaffarian D, Mussolino ME, Nasir K, Neumar RW, Palaniappan L, Pandey DK, Thiagarajan RR, Reeves MJ, Ritchey M, Rodriguez CJ, Roth GA, Rosamond WD, Sasson C, Towfighi A, Tsao CW, Turner MB, Virani SS, Voeks JH, Willey JZ, Wilkins JT, Wu JH, Alger HM, Wong SS, Muntner P, American Heart Association Statistics C, Stroke Statistics S: Heart Disease and Stroke Statistics-2017 Update: A Report From the American Heart Association. Circulation 2017;135:e146-e603.

2 Greer EL, Shi Y: Histone methylation: a dynamic mark in health, disease and inheritance. Nat Rev Genet 2012;13:343-357.

3 Dimitrova E, Turberfield AH, Klose RJ: Histone demethylases in chromatin biology and beyond. EMBO Rep 2015;16:1620-1639.

4 Zaidi S, Choi M, Wakimoto H, Ma L, Jiang J, Overton JD, Romano-Adesman A, Bjornson RD, Breitbart RE, Brown KK, Carriero NJ, Cheung YH, Deanfield J, DePalma S, Fakhro KA, Glessner J, Hakonarson H, Italia MJ, Kaltman JR, Kaski J, Kim R, Kline JK, Lee T, Leipzig J, Lopez A, Mane SM, Mitchell LE, Newburger JW, Parfenov M, Pe'er I, Porter G, Roberts AE, Sachidanandam R, Sanders SJ, Seiden HS, State MW, Subramanian S, Tikhonova IR, Wang W, Warburton D, White PS, Williams IA, Zhao H, Seidman JG, Brueckner M, Chung WK, Gelb BD, Goldmuntz E, Seidman CE, Lifton RP: De novo mutations in histone-modifying genes in congenital heart disease. Nature 2013;498:220-223.

5 Johansson C, Tumber A, Che K, Cain P, Nowak R, Gileadi C, Oppermann U: The roles of Jumonji-type oxygenases in human disease. Epigenomics 2014;6:89-120.

6 Jung J, Mysliwiec MR, Lee Y: Roles of JUMONJI in mouse embryonic development. Developmental dynamics : an official publication of the American Association of Anatomists 2005;232:21-32.

7 Shen X, Kim W, Fujiwara Y, Simon MD, Liu Y, Mysliwiec MR, Yuan GC, Lee Y, Orkin SH: Jumonji modulates polycomb activity and self-renewal versus differentiation of stem cells. Cell 2009;139:1303-1314.

8 Mysliwiec MR, Carlson CD, Tietjen J, Hung H, Ansari AZ, Lee Y: Jarid2 (Jumonji, AT rich interactive domain 2) regulates NOTCH1 expression via histone modification in the developing heart. J Biol Chem 2012;287:1235-1241.

9 Lee Y, Song AJ, Baker R, Micales B, Conway SJ, Lyons GE: Jumonji, a nuclear protein that is necessary for normal heart development. Circ Res 2000;86:932-

938.

10 Takeuchi T, Kojima M, Nakajima K, Kondo S: jumonji gene is essential for the neurulation and cardiac development of mouse embryos with a C3H/He background. Mech Dev 1999;86:29-38.

11 Towbin JA, Lorts A, Jefferies JL: Left ventricular non-compaction cardiomyopathy. Lancet 2015;386:813-825.

12 Zhang W, Chen H, Qu X, Chang CP, Shou W: Molecular mechanism of ventricular trabeculation/compaction and the pathogenesis of the left ventricular noncompaction cardiomyopathy (LVNC). Am J Med Genet C Semin Med Genet 2013;163C:144-156.

13 Chen H, Zhang W, Li D, Cordes TM, Mark Payne R, Shou W: Analysis of ventricular hypertrabeculation and noncompaction using genetically engineered mouse models. Pediatr Cardiol 2009;30:626-634.

14 Stankunas K, Hang CT, Tsun ZY, Chen H, Lee NV, Wu JI, Shang C, Bayle JH, Shou W, Iruela-Arispe ML, Chang CP: Endocardial Brg1 represses ADAMTS1 to maintain the microenvironment for myocardial morphogenesis. Dev Cell 2008;14:298-311.

15 Peng JC, Valouev A, Swigut T, Zhang J, Zhao Y, Sidow A, Wysocka J: Jarid2/Jumonji coordinates control of PRC2 enzymatic activity and target gene occupancy in pluripotent cells. Cell 2009;139:1290-1302.

16 Landeira D, Sauer S, Poot R, Dvorkina M, Mazzarella L, Jorgensen HF, Pereira CF, Leleu M, Piccolo FM, Spivakov M, Brookes E, Pombo A, Fisher C, Skarnes WC, Snoek T, Bezstarosti K, Demmers J, Klose RJ, Casanova M, Tavares L, Brockdorff N, Merkenschlager M, Fisher AG: Jarid2 is a PRC2 component in embryonic stem cells required for multi-lineage differentiation and recruitment of PRC1 and RNA Polymerase II to developmental regulators. Nature cell biology 2010;12:618-624.

17 Jones A, Wang H: Polycomb repressive complex 2 in embryonic stem cells: an overview. Protein & cell 2010;1:1056-1062.

18 Vizan P, Beringer M, Ballare C, Di Croce L: Role of PRC2-associated factors in stem cells and disease. FEBS J 2015;282:1723-1735.

19 Mysliwiec MR, Bresnick EH, Lee Y: Endothelial Jarid2/Jumonji is required for normal cardiac development and proper Notch1 expression. J Biol Chem 2011;286:17193-17204.

20 He A, Ma Q, Cao J, von Gise A, Zhou P, Xie H, Zhang B, Hsing M, Christodoulou

DC, Cahan P, Daley GQ, Kong SW, Orkin SH, Seidman CE, Seidman JG, Pu WT: Polycomb repressive complex 2 regulates normal development of the mouse heart. Circ Res 2012;110:406-415.

21 Moses KA, DeMayo F, Braun RM, Reecy JL, Schwartz RJ: Embryonic expression of an Nkx2-5/Cre gene using ROSA26 reporter mice. Genesis 2001;31:176-180.

22 Jiao K, Kulessa H, Tompkins K, Zhou Y, Batts L, Baldwin HS, Hogan BL: An essential role of Bmp4 in the atrioventricular septation of the mouse heart. Genes Dev 2003;17:2362-2367.

23 Agah R, Frenkel PA, French BA, Michael LH, Overbeek PA, Schneider MD: Gene recombination in postmitotic cells. Targeted expression of Cre recombinase provokes cardiac-restricted, site-specific rearrangement in adult ventricular muscle in vivo. J Clin Invest 1997;100:169-179.

24 Ma Q, Zhou B, Pu WT: Reassessment of Isl1 and Nkx2-5 cardiac fate maps using a Gata4-based reporter of Cre activity. Developmental biology 2008;323:98-104.

25 Chen D, Wang X, Liang D, Gordon J, Mittal A, Manley N, Degenhardt K, Astrof S: Fibronectin signals through integrin α5β1 to regulate cardiovascular development in a cell type-specific manner. Dev Biol 2015;407:195-210.

26 Ffrench-Constant C, Hynes RO: Patterns of fibronectin gene expression and splicing during cell migration in chicken embryos. Development 1988;104:369-382.

27 Lockhart M, Wirrig E, Phelps A, Wessels A: Extracellular matrix and heart development. Birth defects research Part A, Clinical and molecular teratology 2011;91:535-550.

28 Nandadasa S, Foulcer S, Apte SS: The multiple, complex roles of versican and its proteolytic turnover by ADAMTS proteases during embryogenesis. Matrix Biol 2014;35:34-41.

29 Leavesley DI, Kashyap AS, Croll T, Sivaramakrishnan M, Shokoohmand A, Hollier BG, Upton Z: Vitronectin--master controller or micromanager? IUBMB life 2013;65:807-818.

30 Jung J, Kim TG, Lyons GE, Kim HR, Lee Y: Jumonji regulates cardiomyocyte proliferation via interaction with retinoblastoma protein. J Biol Chem 2005;280:30916-30923.

31 Pasini D, Cloos PA, Walfridsson J, Olsson L, Bukowski JP, Johansen JV, Bak M, Tommerup N, Rappsilber J, Helin K: JARID2 regulates binding of the Polycomb repressive complex 2 to target genes in ES cells. Nature 2010;464:306-310.

32 Cai CL, Liang X, Shi Y, Chu PH, Pfaff SL, Chen J, Evans S: Isl1 identifies a cardiac progenitor population that proliferates prior to differentiation and contributes a majority of cells to the heart. Dev Cell 2003;5:877-889.

33 Lu H, Li Y, Wang Y, Liu Y, Wang W, Jia Z, Chen P, Ma K, Zhou C: Wnt-promoted Isl1 expression through a novel TCF/LEF1 binding site and H3K9 acetylation in early stages of cardiomyocyte differentiation of P19CL6 cells. Mol Cell Biochem 2014;391:183-192.

34 Li Y, Yu W, Cooney AJ, Schwartz RJ, Liu Y: Brief report: Oct4 and canonical Wnt signaling regulate the cardiac lineage factor Mesp1 through a Tcf/Lef-Oct4 composite element. Stem Cells 2013;31:1213-1217.

35 Zhang CG, Jia ZQ, Li BH, Zhang H, Liu YN, Chen P, Ma KT, Zhou CY: beta-Catenin/TCF/LEF1 can directly regulate phenylephrine-induced cell hypertrophy and Anf transcription in cardiomyocytes. Biochemical and biophysical research communications 2009;390:258-262.

36 Morita Y, Andersen P, Hotta A, Tsukahara Y, Sasagawa N, Hayashida N, Koga C, Nishikawa M, Saga Y, Evans SM, Koshiba-Takeuchi K, Nishinakamura R, Yoshida Y, Kwon C, Takeuchi JK: Sall1 transiently marks undifferentiated heart precursors and regulates their fate. Journal of molecular and cellular cardiology 2016;92:158-162.

37 Miller EM, Hopkin R, Bao L, Ware SM: Implications for genotype-phenotype predictions in Townes-Brocks syndrome: case report of a novel SALL1 deletion and review of the literature. Am J Med Genet A 2012;158A:533-540.

38 Huang J, Elicker J, Bowens N, Liu X, Cheng L, Cappola TP, Zhu X, Parmacek MS: Myocardin regulates BMP10 expression and is required for heart development. J Clin Invest 2012;122:3678-3691.

39 Laugwitz KL, Moretti A, Caron L, Nakano A, Chien KR: Islet1 cardiovascular progenitors: a single source for heart lineages? Development 2008;135:193-205.

40 Christoffels VM, Smits GJ, Kispert A, Moorman AF: Development of the pacemaker tissues of the heart. Circ Res 2010;106:240-254.

41 Liang X, Zhang Q, Cattaneo P, Zhuang S, Gong X, Spann NJ, Jiang C, Cao X, Zhao X, Zhang X, Bu L, Wang G, Chen HS, Zhuang T, Yan J, Geng P, Luo L, Banerjee I, Chen Y, Glass CK, Zambon AC, Chen J, Sun Y, Evans SM: Transcription factor ISL1 is essential for pacemaker development and function. J Clin Invest 2015;125:3256-3268.

42 Kim TG, Kraus JC, Chen J, Lee Y: JUMONJI, a critical factor for cardiac

development, functions as a transcriptional repressor. J Biol Chem 2003;278:42247-42255.

43 McFadden DG, Barbosa AC, Richardson JA, Schneider MD, Srivastava D, Olson EN: The Hand1 and Hand2 transcription factors regulate expansion of the embryonic cardiac ventricles in a gene dosage-dependent manner. Development 2005;132:189-201.

44 Ilagan R, Abu-Issa R, Brown D, Yang YP, Jiao K, Schwartz RJ, Klingensmith J, Meyers EN: Fgf8 is required for anterior heart field development. Development 2006;133:2435-2445.

45 Panzer AA, Regmi SD, Cormier D, Danzo MT, Chen ID, Winston JB, Hutchinson AK, Salm D, Schulkey CE, Cochran RS, Wilson DB, Jay PY: Nkx2-5 and Sarcospan genetically interact in the development of the muscular ventricular septum of the heart. Sci Rep 2017;7:46438.

46 Terada R, Warren S, Lu JT, Chien KR, Wessels A, Kasahara H: Ablation of Nkx2-5 at mid-embryonic stage results in premature lethality and cardiac malformation. Cardiovasc Res 2011;91:289-299.

47 Chen H, Shi S, Acosta L, Li W, Lu J, Bao S, Chen Z, Yang Z, Schneider MD, Chien KR, Conway SJ, Yoder MC, Haneline LS, Franco D, Shou W: BMP10 is essential for maintaining cardiac growth during murine cardiogenesis. Development 2004;131:2219-2231.

48 Chen H, Zhang W, Sun X, Yoshimoto M, Chen Z, Zhu W, Liu J, Shen Y, Yong W, Li D, Zhang J, Lin Y, Li B, VanDusen NJ, Snider P, Schwartz RJ, Conway SJ, Field LJ, Yoder MC, Firulli AB, Carlesso N, Towbin JA, Shou W: Fkbp1a controls ventricular myocardium trabeculation and compaction by regulating endocardial Notch1 activity. Development 2013;140:1946-1957.

49 Luxán G, Casanova JC, Martínez-Poveda B, Prados B, D'Amato G, MacGrogan D, Gonzalez-Rajal A, Dobarro D, Torroja C, Martinez F, Izquierdo-García JL, Fernández-Friera L, Sabater-Molina M, Kong YY, Pizarro G, Ibañez B, Medrano C, García-Pavía P, Gimeno JR, Monserrat L, Jiménez-Borreguero LJ, de la Pompa JL: Mutations in the NOTCH pathway regulator MIB1 cause left ventricular noncompaction cardiomyopathy. Nat Med 2013;19:193-201.

50 Li D, Hallett MA, Zhu W, Rubart M, Liu Y, Yang Z, Chen H, Haneline LS, Chan RJ, Schwartz RJ, Field LJ, Atkinson SJ, Shou W: Dishevelled-associated activator of morphogenesis 1 (Daam1) is required for heart morphogenesis. Development 2011;138:303-315.

51 Tian X, Li Y, He L, Zhang H, Huang X, Liu Q, Pu W, Zhang L, Zhao H, Wang Z, Zhu J, Nie Y, Hu S, Sedmera D, Zhong TP, Yu Y, Yan Y, Qiao Z, Wang QD, Wu

SM, Pu WT, Anderson RH, Zhou B: Identification of a hybrid myocardial zone in the mammalian heart after birth. Nat Commun 2017;8:87.

52 Tian X, Hu T, Zhang H, He L, Huang X, Liu Q, Yu W, Yang Z, Yan Y, Yang X, Zhong TP, Pu WT, Zhou B: Vessel formation. De novo formation of a distinct coronary vascular population in neonatal heart. Science 2014;345:90-94.

53 Dorn T, Goedel A, Lam JT, Haas J, Tian Q, Herrmann F, Bundschu K, Dobreva G, Schiemann M, Dirschinger R, Guo Y, Kuhl SJ, Sinnecker D, Lipp P, Laugwitz KL, Kuhl M, Moretti A: Direct nkx2-5 transcriptional repression of isl1 controls cardiomyocyte subtype identity. Stem Cells 2015;33:1113-1129.

54 Zhang Z, Jones A, Sun CW, Li C, Chang CW, Joo HY, Dai Q, Mysliwiec MR, Wu LC, Guo Y, Yang W, Liu K, Pawlik KM, Erdjument-Bromage H, Tempst P, Lee Y, Min J, Townes TM, Wang H: PRC2 complexes with JARID2, MTF2, and esPRC2p48 in ES cells to modulate ES cell pluripotency and somatic cell reprogramming. Stem Cells 2011;29:229-240.

55 Schmitges FW, Prusty AB, Faty M, Stützer A, Lingaraju GM, Aiwazian J, Sack R, Hess D, Li L, Zhou S, Bunker RD, Wirth U, Bouwmeester T, Bauer A, Ly-Hartig N, Zhao K, Chan H, Gu J, Gut H, Fischle W, Müller J, Thomä NH: Histone methylation by PRC2 is inhibited by active chromatin marks. Mol Cell 2011;42:330-341.

56 Kim DH, Tang Z, Shimada M, Fierz B, Houck-Loomis B, Bar-Dagen M, Lee S, Lee SK, Muir TW, Roeder RG, Lee JW: Histone H3K27 trimethylation inhibits H3 binding and function of SET1-like H3K4 methyltransferase complexes. Mol Cell Biol 2013;33:4936-4946.

57 Albert M, Schmitz SU, Kooistra SM, Malatesta M, Morales Torres C, Rekling JC, Johansen JV, Abarrategui I, Helin K: The histone demethylase Jarid1b ensures faithful mouse development by protecting developmental genes from aberrant H3K4me3. PLoS Genet 2013;9:e1003461.

58 Delgado-Olguin P, Huang Y, Li X, Christodoulou D, Seidman CE, Seidman JG, Tarakhovsky A, Bruneau BG: Epigenetic repression of cardiac progenitor gene expression by Ezh2 is required for postnatal cardiac homeostasis. Nature genetics 2012;44:343-347.

59 Pereira RM, Martinez GJ, Engel I, Cruz-Guilloty F, Barboza BA, Tsagaratou A, Lio CW, Berg LJ, Lee Y, Kronenberg M, Bandukwala HS, Rao A: Jarid2 is induced by TCR signalling and controls iNKT cell maturation. Nat Commun 2014;5:4540.

60 da Rocha ST, Boeva V, Escamilla-Del-Arenal M, Ancelin K, Granier C, Matias NR, Sanulli S, Chow J, Schulz E, Picard C, Kaneko S, Helin K, Reinberg D, Stewart AF, Wutz A, Margueron R, Heard E: Jarid2 Is Implicated in the Initial Xist-Induced

Targeting of PRC2 to the Inactive X Chromosome. Mol Cell 2014;53:301-316.

61 Mysliwiec MR, Chen J, Powers PA, Bartley CR, Schneider MD, Lee Y: Generation of a conditional null allele of jumonji. Genesis 2006;44:407-411.

62 Brody MJ, Cho E, Mysliwiec MR, Kim TG, Carlson CD, Lee KH, Lee Y: Lrrc10 is a novel cardiac-specific target gene of Nkx2-5 and GATA4. Journal of molecular and cellular cardiology 2013;62:237-246.

63 Brody MJ, Hacker TA, Patel JR, Feng L, Sadoshima J, Tevosian SG, Balijepalli RC, Moss RL, Lee Y: Ablation of the cardiac-specific gene leucine-rich repeat containing 10 (lrrc10) results in dilated cardiomyopathy. PloS one 2012;7:e51621.

64 Tietjen JR, Zhang DW, Rodriguez-Molina JB, White BE, Akhtar MS, Heidemann M, Li X, Chapman RD, Shokat K, Keles S, Eick D, Ansari AZ: Chemical-genomic dissection of the CTD code. Nature structural & molecular biology 2010;17:1154-1161.

65 Mysliwiec MR, Kim TG, Lee Y: Characterization of zinc finger protein 496 that interacts with Jumonji/Jarid2. FEBS Lett 2007;581:2633-2640.

Chapter 3

Myocardial-specific ablation of *Jarid2* leads to dilated cardiomyopathy in mice

Eunjin Cho, HyunJun Kang, Dae-Ki Kang, Timothy A. Hacker, and Youngsook Lee

Abstract

Cardiomyopathy is a common human disorder leading to disability and sudden death. However, the molecules and precise mechanisms causing cardiomyopathy are not fully clarified. In this study, we investigated myocardial-specific deletion of *Jarid2* (*Jarid2*$^{\alpha MHC}$) using *αMHC*-Cre mice. Jarid2 is a critical cardiac factor in embryonic heart development, but the function of Jarid2 in the adult heart remains to be elucidated. *Jarid2*$^{\alpha MHC}$ mice exhibited no overt defects during cardiac development and survived to adulthood. However, *Jarid2*$^{\alpha MHC}$ mice developed dilated cardiomyopathy and revealed premature death. We performed RNA-seq analyses at different stages, postnatal day 10 and 7 months of age, to determine functions of Jarid2 in the adult heart. In the *Jarid2*$^{\alpha MHC}$ heart, heart failure-related genes including *Ankrd1* and *Gyg* were up-regulated, and fetal genes, such as *Tnni1* and *Acta2*, were continuously increased during adult stages. We suggest that Jarid2 is necessary to repress immature contractile gene expression in neonatal stages and that ErbB4 signaling is involved in the repression process. Importantly, this study demonstrates that Jarid2 is essential in the postnatal heart.

Introduction

Heart failure is a major cause of mortality, presenting in 40 million people globally [1]. Prolonged exposure to pathological and physiological stresses in the adult myocardium triggers adaptive responses, including the disruption of transcriptional homeostasis. As adaptive responses, the fetal gene program re-emerges, bringing with it fetal metabolism and the use of glycolysis and carbohydrate substrates for ATP generation. Persistent volume overload induces axial cardiomyocyte lengthening and chamber dilation, known as eccentric or dilated cardiomyopathy (DCM), resulting in reduced systolic function [2]. In contrast, pressure overload incudes radial cardiomyocyte widening and ventricular wall thickening, resulting in concentric or hypertrophic cardiomyopathy (HCM) with diastolic dysfunction [3]. DCM and HCM are the most common forms of cardiomyopathy that can lead to heart failure and sudden death [4]. Inherited HCM and DCM can occur by mutations in the genes encoding sarcomeric proteins, which regulate tension and subsequent contraction through excitation-contraction coupling [2]. Many mutations in sarcomere genes, such as *myosin heavy chain 7* (*Myh7*, βMHC), *tropomyosin 1* (*Tpm1*) and *cardiac troponin T* (*Tnnt2*) cause both DCM and HCM. However, molecular causes of DCM are more heterogenous than HCM [5-7], including not only sarcomeric proteins, but also cytoskeletal and nuclear membrane proteins [8]. Thus, the molecular and cellular mechanisms underlying DCM are not fully understood.

Cardiomyocytes undergo dramatic molecular, physiological and developmental changes during the first two weeks after birth (herein, referred to as a ‘neonatal’ period),

to generate mature functioning cardiomyocytes [9, 10]. These changes include the regulation of gene expression, and isoform switching from fetal to adult forms, which are involved in contractility, calcium handling, energy utilization, and cell proliferation. Various genes that are highly expressed in utero become down-regulated or vice versa during perinatal and neonatal stages. Cytoskeletal and sarcomeric genes required for optimal contraction, and calcium handling genes required for exquisite calcium sensitivity and EC coupling, often switch from fetal to adult forms. In the mouse ventricle, βMHC is the predominant isoform during fetal stages and is replaced by αMHC after birth [9]. Expression of metabolic genes responsible for glycolytic process is decreased, whereas oxidative and fatty acid metabolisms are induced in the normal postnatal heart. The metabolic shift is to support a high-energy demand due to increased cardiac output. Mitochondrial density increases as the metabolic rate increases [11]. Cardiomyocyte proliferation in mice ceases during the neonatal period, and physiological hypertrophic growth occurs [12]. However, it is poorly understood how fundamental transition and molecular mechanisms are integrated and coordinated during neonatal stages.

Neuregulin (Nrg) is a ligand for the epidermal growth factor receptor family. Nrgs are made from alternative spliced transcriptions, and proteins are secreted from the endocardium/endothelial cells by matrix metalloproteases [13]. The membrane-bound tyrosine kinase receptors ErbB2 and ErbB4 are expressed in the cardiomyocytes during embryonic and postnatal stages. Nrg1 and its receptors have crucial roles in cardiac development and maintenance of cardiac function in the adult heart [14]. Nrg1-ErbB signaling activates Akt, Erk, or Jnk pathways required for cell maintenance, growth, and survival. [15]. Nrg1 and recombinant Nrg1 have been investigated for heart failure

treatment based on the evidence that Nrg1 improves heart function and prevents cardiac fibrosis in animal models [15]. However, it is unclear how Nrg1-ErbB signaling is regulated in the heart.

Jarid2 is required for normal embryonic development. Knockout (KO) of *Jarid2* in mice causes developmental defects in the brain, heart, liver or hematopoietic tissues and lethality [16]. Endothelial/endocardial-specific deletion of *Jarid2* shows cardiac defects recapitulating in *Jarid2* knockout mice [17]. Early deletion of *Jarid2* in the myocardium using *Nkx2.5*-Cre mice leads to cardiac defects and death within one day after birth, but *Jarid2* deletion in the differentiated myocardium does not exhibit abnormalities in mice [18]. During development, Jarid2 functions as an epigenetic regulator by interacting with methyltransferase enzymes [19]. Jarid2 is a component of Polycomb repressive complex 2 (PRC2), a methyltransferase of histone H3 lysine 27 (H3K27) in embryonic stem cells for an efficient accumulation of PRC2 on the chromatin. We have demonstrated that Jarid2 and PRC2 accumulate on the *Isl1* promoter during embryonic heart development and repress Isl1 expression [18]. Moreover, Jarid2 recruits Setdb1 on the *Notch1* promoter and represses Notch1 expression via H3K9 methylation in endothelial/endocardial cells of the developing heart [20]. Thus, Jarid2 functions as a transcriptional repressor in part by recruiting histone modifying enzymes such as PRC2 or Setdb1, regulating methylation of H3K27 or H3K9, respectively. In addition, Jarid2 can repress transcriptional activity of cardiac transcription factors, including Nkx2.5, GATA4 and Mef2 [19]. Although roles of Jarid2 have been studied in the embryonic heart, its function in the adult heart remains largely unknown. Interestingly, JARID2 expression is reduced in heart failure patients [21]. In mice, reduced Jarid2 expression is associated

with cardiac hypertrophy [22]. These studies imply potential roles of Jarid2 in the adult heart.

Here, we investigated the myocardial-specific function of Jarid2 in the adult heart by using *αMHC*-Cre mice (*Jarid2*$^{\alpha MHC}$). *Jarid2*$^{\alpha MHC}$ mice exhibited premature death at 7-9 months (m) of age with dilated cardiomyopathy. We performed gene expression profiling using RNA-seq analysis on postnatal day (p) 10 and 7m hearts to determine the role of Jarid2 before the onset of DCM as well as defective molecular pathways in DCM development, respectively. The neonatal heart from *Jarid2*$^{\alpha MHC}$ mice showed increased muscle contraction and heart developmental genes although the heart morphology was normal. Specifically, immature sarcomere genes, such as *troponin I type 1* (*Tnni1*) and *smooth muscle alpha-actin 2* (*Acta2*), and DCM-associated genes were up-regulated in *Jarid2*$^{\alpha MHC}$ hearts at p10. At 7m, pathways involved in collagen fibril organization and metabolic process were enriched in *Jarid2*$^{\alpha MHC}$ hearts. We identified sarcomere or their associated genes that were increased at 7m as compared to p10 in the normal heart. However, *Jarid2*$^{\alpha MHC}$ mice did not show increases in those genes for contractility such as *cardiac a-actin* (*Actc1*), *Myh6*, *Tnni3*, *Tnnt2*, *tropomyosin* (*Tpm1*), *myosin regulatory light chain* (*Myl2*) and *phospholamban* (*Pln*). In the *Jarid2*$^{\alpha MHC}$ heart, *Nrg1*, *ErbB4*, and *Ankrd1* expression levels were already dysregulated in the pre-DCM heart, which continued during DCM development. Therefore, Jarid2 is required for myocardial maturation after birth, and the early postnatal function of Jarid2 is critical for maintaining normal cardiac function later during adulthood.

Results

Generation of mice with cardiac-specific deletion of Jarid2

Jarid2 is indispensable for normal embryonic development including cardiac development [17, 18, 23]. However, cardiac-specific roles of Jarid2 in the adult heart remain to be elucidated. To understand the role of Jarid2 in the cardiomyocytes after birth, we generated *αMHC*-Cre;*Jarid2f/f* (*Jarid2*$^{\alpha MHC}$) mice, in which *αMHC*-Cre specifically inactivates the conditional *Jarid2fl* allele in differentiated cardiomyocytes [24, 25]. PCR analyses of genomic DANs isolated from the heart or tail showed that *Jarid2* was deleted only in the heart, but not in the tail of *Jarid2*$^{\alpha MHC}$ mice since a *Jarid2* floxed out band (354 bp) was detected only in the heart of *Jarid2*$^{\alpha MHC}$, but not in the control heart or in the tail (Fig. 3-1A). A faint *Jarid2f/f* band (1054 bp) likely indicates the *Jarid2f/f* allele from noncardiomyocytes in the heart of *Jarid2*$^{\alpha MHC}$. qRT-PCR data confirmed a reduction in *Jarid2* transcripts in *Jarid2*$^{\alpha MHC}$ vs. control hearts at p10 (Fig. 3-1B). Residual *Jarid2* mRNAs may be from noncardiac lineages such as endothelial cells, and fibroblasts. Immunostaining and Western blotting data also showed a marked reduction of Jarid2 levels in *Jarid2*$^{\alpha MHC}$ hearts (Fig. 3-1C and 1D). To examine Jarid2 levels in the heart at different stages, we performed X-gal staining on tissue sections from heterozygous *Jarid2* gene trapped mice, in which *LacZ e*xpression recapitulates endogenous *Jarid2* expression [23]. X-gal staining was readily detected in the ventricle of embryonic (e) and p10 hearts but was reduced at 1 and 4 m of age (Fig. 3-1E). Western blotting performed on different ages showed that Jarid2 expression was high until p2 but significantly reduced in the adult heart (Fig. 3-1F). These data indicate that Jarid2 continues to be

expressed in the neonatal heart followed by a marked decrease by 1-2 m of age, suggesting an important role of Jarid2 in the heart during neonatal stages.

Jarid2$^{\alpha MHC}$ hearts exhibited dilated cardiomyopathy and premature death

The *Jarid2*$^{\alpha MHC}$ mice showed an expected birth rate, and no gross morphological abnormalities in the embryonic [17] or young adult heart (Fig. A1-8A, Table A2-4). However, the mutant mice exhibited 100% mortality by 9 m (Fig. 3-2A), likely due to heart failure. Thus, *Jarid2*$^{\alpha MHC}$ hearts at 7 m were subjected to histological examination. The mutant heart was enlarged compared to controls at 7 m (Fig. 3-2B). H&E staining images showed similar ventricular wall or septal thickness but suggested the necrotic myocardium in the mutant heart (Fig. 3-2C). Apoptosis levels were marginally increased as indicated by cleaved-caspase 3 expression levels in mutant hearts compared to controls (Fig. A1-8B). The cross-sectional area (CSA) of cardiomyocytes was measured by wheat germ agglutinin (WGA) staining to demarcate plasma membrane boundaries in the ventricular wall (Fig. 3-2D). Although CSA in *Jarid2*$^{\alpha MHC}$ hearts seems larger as shown in Fig 3-2D, the average CSA (Fig. 3-2F, left) and a total number of cells in the same square area (Fig. A1-8C) were not significantly different between control and mutant hearts. However, percentages of the big (CSA>400um^2) or small cells (CSA<150um^2) were significantly increased in *Jarid2*$^{\alpha MHC}$ vs. control hearts (Fig. 3-2F, right), suggesting abnormal hypertrophic processes in *Jarid2*$^{\alpha MHC}$ hearts. Increased fibrosis was detected in mutant hearts compared to controls as indicated by PicroSirius red staining (Fig. 3-2E). We analyzed expression of a panel of cardiac failure markers by qRT-PCR. The mRNA expression levels of hypertrophic markers, *Nppa*, *Nppb*, *Myh7* and *Acta1* were normal at

3 m in *Jarid2*$^{\alpha MHC}$ hearts, but significantly increased at 7 m as compared to controls (Fig. 3-2G). These data suggest that *Jarid2*$^{\alpha MHC}$ mice do not exhibit heart failure at 3 m but progress to severe heart failure leading to premature death between 6-9 m of age.

Next, we investigated cardiac structural and functional parameters by echocardiography at 3 and 7 m of age (Table 3-1). *Jarid2*$^{\alpha MHC}$ mice at 7 m showed increases in left ventricular inner diameter at end diastole (LVID;d) and end systole (LVID;s), and LV mass/body weight ratios (Fig. 3-3A-3C). The dilation was not accompanied by an alternation in interventricular septal (LVAW) or posterior wall (LVPW) thickness, while left ventricular volumes were significantly increased at end diastole and end systole, indicating the enlarged and dilated left ventricle (Table 3-1). The H/R ratio (left ventricular wall thickness/chamber radius) was significantly reduced in *Jarid2*$^{\alpha MHC}$ vs. control hearts, indicating ventricular dilation. Decreases in ejection fraction (EF, Fig. 3-3D) and fractional shortening (FS, Fig. 3-3F) were detected at 7m, indicating defective cardiac contractility and DCM.

To determine the time-dependent changes in cardiac parameters of *Jarid2*$^{\alpha MHC}$ mice, echocardiography was performed at 3 m of age (Table 3-1). Interestingly, *Jarid2*$^{\alpha MHC}$ mice showed hyper-performing hearts as evidenced by the increases in stroke volume, cardiac output, EF, and FS (Fig. 3-3D-3F). However, left ventricular chamber dimensions remained similar to controls. Histological analyses of *Jarid2*$^{\alpha MHC}$ hearts at 3 m did not show morphological defects (Fig. A1-9). Thus far, our data indicate that *Jarid2*$^{\alpha MHC}$ mice exhibit hyper-performing compensating hearts at 3 m during young adult stages followed by decompensating pathological remodeling that progresses to DCM/heart failure by 6-7m of age. All together, we demonstrated for the first time that Jarid2 within the

myocardium is required for maintaining normal cardiac function in the adult heart.

Genome-wide analyses of gene expression profiling in the Jarid2$^{\alpha MHC}$ heart at neonatal stages

The heart undergoes crucial maturation processes during the first two weeks after birth to achieve normal adult cardiac morphology and function [11]. Jarid2 expression was significantly reduced by 1 m of age (Fig. 3-1), but *Jarid2*$^{\alpha MHC}$ mice did not show DCM/heart failure until much later. Thus, we reasoned that early defects during neonatal stages in the mutant heart may play critical roles in the initiation and progression to DCM later in life. We set out to determine molecular changes in *Jarid2*$^{\alpha MHC}$ hearts at p10, which will provide crucial information on the function of Jarid2 in the postnatal hearts as well as defective molecular pathways in the mutant heart that may be causal to DCM development. These analyses will also help determine critical mechanisms in preventing cardiomyopathy. The whole heart and H&E stained sections showed that *Jarid2*$^{\alpha MHC}$ hearts appeared normal compared to controls at p10 (Fig. 3-4A and 4B). The hypertrophic marker genes, *Nppa*, *Nppb*, *Myh7* and *Acta1* were unchanged in *Jarid2*$^{\alpha MHC}$ vs. control hearts (Fig. 3-4D). CSA (Fig. 3-4C) and cell proliferation by immunostaining of Ki67 or phospho-histone H3 (Fig. A1-8D) seemed normal in *Jarid2*$^{\alpha MHC}$ heart. Altogether, *Jarid2*$^{\alpha MHC}$ hearts present grossly normal phenotypes at p10.

Thus, *Jarid2*$^{\alpha MHC}$ hearts at p10 would provide an excellent opportunity to investigate the molecular function of Jarid2 in the postnatal heart as well as molecular etiology that causes DCM later before the onset of pathological remodeling or secondary compensatory process of the heart. We next determined gene expression profiling in

Jarid2$^{\alpha MHC}$ vs control hearts by performing RNA-seq at p10 (Fig. 3-5). We employed two different analysis methods, EBSeq (Fig. 3-5A) and DESeq2 (Fig. A1-10A) to determine differentially expressed (DE) genes between *Jarid2*$^{\alpha MHC}$ and control hearts [26]. As shown in Fig. 3-5B, 61 DE genes were identified by EBSeq analysis, whereas 20 DE genes were identified by DESeq2 analysis. First, we analyzed all 72 DE genes identified by either DESeq2 or EBSeq analysis (Table A2-5). The majority of DE genes (54 genes, 75%) were up-regulated in the absence of *Jarid2* at p10 (Fig. 3-5C, Table A2-5), likely reflecting the function of Jarid2 as a transcriptional repressor at neonatal stages. Gene ontology (GO) term analysis on biological process (BP) showed that organ morphogenesis, ion transmembrane transport, heart development, and muscle contraction were significantly dysregulated (Fig. 3-5C and 5D). The genes enriched in organ morphogenesis were involved mainly in non-cardiac organ development such as lung (*Irx1* and *Irx2*), neuron (*Ntn1*, *Cdh2* and *Gli1*), epidermal stem cell and intestinal stem cell (*Lrig1*), and kidney (*Wnk4*). These results suggest that other organ developmental genes are repressed by Jarid2 in the heart at neonatal stages. The genes enriched in heart development included the genes whose mutation is known to cause heart failure. Among the 54 up-regulated genes, the 5 genes (*Ankrd1, Abcc9, Actc1, Pln, and Gyg*) have been shown to be mutated in human DCM and HCM [2]. GO term analysis on cellular component (CC) showed myofibril, contractile fiber, sarcomere, and T-tubule at p10. These included increased contractility related genes (*Actc1, Slc8a1, Abcc9, Atp2a1, Ankrd1, Myl12a, Myl1* and *Tmod1*), which precede hyper-performing hearts at 3 m in *Jarid2*$^{\alpha MHC}$.

To determine potential targets of Jarid2, we overlapped 72 DE genes with Jarid2 ChIP-chip data [20], yielding 15 genes (Table A2-6). Among these, the promoter region

of *Gli1, Ttll1* and *Prph* were co-occupied by Jarid2 and H3K27 tri-methylation. Gli1, a zinc finger transcription factor, is a modulator and target of hedgehog signaling during embryo development [27]. Gli1 has been studied in the generation of vascular smooth muscle cells and regulation of fibrosis [28]. Prph is a type III intermediate filament protein presenting in neurons of the mammalian peripheral nervous system and neuroblastoma cells [29]. Ttll1 is a member of the tubulin tyrosine ligase superfamily that adds polyglutamylation to tubulin and other proteins for interaction and axoneme motility [30]. Tmem100 is a two-transmembrane protein expressing in endothelial cells and involved in endothelial differentiation and vascular morphogenesis [31]. *Tmem100* KO mice are embryonic lethal showing cardiovascular failure [32]. The sarcoplasmic reticulum calcium-ATPase (SERCA) is a major component of Ca2+ cycling in the diastole heart. Reduction of SERCA pump expression and activity has been linked to diastolic dysfunction in hypertrophied and failing hearts [33]. Although SERCA2a is the major cardiac-specific isoform, SERCA1a overexpression in the heart reveals faster Ca2+ transport kinetics by reduction in endogenous SERCA2a pump levels [33]. Thus, Increased *Atp2a1* (SERCA1a) levels in *Jarid2*$^{\alpha MHC}$ may impact on SERCA2a expression and thus Ca2+ uptake and cardiac contractility.

There were 7 DE genes identified by both EBSeq and DESeq2 analyses (Table 3-2). ADP-ribosylhydrolase like 1 (Adprhl1) is a member of the ADP-ribosylhydrolase (ARH) protein family which cleaves the ADP-ribose linkage with arginine side chains [34]. Although, Adprhl1 is enzymatically inactive, it is important for heart chamber outgrowth and myofibril assembly in Xenopus embryos [35]. The function of Adprhl1 in the mouse heart has not been studied, but elevated *Adprhl1* expression levels may lead to abnormal

orientation of myofibril or contractile defects in *Jarid2*$^{\alpha MHC}$ hearts. Glycogen is a primary form of energy storage in eukaryotes. Glycogenin (Gyg) is a glycosyltransferase that catalyzes the addition of glucose as a primer for glycogen synthesis [36]. *GYG1* deficiency has been associated with cardiomyopathies due to an abnormal storage material, polyglucosan in the heart [37]. The elevated *Gyg* and another up regulated gene, *glycogen branching enzyme 1* (*Gbe1*), in *Jarid2*$^{\alpha MHC}$ hearts suggest that the glucose metabolism may be altered. Sodium-calcium exchanger 1 (Slc8a1, NCX1) is an antiporter membrane protein, which maintains cytosolic Ca2+ homeostasis. NCX1 appears in sarcolemma and regulates the movement of Ca2+ across the sarcolemma to the extracellular space [38]. Dysregulation of *NCX1* in humans is observed in end-stage heart failure, and expression and function of NCX1 are increased during heart failure [38]. Therefore, increased *Slc8a1* expression in *Jarid2*$^{\alpha MHC}$ hearts may cause a disruption in Ca2+ homeostasis. Abcc9 is an ATP-binding cassette family member and encodes a membrane-associated receptor, SUR2 in the mitochondria and cell membrane. *ABCC9* mutation causes DCM in humans, and KO mice die in the neonatal period with progressive cardiac dysfunction and a failure to transition from fetal to mature myocardial metabolism [39]. Abcc9 expression is increased by low oxygen stress mediated by ERK or AKT signaling as a protective effect [40]. In *Jarid2*$^{\alpha MHC}$ hearts, elevated *Abcc9* levels may imply cardiac dysfunction or defective maturation. Sulfatase 2 (Sulf2) is an extracellular endosulfatase and removes the 6-O-sulfate from heparan sulfate. Heparan sulfate is a dynamic molecule in the extracellular matrix and involved in signaling by interacting with growth factors [41]. N-myc downstream regulated gene 4 (Ndrg4) is a cytoplasmic protein highly expressed in the brain and heart. Down regulation of Ndrg4

leads to hypoplastic hearts in zebrafish, and Ndrg4 expression is down-regulated by Tbx2 in mice [42, 43]. In our RNA-seq data, *Tbx2* expression was down-regulated, suggesting that an increase in *Nrdg4* expression is mediated by reduced *Tbx2* expression. Ankyrin repeat domain 1 (Ankrd1) protein is a part of the muscle ankyrin repeat protein family and a cardiac-specific stress-response protein. Ankrd1 plays as a transcription co-factor in the nucleus and maintains sarcomere assembly by interacting with titin in the heart [44]. Although *Ankrd1* KO mice are viable and display normal heart function, Ankrd1 has been proposed as a potential biomarker for heart failure. *Ankrd1* transcription is directly activated by Nkx2.5 and GATA4, and their transcriptional activities can be repressed by Jarid2 [45]. Thus, increased Nkx2.5 and GATA4 activities in *Jarid2*$^{\alpha MHC}$ hearts may activate *Ankrd1* expression. These 7 up-regulated genes in *Jarid2*$^{\alpha MHC}$ hearts indicate alterations in expression of critical genes at p10. Interestingly, among the 7 genes, 4 genes (*Gyg*, *Slc8a1*, *Abcc9* and *Ankrd1*) are associated with heart failure.

Genome-wide analyses of gene expression profiling in the Jarid2$^{\alpha MHC}$ heart during DCM/heart failure

To gain insights into the mechanisms underlying DCM progression in *Jarid2*$^{\alpha MHC}$ hearts, we performed RNA-seq on 7m hearts (Fig. 3-6). A total of 2375 genes were significantly dysregulated in *Jarid2*$^{\alpha MHC}$ hearts by either EBSeq (Fig. 3-6A) or DESeq2 analysis (Fig. A1-10B). Among those, 1005 genes were common DE genes identified by both analyses (Fig. 3-6B). Major gene ontology of the 1005 genes by BP analysis indicated collagen fibril organization and fatty acid metabolic process, which consist of mostly up- and down-regulated genes, respectively (Fig. 3-6C). Likewise, the extracellular

region and mitochondrion were identified by CC, which consist of mostly up- and down-regulated genes, respectively. Similarly, fibronectin binding and oxidoreductase activity were identified by MF, consisting of up- and down-regulated genes, respectively. Specifically, aerobic metabolism, including fatty acid oxidation and oxidation-reduction process by BP was enriched with down-regulated genes.

Since highly dysregulated genes in the mutant heart may play important roles in mediating DCM at 7m, we analyzed 319 dysregulated genes that showed more than two-fold changes (Fig. 3-6D). Among the 319 DE genes, 128 were down-regulated and 191 genes up-regulated. GO term analyses on the down-regulated genes showed action potential, single-organism metabolic process, and regulation of transmembrane transport by BP analysis. The CC analysis indicated that sarcolemma, and T-tubule, and MF analysis showed voltage-gated ion channel activities. The up-regulated genes were mainly involved in extracellular region (84/191). Interestingly, PI3K-Akt signaling pathway was identified by KEGG analyses, which included many extracellular matrix genes (*Col1a1, Col1a2, Col3a1, Col5a2, Col6a3, Col11a1, Cdkn1a*, *Gng8*, *Itga11*, *Lpar3*, *Myc*, *Spp1*, *Tnc*, and *Thbs4*). Additionally, heart failure associated genes or extracellular matrix genes were up-regulated, including *tissue inhibitor of metaolloprotease-1* (*Timp1*), *a disintegrin and metalloproteinase with thrombosponding repeats-like 2* (*Adamtsl2*), and *small proline-rich repeat protein 1a* (*Sprr1a*). Timp1 is a collagenase inhibitor [46]. Adamtsl2 mutation causes Geleophysic dysplasia with cardiac defects, including ventricular septal defect and thickened and nonstenotic aortic valve [47]. Sprr1a is overexpressed in myocytes after mechanical stress and may prevent the myocytes against permanent damages [48]. Therefore, *Jarid2*$^{\alpha MHC}$ hearts exhibited increases in

stress-response genes and fibrosis related genes.

Jarid2 was required for myocardial maturation

Next, we determined genes that are continuously dysregulated at both p10 and 7m in the mutant heart to increase mechanistic insights into the Jarid2 function or DCM progression. Our RNA-seq data indicated that only 12 genes were significantly dysregulated in *Jarid2*$^{\alpha MHC}$ hearts at both p10 and 7m (Fig. 3-7A). Most of these genes (*Lpar3*, *Sulf2*, *Gsg1l*, *Irx2*, *Pam*, *Ankrd1*, *Gyg*, *Lnx1* and *Adprhl1*) continued to be up-regulated in *Jarid2*$^{\alpha MHC}$ hearts at p10 and 7m compared to controls, implying that Jarid2 may function in suppressing these genes in normal hearts. Lpar3 is a receptor for lysophosphatidic acid belonging to the G-protein coupled receptor family, and is expressed in the myocardium during postnatal maturation stages [49]. Pam is an integral membrane protein containing peptidylglycine α-hydroxylating monooxygenase and α-amidating enzymes [50]. Pam has been studied in the atrium for α-amidation and pro-ANP packaging in secretory granules [51]. Lnx1 is an E3 ubiquitin ligase that mediates the ubiquitination and degradation of Numb and also ubiquitinates ErbB2 receptors in Schwann cells for the maturation [52]. Therefore, increased Lnx1 might regulate Nrg1-ErbB signaling pathways in *Jarid2*$^{\alpha MHC}$ hearts. Gsg1l is a transmembrane auxiliary subunit of AMPA-receptors, which are ionotropic glutamate receptors in the central nervous system [53]. *lectin galactoside-binding soluble 4* (*Lgals4*) and *with no lysine kinase 4* (*Wnk4*) were expressed higher in control hearts at p10 and 7m compared to mutants. *Gli1* was down-regulated at p10 but up-regulated at 7m in mutant hearts. However, *Gli1* expression level was very low in the adult heart.

Since the heart undergoes postnatal development, we reasoned that comparing normal time-dependent changes in gene expression patterns from p10 to 7m in control hearts vs. mutant hearts may provide important information to identify developmental defects in the mutant heart (Fig. 3-7B). There were 16 genes showing significantly different time-dependent patterns between control and *Jarid2*$^{\alpha MHC}$ hearts. In *Jarid2*$^{\alpha MHC}$ hearts, *eukaryotic elongation factor 1* (*Eef1a1*), *Nppa*, *Nppb* and *Ankrd1* were significantly increased compared to controls, which are linked to heart failure. In contrast, metabolic process related genes, such as *cytochrome c oxidase subunit 7a1* (*Cox7a1*) and *enoyl coenzyme A hydratase 1* (*Ech1*) were down-regulated in mutant hearts compared to controls. Cox7a1 is a complex of the mitochondrial respiratory chain and a heart and skeletal muscle-specific enzyme. *Cox7a1* KO mice develop DCM with reduced Cox activities in the muscle [54]. Ech1 is the second enzyme of mitochondrial fatty acid beta-oxidase pathways and associated with cell growth and apoptosis [55].

Interestingly *Ankrd1* and *Nppb* expression levels were slightly up regulated in control hearts from p10 to 7m (1.6-fold and 1.4-fold, respectively), even though these genes were highly up regulated in *Jarid2*$^{\alpha MHC}$ hearts (2.5-fold and 3.2-fold, respectively). These results suggest that Jarid2 prevents heart failure related gene expression in adult hearts. Contractile gene expression (*Tpm1*, *Myl2*, *Myh6*, *Actc1*, *Pln*, *Tnnt2*, and *Tnni3*) was increased in control hearts from p10 to 7m, whereas these were not increased as much in *Jarid2*$^{\alpha MHC}$ hearts. Indeed, expression levels of *Tpm1*, *Myl2*, *Myh6*, *Actc1*, and *Pln* were reduced from p10 to 7m in *Jarid2*$^{\alpha MHC}$ hearts. These results suggest that Jarid2 is important to increase or maintain the expression of contractile genes for mature cardiomyocytes.

To analyze sarcomere gene expression, we examined expression levels of fetal isoforms such as *Myl7*, *Tnni1* and *Acta2* by qRT-PCR on p10 and 7m hearts (Fig. 3-7C). In general, these fetal genes are switched to the adult forms or reduced their expression levels during myocardial maturation [56]. *Tnni1* and *Acta2* were significantly increased in the mutant neonatal heart. Ankrd1 is another fetal gene, which is expressed at a higher level in the embryonic heart than the adult heart [44]. *Ankrd1* expression was continuously increased in p10 and 7m *Jarid2*$^{\alpha MHC}$ hearts. *Myh7,* a fetal isoform*,* was only increased at 7m, indicating that increased *Myh7* in combination with decreased *Myh6* levels were the known phenotype of heart failure, namely 'fetal gene re-expression'. *Tpm1*, *Myl2* and *Pln* are important contractile genes that are increased as the heart matures, and dysregulations of these genes are linked to DCM [57]. However, these genes were down-regulated in 7m *Jarid2*$^{\alpha MHC}$ hearts although *Myl2* and *Pln* expression levels were not altered at p10 (Fig. 3-7C). These data suggest that Jarid2 is necessary to repress expression of fetal genes and maintain mature genes in the adult heart.

Nrg1-ErbB4 signaling pathway may be dysregulated in Jarid2 deficient hearts

We have previously shown that Notch1-Nrg1-ErbB signaling pathways were increased in *Jarid2* KO embryonic hearts [17]. Myocardial-specific induction of ErbB2 exhibits cardiac hypertrophy and dedifferentiation of the cardiomyocytes mediated by ERK and AKT signaling pathways [14]. In our RNA-seq data, *Nrg1* was highly up-regulated, whereas *ErbB4* was down-regulated in *Jarid2*$^{\alpha MHC}$ hearts at 7m (Fig. 3-6A). Therefore, we examined whether the altered immature gene expression is correlated with Nrg1-ErbB signaling. First, we determined the expression levels of *Nrg1* and *ErbB4* by

qRT-PCR (Fig. 3-8A and 8B). Interestingly, *Nrg1* expression was continuously increased in *Jarid2*$^{\alpha MHC}$ hearts from 1m (pre-DCM) to 7m (DCM/heart failure). In contrast, *ErbB4* expression in the myocardium was temporarily increased at p10 but down-regulated by 7m in *Jarid2*$^{\alpha MHC}$ hearts. Since Nrg1-ErbB signaling activates AKT and ERK pathways [14], we examined ErbB4 protein levels and downstream signals (Fig. 3-8C and 8D). ErbB4 protein expression was increased in *Jarid2*$^{\alpha MHC}$ hearts compared to controls at p10, correlating with mRNA levels. Phospho-AKT and phospho-ERK1/2 expression levels were significantly elevated, while total AKT and ERK1/2 expression levels were not changed. To determine whether increased ErbB4 signaling pathways directly regulate fetal gene expression, the isolated cardiomyocytes from control and *Jarid2*$^{\alpha MHC}$ hearts were incubated in ErbB inhibitors. Under the control condition, *Tnni1* and *Acta2* expression levels were significantly up-regulated in *Jarid2*$^{\alpha MHC}$ vs. control hearts (Fig. 3-8E). However, these increases returned to control levels by the treatment with an ErbB receptor inhibitor (Fig. 3-8F). These results suggest that Jarid2 may mediate transition from fetal to adult gene expression via ErbB4 signaling pathways during neonatal stages. Further experiments are required to determine whether Jarid2 is a direct regulator of ErbB4 signaling. Intriguingly, *Ankrd1* expression was marginally increased in the isolated cardiomyocytes from the *Jarid2*$^{\alpha MHC}$ heart, and its expression was not altered by the treatment with an ErbB inhibitor. It suggests that increased Ankrd1 expression is regulated by different signaling pathways, or *Ankrd1* expression in the cultured cardiomyocytes is differently regulated as compared to an intact mouse heart.

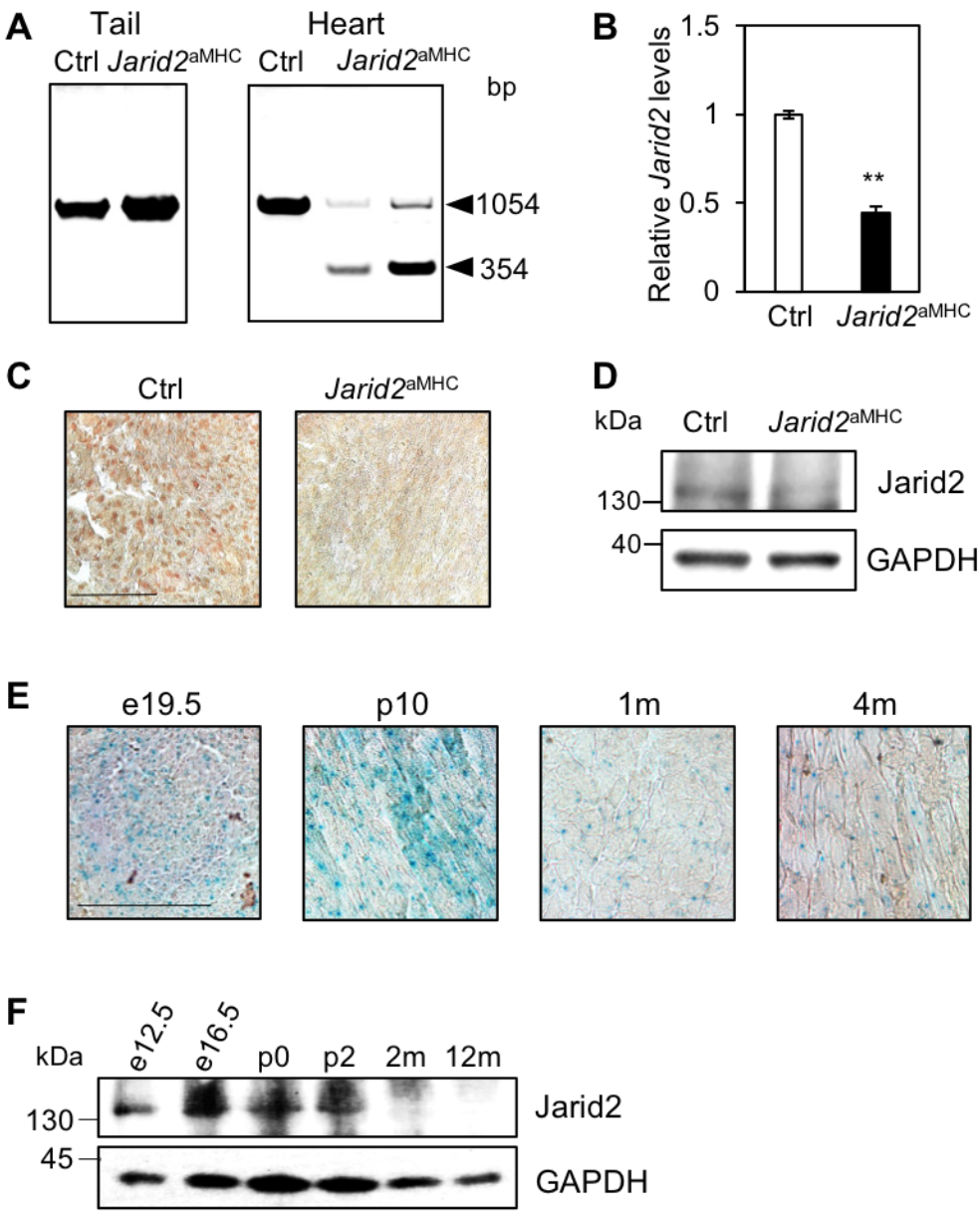

Figure 3-1. Jarid2 expressed in the heart during early-postnatal stages.

A, Genomic DNAs were isolated from the tail and the heart, and PCR was performed with primers detecting *Jarid2fl* (1054bp) or floxed out *Jarid2* (354bp) band. B, qRT-PCR was performed on p10 hearts to determine *Jarid2* expression levels. The expression levels were normalized to control levels. n=3. C, Immunostaining analysis was performed on

p10 hearts with Jarid2 antibody (brown). Scale bar, 100um. D, Jarid2 protein levels were detected by Western blotting on p10 hearts. The GAPDH was used as a loading control. E, LacZ staining was performed on the frozen sections of *Jarid2* heterozygous hearts [23]. Embryonic hearts (e19.5) and postnatal hearts (p10, 1m and 4m) were used to compare *Jarid2* expression. Scale bar, 100um. F, Jarid2 protein levels were detected by Western blotting on embryonic (e12.5 and e16.5) and postnatal (p0, p2, 2m and 12m) hearts. The GAPDH was used as a loading control.

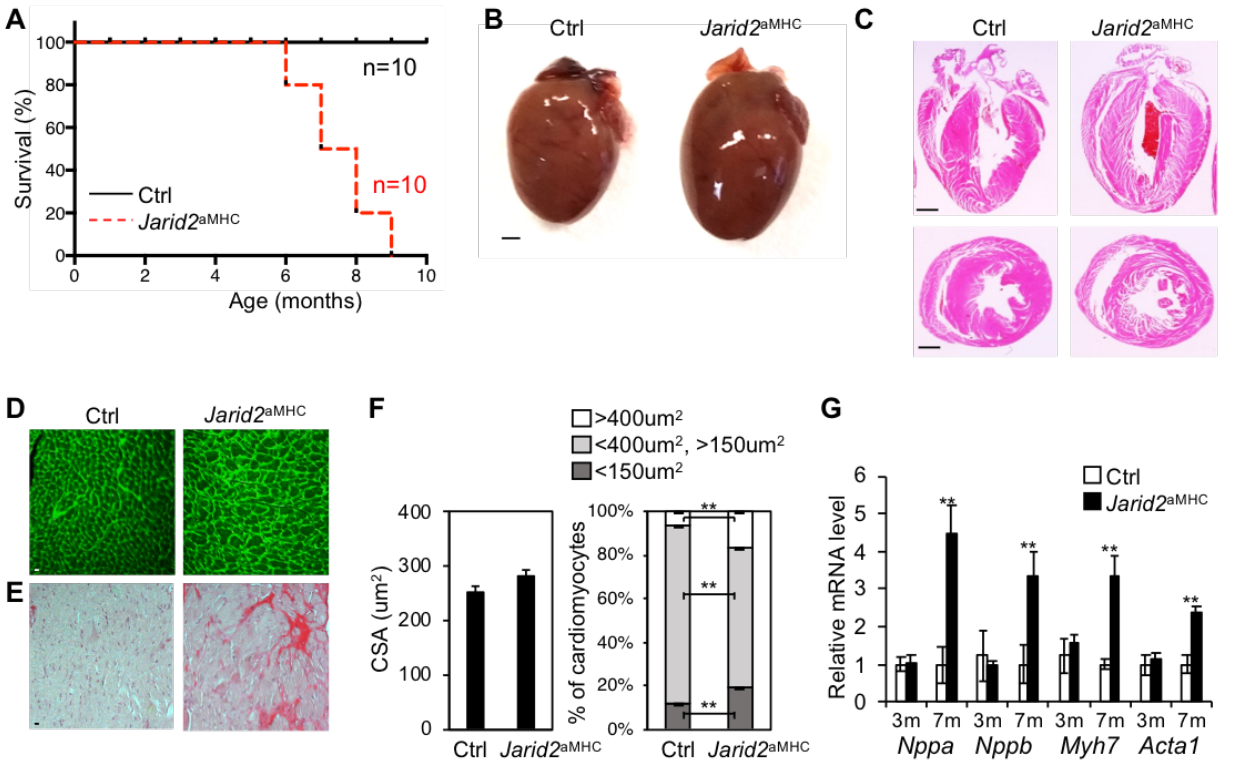

Figure 3-2. *Jarid2*$^{\alpha MHC}$ mice died with enlarged hearts.

A, Kaplan-Meier survival curves of control and *Jarid2*$^{\alpha MHC}$ mice were assessed by log-rank test. *P*<0.001, n=10. B, Cardiac dilation and hypertrophy were observed by gross morphology in *Jarid2*$^{\alpha MHC}$ hearts at 7m. Scale bar, 1mm. C-E, The frontal or transverse midline heart sections were stained with H&E (C), WGA (D) or PicroSirius red (E) on control and *Jarid2*$^{\alpha MHC}$ hearts at 7m. scale bar, 1mm. F, Cardiomyocyte surface cross-sectional area (CSA) in the left ventricular wall was measured by WGA staining using Image J software. CSA was evaluated in at least 200 cardiomyocytes of the left ventricle. n=3. G, Expression levels of the hypertrophy marker genes, *Nppa*, *Nppb, Myh7* and *Acta1*, were evaluated by qRT-PCR on control and *Jarid2*$^{\alpha MHC}$ hearts at 3m or 7m. The expression levels were normalized to control levels. n=3-5.

Table 3-1. Echocardiographic assessment of cardiac structure and function in *Jarid2*$^{\alpha MHC}$ mice.

Age (months)	3 months		7months	
	Ctrl	*Jarid2*^{aMHC}	Ctrl	*Jarid2*^{aMHC}
n	9	10	9	9
LVID; d (mm)	4.12 ± 0.1	4.34 ± 0.1	4.23 ± 0.1	**5.22 ± 0.3****
LVID; s (mm)	3.33 ± 0.1	3.20 ± 0.2	3.02 ± 0.09	**4.36 ± 0.37****
LVPW; d (mm)	0.60 ± 0.03	0.65 ± 0.02	0.67 ± 0.02	0.64 ± 0.02
LVPW; s (mm)	0.77 ± 0.03	**0.90 ± 0.03****	0.78 ± 0.02	0.77 ± 0.02
LVAW; d (mm)	0.60± 0.03	0.66 ± 0.02	0.67 ± 0.02	0.64 ± 0.02
LVAW; s (mm)	0.82 ± 0.04	0.89 ± 0.03	0.77 ± 0.02	0.76 ± 0.02
H/R	0.29 ± 0.01	0.30 ± 0.01	0.32 ± 0.01	**0.25 ± 0.01****
LV volume; d (μL)	79.04 ± 4.5	86.39 ± 6.9	80.83 ± 5.2	**135.34 ± 19.1****
LV volume; s (μL)	45.54 ± 3.6	42.49 ± 5.5	35.96 ± 2.6	**93.06 ± 20.8***
Stroke volume (μL)	33.50 ± 1.9	**43.90 ± 2.3****	44.87 ± 3.1	42.28 ± 3.7
% E.F.	42.71 ± 2.1	**51.95 ± 2.7***	55.37 ± 1.5	**35.21 ± 4.3****
% F.S.	20.87 ± 1.1	**26.64 ± 1.7****	28.65 ± 1.0	**17.25 ± 2.3****
Heart Rate (bpm)	424.44 ± 6.3	419.20 ± 11.9	485.67 ± 13.1	448.11 ± 18.1
Cardiac Output (ml/m)	14.17 ± 0.7	**18.47 ± 1.2****	21.75 ± 1.5	19.10 ± 2.0
IVRT (ms)	23.75 ± 1.5	**18.46 ± 1.1****	19.52 ± 1.7	22.22 ± 1.7
MV E/A	1.65 ± 0.1	**1.32 ± 0.1***	1.37 ± 0.1	1.23 ± 0.2
LV Mass (mg)	90.27 ± 8.9	106.29 ± 9.7	101.87 ± 5.2	**142.50 ± 14.1***
Body weight (g)	27.67 ± 2.0	26.70 ± 1.5	33.78 ± 1.9	33.22 ± 1.7
LV Mass/BW (mg/g)	3.24 ± 0.1	**3.98 ± 0.3***	3.06 ± 0.2	**4.37 ± 0.5***

Evaluation of cardiac structural and functional parameters by echocardiography in *Jarid2*^{aMHC} and control mice at 3 or 7 months. Values are means ± SEM. *LV*, left ventricle; *ID*, inner diameter; *PW*, posterior wall; *AW*, anterior wall; *d*, diastole; *s*, systole; H/R, left

ventricular thickness/radius; *E.F.*, ejection fraction; *F.S.*, fractional shortening; IVRT, isovolumic relaxation time; MV E/A, the ratio of peak velocity of early to late filing of mitral inflow. **P*<0.05, ***P*<0.01 compared with controls (in bold), n=9-10.

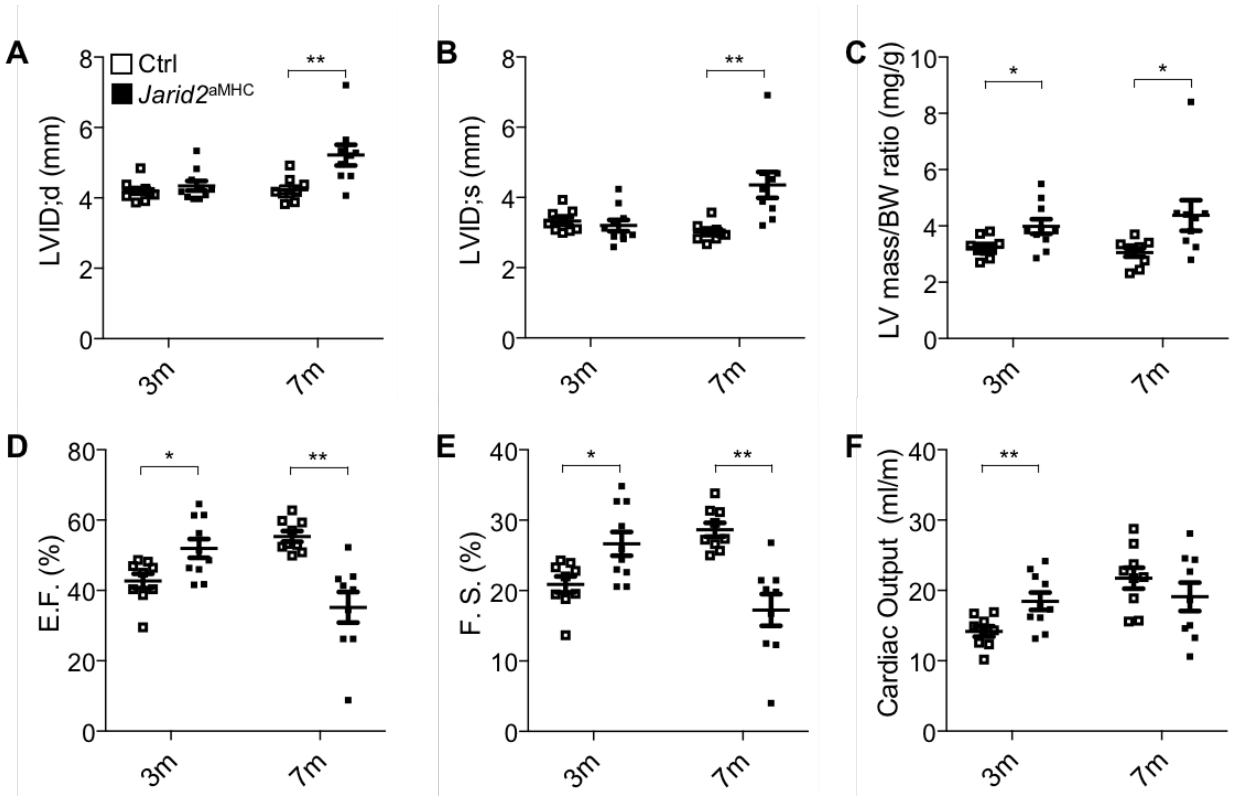

Figure 3-3. *Jarid2*$^{\alpha MHC}$ mice developed dilated cardiomyopathy.

Cardiomyopathy was evaluated by echocardiography at 3m or 7m of age. Cardiac dilation in *Jarid2*$^{\alpha MHC}$ mice was observed by left ventricular inner diameters at diastole (LVID;d, A) and systole (LVID;s, B), and left ventricular mass to body weight ratio (C). Heart function was measured by echocardiography as ejection fraction (EF, D), fractional shortening (EF, E) and cardiac output (F). Mean ± SEM, n=9-10.

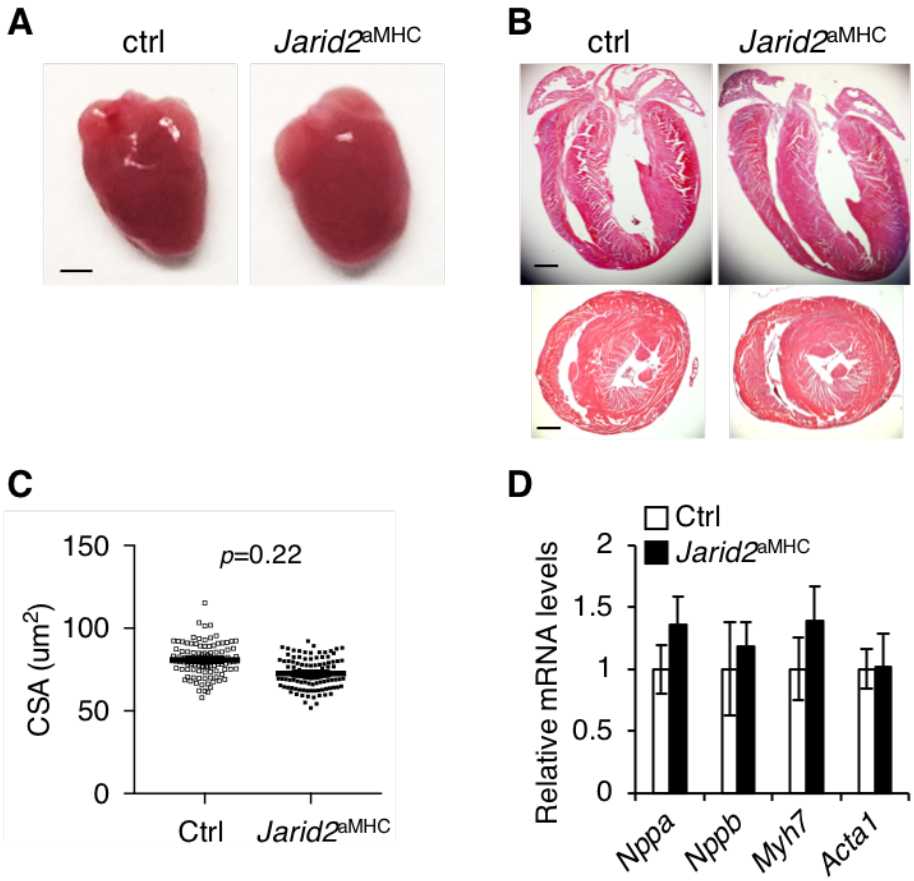

Figure 3-4. *Jarid2*$^{\alpha MHC}$ hearts revealed normal phenotypes at p10.

A, Whole images of control and *Jarid2*$^{\alpha MHC}$ hearts at p10. Scale bar, 1mm. B, H&E staining was performed on p10 hearts on longitudinal and transverse sections. Scale bar, 500um. C, CSA was measured by WGA staining at p10. Mean ± SEM, n=6. D, Expression of the hypertrophy marker genes were evaluated by qRT-PCR on p10 hearts. n=3-5.

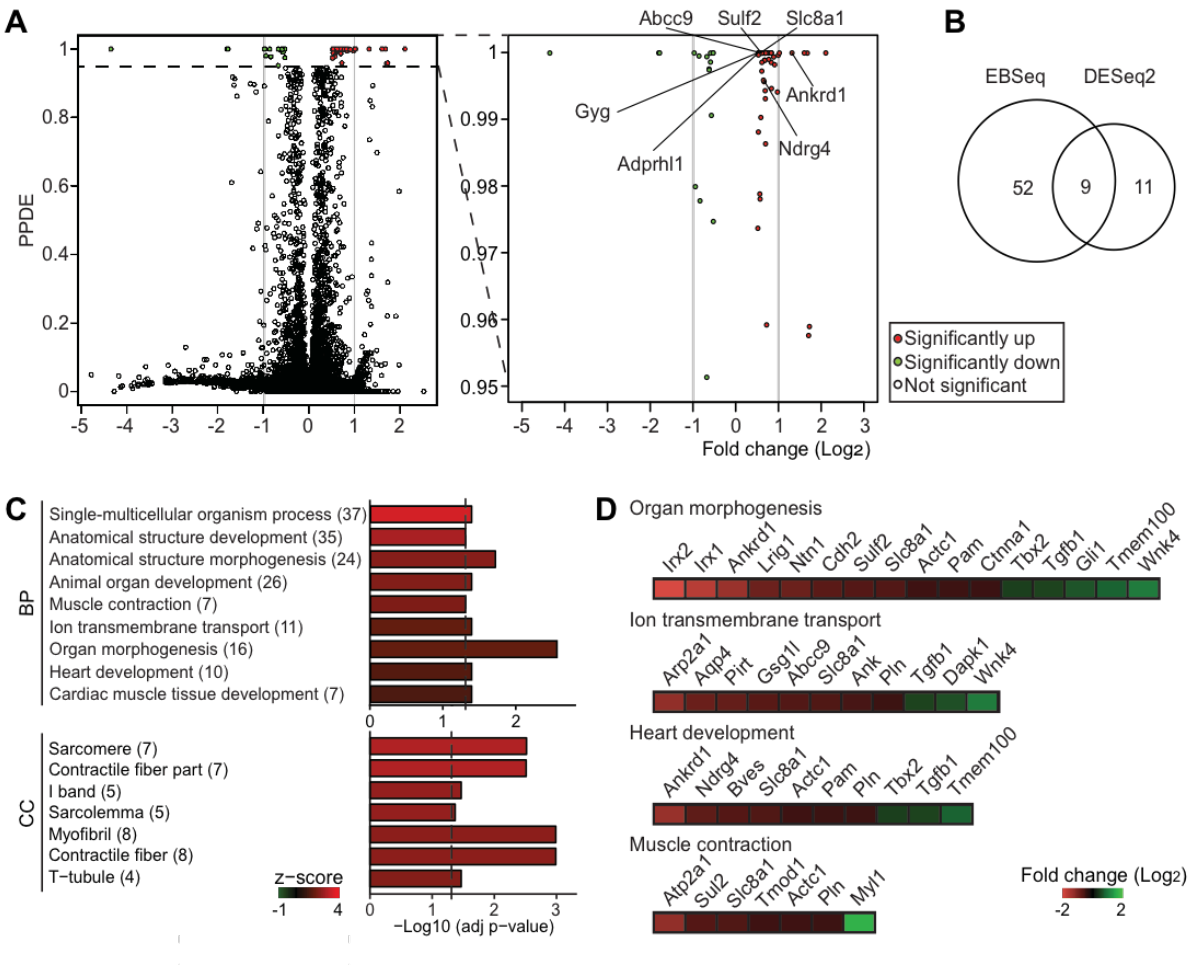

Figure 3-5. RNA-seq was performed on p10 hearts.

A, Volcano plot showed differentially expressed genes by EBSeq. 61 genes were statistically significant (Posterior probability of being differentially expressed, PPDE>0.95) and magnified (right). Gray lines indicate ±1-fold change. All genes are indicated by a dot. B, Venn diagram demonstrates numbers of DE genes by EBSeq and DESeq2. C, GO term analysis was performed with all DE genes (72) to indicate significant BP and CC (adj *p*-value<0.05, dotted lines). Colors reflect the z-score. D, Heat map indicates genes involved in organ morphogenesis, ion transmembrane transport, heart development and muscle contraction. colors reflect the fold change. Increased genes are indicated in red, intermediate in black and decreased in green.

Table 3-2. List of 7 DE genes in EBSeq and DESeq2 at p10.

Gene	Fold change	PPDE	Name
Ankrd1	1.31	1.00	Ankyrin repeat domain 1 (cardiac muscle)
Ndrg4	0.65	1.00	N-myc downstream regulated gene 4
Sulf2	0.61	1.00	Sulfatase 2
Slc8a1	0.58	1.00	Solute carrier family 8 (sodium/calcium exchanger), member 1
Abcc9	0.55	1.00	ATP-binding cassette, sub-family C (CFTR/MRP), member 9
Adprhl1	0.53	1.00	ADP-ribosylhydrolase like 1
Gyg	0.53	1.00	Glycogenin

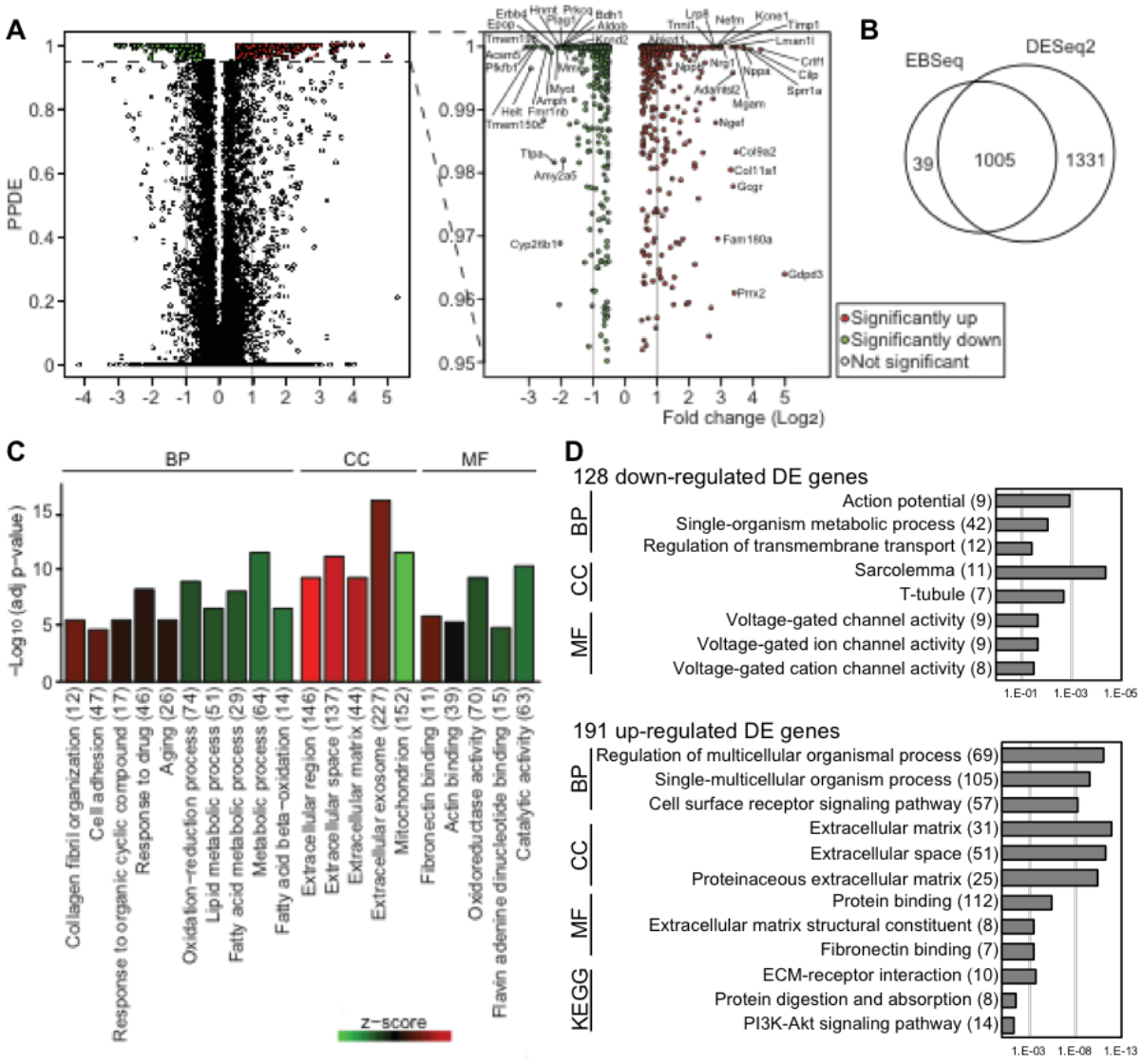

Figure 3-6. RNA-seq was performed on 7m hearts.

A, Volcano plot showed differentially expressed genes by EBSeq. 1044 genes were statistically significant (PPDE>0.95) and indicated by dotted line and magnified (right). All genes are indicated by dots. B, Venn diagram demonstrates numbers of differentially expressed genes by EBSeq and DESeq2. 1005 genes were common differentially expressed genes in EBSeq and DESeq2. C, GO term analysis was performed with 1005 genes. Among the significant categories, top 10 BPs, and top 5 CCs and MFs were

indicated (adj *p*-value<0.05). D, GO term analysis was performed with 319 DE genes (fold change >1). Down-regulated genes reveled all significant categories, whereas up-regulated genes revealed top 3 significant categories (FDR<0.05).

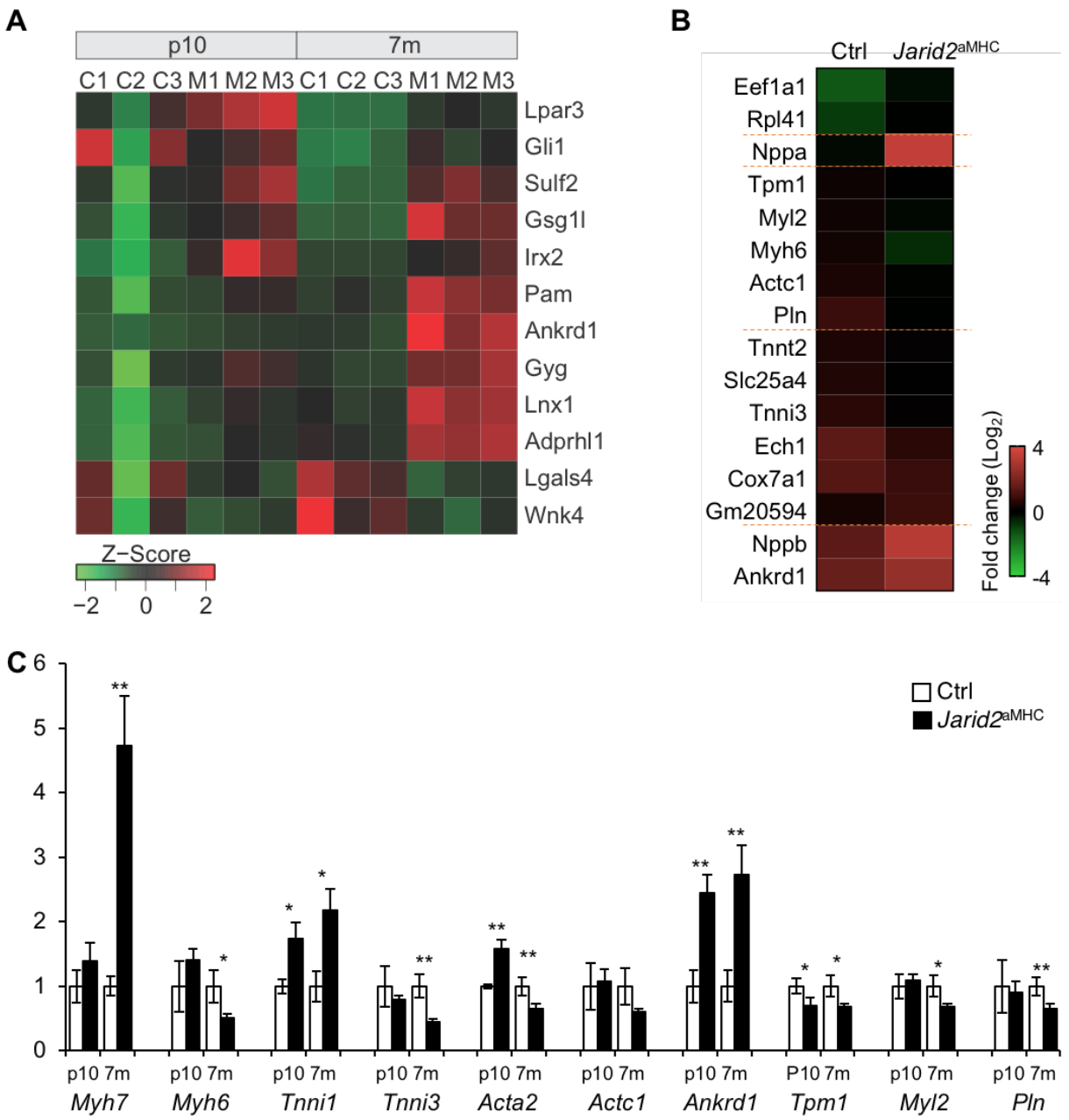

Figure 3-7. Jarid2 was required for myocardial maturation.

A, The heat map showed statistically significantly dysregulated genes in *Jarid2*$^{\alpha MHC}$ at p10 and 7m. 12 genes were only dysregulated genes among 72 genes and 2375 genes at p10 and 7m, respectively. B, The heat map displayed TDDE (time-dependent

differential expression). 16 genes were statistically significant in our analysis, and the fold changes from p10 to 7m were presented by colors. C, qRT-PCR was performed to determine expression levels of DE genes in p10 and 7m hearts. n=3-5.

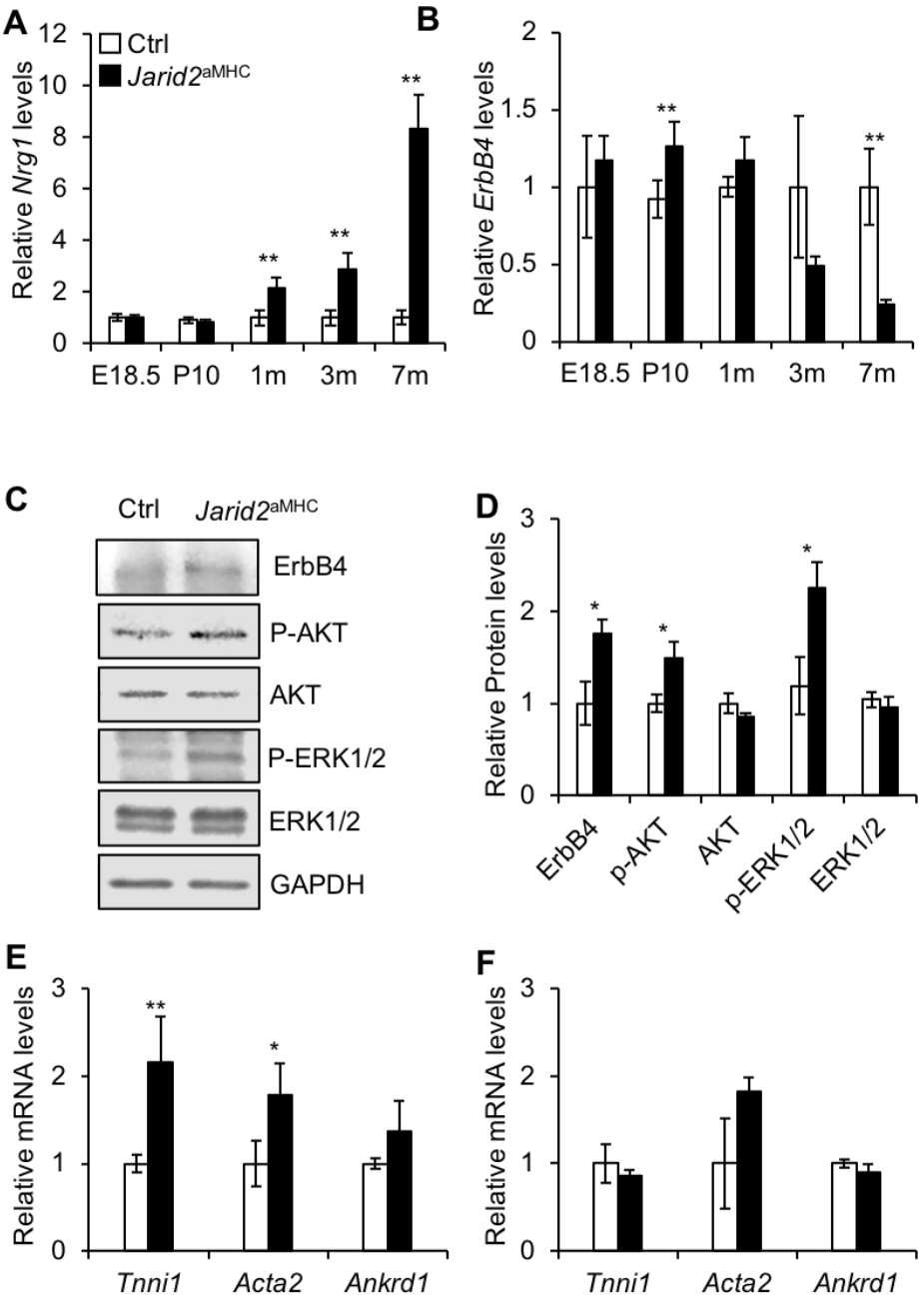

Figure 3-8. ErbB4 was highly expressed in *Jarid2*$^{\alpha MHC}$ hearts at p10.

A, *Nrg1* levels were determined by qRT-PCR on the heart at e18.5, p10, 1m, 3m and 7m of age. The expression levels were normalized to each control levels. n=3-5. B, *ErbB4* expression levels were measured by qRT-PCR on control and *Jarid2*$^{\alpha MHC}$ hearts. n=3-5.

C, Western blotting was performed to determine ErbB4, AKT and ERK pathways on p10 hearts. D, The graph showed the protein levels of ErbB4, AKT and ERK by standardization to GAPDH and normalization to control levels. qRT-PCR was performed on cardiomyocytes from new born hearts incubated in vehicle (E) or ErbB inhibitor, AG1478 (5uM) (F). n=3-5.

Discussion

In the present study, the molecular and developmental function of Jarid2 were determined in the postnatal heart by employing cardiac-specific Cre mice. *Jarid2*$^{\alpha MHC}$ mice exhibited dilated cardiomyopathy with contractility defects, leading to premature death around 7-9m of age. Since Jarid2 expression was maintained in the neonatal heart but significantly decreased thereafter, we reasoned that Jarid2 functions critically in the neonatal hearts. These studies will increase our understanding on the molecular etiology of DCM. Thus, we analyzed gene expression profiling in the neonatal heart at p10 (pre-DCM) and in DCM/failing hearts at 7m. At p10, dysregulated genes in *Jarid2*$^{\alpha MHC}$ hearts represented mainly heart development and muscle contraction pathways although the mutant heart appear normal. Further analyses showed that heart failure-related genes were significantly elevated in the mutant heart. At 7m, the metabolic process and ion channel activity were enriched with down-regulated genes, and extracellular matrix components were enriched with up-regulated genes. These data indicate that Jarid2 is important for regulating genes for neonatal heart development and muscle contraction at p10, even when the heart morphology and function seems normal. These early changes in gene expression may have contributed to heat failure at 7m. To determine whether Jarid2 plays important roles in maturation of cardiomyocytes postnatally, we analyzed gene expression patterns from p10 to 7m. In normal hearts, sarcomere and contractile associated genes were up-regulated from p10 to 7m in an age-dependent manner, while these genes were not sufficiently increased in *Jarid2*$^{\alpha MHC}$ hearts. These data suggest that Jarid2 plays important roles in inducing mature cardiomyocytes and normal sarcomere

development and in inhibiting the expression of DCM-related genes during neonatal stages.

Jarid2 is an important transcription factor in heart development. *Jarid2* KO mice develop congenital cardiac defects such as thin myocardium, hypertrabeculation and ventricular septal defect during embryonic stages [23]. Although Jarid2 is an enzymatically inactive member of the JMJ histone demethylase family, Jarid2 can function as an epigenetic regulator by recruiting histone methyltransferases in the developing heart [19]. However, the function of Jarid2 in the adult heart is not fully understood. The p10 RNA-seq data were overlapped with our Jarid2 Chip-chip on the promoters identified in the developing heart [20] to determine potential targets of Jarid2 (Table A2-6). Among the 72 DE genes, Jarid2 occupies the promoters of the 15 genes, which are potential direct targets of Jarid2. Cell proliferation and differentiation related genes (*Tmem100*, *Gli1*, *Tgfb1* and *Egfl7*) were down-regulated in mutant hearts, implying transcriptional activation functions of Jarid2 in the neonatal heart. However, since ChIP-chip assays were performed using e17.5 embryonic hearts, this overlapping has limitations due to age and environmental differences. Further investigation into Jarid2 occupancy in the postnatal heart would be important to determine direct targets of Jarid2. Myocardial noncompaction and hypertrabeculation in early childhood are associated with the increased risk for developing DCM [58]. In *Jarid2*$^{\alpha MHC}$ hearts at p10, the heart morphology looked normal, yet altered gene expression has already occurred for the genes involved in ion transmembrane transport and muscle contraction. This suggests that dysregulation of these genes is not sufficient to develop morphological and functional defects at p10 but may be causal to hyper-functioning hearts at 3m and DCM later.

Jarid2$^{\alpha MHC}$ mice exhibited DCM and increased gene expression involved in collagen fibril organization, and extracellular matrix remodeling, indicating increased fibrosis, a common feature of the pathological remodeling in the failing heart. Cardiac fibrosis can cause disruption of the myocardial architecture and impairment of systolic and diastolic function [59, 60]. *Jarid2*$^{\alpha MHC}$ hearts showed dysregulated collagen synthesis (*Col6a3*, *Col1a2*, *Col5a2*, *Col3a1*, *Col1a1*, *Col14a1*, *Col11a1* and *Col9a2*). In addition, genes involved in extracellular matrix degradation were dysregulated such as metalloproteases (*Mmp19*, *Mmp2*, *Mmp14*, *Mmp23*, *Adam7*, *Adam3*, *Adam2*, *Adamtsl2*, *Adam22* and *Adam 11*), and metalloproteases inhibitor (*Timp1*). The secreted factors regulating fibrosis (*Fgf11*, *Fgf9*, *Ptn* and *Fstl3*) were also dysregulated in *Jarid2*$^{\alpha MHC}$ hearts. Interestingly, Serpin isoforms (*Serpin1f*, *Serpina3n*, *Serpine1* and *Serpinb1c*) were highly increased in *Jarid2*$^{\alpha MHC}$ hearts at 7m by our RNA-seq data. Serpins are serine protease inhibitors, which regulate anti-fibrinolysis. Serpine1 (PAI1) inhibits the Mmp activity involved in fibrosis [61]. Together, these findings suggest that increased fibrosis in *Jarid2*$^{\alpha MHC}$ hearts is mediated by dysregulation of collagens, Mmps and Serpins expression.

The adult heart produces 90 % of ATP using fatty acid oxidation. However, this energy metabolism is changed to glycolysis in the failing heart [62]. *Jarid2*$^{\alpha MHC}$ hearts at 7m displayed a reduction of fatty acid metabolic process. Peroxisome proliferator-activated receptor (PPAR) pathway is a key regulator in heart metabolism, which is inhibited in DCM mouse models [63]. PPAR downstream signaling was significantly reduced in *Jarid2*$^{\alpha MHC}$ hearts at 7m (*Slc27a1*, *Acadl*, *Esrrb* and *Ppargc1a*). However, this pathway was not altered in p10 hearts, suggesting that reduced fatty acid metabolism is a DCM phenotype. PPAR gamma coactivator 1 alpha (PGC1α, ppargc1a) regulates

mitochondrial biogenesis and oxidative phosphorylation in the heart [63], implying that mitochondrial function is perturbated in *Jarid2*$^{\alpha MHC}$ hearts (Fig. 3-6C). Glucose metabolism process was not identified as a significantly dysregulated pathway in *Jarid2*$^{\alpha MHC}$ hearts at 7m. However, RNA-seq data exhibited decreases in glycolysis and gluconeogenesis related genes (*Ldhb*, *Galm*, *Acss1*, *Aldob*, *Fbp2* and *Aldh9a1*), and increases in glucose synthesis enzymes (*Ptges3*, *Prkag3*, *Gck* and *Gyg*), implying that a shift from aerobic metabolism to nonoxidative glucose metabolism may have occurred in *Jarid2*$^{\alpha MHC}$ hearts at 7m.

In mouse models of heart failure, Nrg1 expression is higher, while ErbB2 and ErbB4 expression levels are decreased during the transition from compensatory hypertrophy to heart failure [15]. Nrg1 improves heart function and prevents cardiac fibrosis in animal models and heart failure patients [15]. Increases in Nrg1 and ErbB4 expression correlate with increases in contractility in animal models of heart failure [64]. It is interesting that in our study, an increase in *Nrg1* expression was detected from 1m, which was much earlier than onset of DCM. Thus, it is plausible that early increases in *Nrg1* lead to the hyper-performing heart at 3m as indicated by increased FS. Elevated levels of *Nrg1* and decreased *ErbB4* in 7m *Jarid2*$^{\alpha MHC}$ hearts correlate with a general heart failure phenotype. Induction of constitutively active ErbB2 in neonatal hearts re-enters the cell cycle mediated by Nrg1 [14], and activation of Nrg1 and ErbB4 induces proliferation of differentiated cardiomyocytes [65]. Although *ErbB4* expression was altered in *Jarid2*$^{\alpha MHC}$ hearts at p10, the cell proliferation was not changed. It may be due to an increase in *ErbB4* expression is not sufficient to induce cell proliferation because endogenous *Nrg1* level is not increased, or absence of *Jarid2* in the myocardium does

not regulate cell proliferation which correlates with our previous result of Jarid2 in the embryonic heart [18]. In our qRT-PCR data, *Nrg1* expression was up-regulated from 1m hearts, implying that increased *Nrg1* may serve as a sensitive indicator of heart failure.

Ankrd1 was highly increased in neonatal as well as failing hearts of *Jarid2*$^{\alpha MHC}$ mice. *Ankrd1* overexpression mouse displays normal cardiac morphology [44], and the function of increased Ankrd1 in the adult heart is controversial; Ankrd1 mediates adaptive and protective responses against pathological damages [66, 67], or Ankrd1 accelerates the progression to hypertrophy [68-70]. It is possible that increased *Ankrd1* at p10 plays a protective role to maintain normal heart morphology and functions, which may lead to the hyper-functioning heart at 3m. It is not clear that chronic overexpression of *Ankrd1* is protective or accelerates the progression of heart failure at 7m. Nonetheless, it is interesting that *Ankrd1* expression is already increased at p10, which is much earlier than the onset of heart failure, and thus may serve as an early sensitive DCM/heart failure marker. It would be interesting to determine the role of early increases in *Nrg1* and *Ankrd1 in Jarid2*$^{\alpha MHC}$ mice.

In our RNA-seq data, only 72 genes were differentially expressed in p10 mutant hearts compared to controls, while 2375 genes were dysregulated at 7m, suggesting that *Jarid2*$^{\alpha MHC}$ hearts is not severely perturbed in neonatal stages. However, of 72 genes, 12 genes were also differentially expressed at 7m, in which 2 genes were maintained down-regulation and 9 genes were maintained up-regulation in *Jarid2*$^{\alpha MHC}$ hearts compared to controls, implying that Jarid2 function is critical in regulating certain gene expression from the neonatal to adult stages. Moreover, in control hearts, sarcomere and contractile associated genes were increased in an age-dependent manner (Fig. 3-7B and 7C)

whereas these genes were not increased in *Jarid2*$^{\alpha MHC}$ hearts.

Time-dependent gene expression profiling data have been reported in other DCM mouse model with a phospholamban (PlnR9C) mutation [63]. By comparing the published dysregulated genes in pre-DCM mutant hearts with our data at p10, we identified the dysregulated genes common to both pre-DCM hearts. These include *Ttll1*, *Myl1*, *Gyg*, and *Ankrd1* (in cardiomyocytes), and *Ampd3*, *Atp2a1*, *Kctd17*, *Sulf2*, and *Tgfb1* (in non-cardiomyocytes). Interestingly, the genes that are decreased in PlnR9C mice at the DCM stage (*Abcc9*, *Ank*, *Esrrg*, *Irx1*, *Mdh1*, *Pln*, *Suclg2* and *Ttll1*) were up-regulated in *Jarid2*$^{\alpha MHC}$ hearts at p10. Of note, the genes increased in PlnR9C mice at the DCM stage were increased in p10 *Jarid2*$^{\alpha MHC}$ hearts, such as *Gbe1*, *Ndrg4*, *Gyg* and *Ankrd1*. Thus, Jarid2 may control the gene expression at neonatal stages, which are involved in DCM development at later stages. Further studies are necessary to determine whether up-regulation of these DCM-related genes at p10 leads to DCM in mutant hearts. Together, we demonstrate for the first time that Jarid2 plays crucial roles in the adult heart, which will provide important molecular and genetic basis of DCM/heart failure in humans.

Materials and Methods

Animal husbandry and genotyping

All studies using animals were housed in accordance with University of Wisconsin Research Animal Resource Center policies and the National Institutes of Health (NIH) *Guide for the Care and Use of Laboratory Animals*. All animal research has been reviewed and approved by an Institutional Animal Care and Use Committee (protocol M005971). All mice were littermate or age-matched controls and mutants. Studies were not blinded. Herein, *Jarid2* conditional deletion mice using *αMHC*-Cre mice [24], $\alpha MHC^{Cre/+};Jarid2^{f/f}$, were designated as $Jarid2^{\alpha MHC}$. To generate $Jarid2^{\alpha MHC}$ mice, females with floxed *Jarid2* allele ($Jarid2^{f/f}$) [25] were mated with $\alpha MHC^{Cre/+};Jarid2^{f/+}$ males. All mice employed in this study were bred to a mixed 129/Svj and C57BL/6 genetic background, and genotyping was performed using specific PCR primers as described previously [25].

Echocardiography

Transthoracic echocardiography was performed on mice under 1% isoflurane gas anesthesia using a Visual Sonics 770 ultrasonograph with a 30 or 40-MHz transducer (RMV 707B) (Visual Sonics) as described previously [71]. Two-dimensionally guided M-mode images of the left ventricle (LV) and Doppler studies were acquired at the tip of the papillary muscles. LV mass-to-body weight ratio (LVmass/BW), LV dimension in diastole (LVID;d), thickness of the posterior walls in diastole, and isovolumic relaxation time were recorded. Endocardial fractional shortening was calculated as (LVIDd-LVIDs)/LVIDd X100, where LVIDs is LV dimension in systole. All parameters were measured over at least three

consecutive cycles.

Western blotting and Cardiomyocyte culture

To determine the protein levels, Western blotting was performed using embryonic heart extracts as described previously [17]. Primary antibodies used were anti-Jarid2 peptide antibodies [17], anti-ErbB4 (Santa Cruz), anti-Phospho-AKT (CST), anti-AKT (CST), anti-Phospho-ERK (CST), anti-ERK (CST), anti-Cleaved-Caspase3 (CST), and anti-GAPDH (Millipore) followed by HRP conjugated secondary antibodies (Santa Cruz). Protein bands were detected by chemiluminescence (Thermo Scientific) and quantitated with NIH Image J software. Cultured primary cardiomyocytes were prepared from newborn (p1) mouse hearts as we described [72], yielding about 70 % cardiomyocytes under our culture condition. Cells were plated in Dulbecco's modified Eagle's medium (DMEM) with 10% horse serum and 5% fetal bovine serum. ErbB inhibitor, AG1478 (Sigma) or vehicle was treated in serum free medium for two days for qRT-PCR experiments.

Histology, Lac Z staining, and immunohistochemistry

Hematoxylin and eosin (H&E) staining was performed according to standard protocols [23]. Immunohistochemistry was performed on paraffin-embedded sections as described [17]. Briefly, tissue sections were incubated with primary antibodies, anti-Jarid2, anti-MF-20 (DSHB), anti-Ki-67 (CST) and anti-Phospho-H3 (Millipore). Alexa dye-conjugated secondary antibodies (Invitrogen) or DAB substrate kit (Vector Laboratories) was used for visualization. LacZ staining was performed as described previously [23].

Briefly, the hearts were isolated and fixed with 0.5% glutaraldehyde from heterozygous of *Jarid2* KO mice at e19.5, p10, 1m and 4m of age. The cryosections were incubated in X-gal staining solution at 37 C degrees for 2 hrs. Cardiomyocyte CSA was measured in WGA (Invitrogen) stained cardiac sections as described [71]. CSA was evaluated in at least 200 cardiomyocytes per animal from identical areas of the left ventricular wall at a 50X magnification. Myocyte cross-sectional area was measured per nucleus and only myocytes that were cut in the same direction were included in the measurements. As criteria, the position and shape of the nucleus within the myocyte were used. Hoechst dye was used for counter-staining of nuclei. Images were taken using a Zeiss Axiovert 200 microscope and an AxoiCam HRc camera. Picrosirius staining for collagen were performed as described [23, 71].

Quantitative real time PCR (qRT-PCR)

qRT-PCR was performed as we described [17]. Briefly, mRNAs extracted from mouse ventricles were reverse transcribed to cDNA using cDNA synthesis kit (Thermo Fisher) followed by qRT-PCR using FastStart SYBR Green Master (Roche) on a BioRad iCycler. The appropriate primers for each gene are listed in Table A2-7. All primers were thoroughly evaluated by melt curve analysis to ensure the amplification of a single, desired amplicon. All samples were assayed in duplicate with nearly identical replicate values. Data were generated using the standard curve method and normalized to 18S expression. qRT-PCR data were analyzed by the RQ analysis algorithm (BioRad).

RNA-sequencing (RNA-seq)

RNA-seq experiments were performed as described [73]. Briefly, the hearts at p10 or 7 m of age from control or *Jarid2*$^{\alpha MHC}$ mice were dissected and snap frozen in liquid nitrogen. Total RNA extraction was performed with TRIzol (Thermo Fisher) according to manufacturer's instruction. For each group, three biological replicates were obtained. Total RNA submitted to the University of Wisconsin-Madison Biotechnology Center was verified for purity and integrity via the NanoDrop One Spectrophotometer and Agilent 2100 BioAnalyzer, respectively. Samples using the Illumina® TruSeq® Stranded mRNA Sample Preparation kits (Illumina Inc.). For each library preparation, mRNA is purified from 200ng total RNA using poly-T oligo-attached magnetic beads. Subsequently, each poly-A enriched sample was fragmented using divalent cations under elevated temperature. The fragmented RNA was synthesized into double-stranded cDNA using SuperScript II Reverse Transcriptase (Invitrogen) and random primers. The cDNA products were incubated with Klenow DNA Polymerase to add an 'A' base (Adenine) and ligated to Illumina adapters, which have a single 'T' base (Thymine) overhang at their 3'end. Adapter ligated DNA was amplified and then purified by paramagnetic beads. Quality and quantity of the finished libraries were assessed using an Agilent HS DNA or DNA1000 chip (Agilent Technologies) and Qubit® dsDNA HS Assay Kit (Invitrogen), respectively. Libraries were standardized to 2nM. Cluster generation was performed using standard Cluster Kits (v4) and the Illumina cBot. Single end 100bp sequencing was performed, using standard SBS chemistry (v4) on an Illumina HiSeq2500 sequencer. Images were analyzed using the standard Illumina Pipeline, version 1.8.2. Following quality assessment using FASQC (http://www.bioinformatics.babraham.ac.uk/projects/fastqc/), the sequencing reads were aligned to reference sequences of transcriptome

obtained from NCBI (GRCm38.p6) using Bowtie v 1.1.2 allowing 2 mismatches [74]. Based on the aligned reads, countable values, expected counts (EC) and transcript per million (TPM) for each transcript were estimated by RSEM v 1.3.0 [75]. The statistical programming language R (ver 3.4.4) was used for further data processing and analysis, unless otherwise mentioned.

Analysis of RNA-seq data

Data analysis was performed as described [26]. DESeq2 was used to identify differentially expressed genes with high precision and accuracy. Genes that have FDR-adjusted p value < 0.05 were considered as DE genes with statistical significance. DE genes were displayed in MA plot. Another DE analytic tool, EBSeq, was used to identify differentially expressed genes based on the Bayesian empirical approach. Genes with value of posterior probability of differential expression (PPDE) ≥ 0.95 were considered as DE genes that were plotted on volcano plot.

Gene ontology (GO) term enrichment on DE genes were assessed using Database for Visualization and Integrative Discovery (DAVID) functional analysis software (www.david.ncifcrt.gov). GO terms were obtained from three categories: biological process (BP), cellular component (CC), and molecular function (MF). Significance of enrichment for each GO term was determined by FDR-adjusted *p*-value < 0.05 based on EASE scores, modified Fisher's exact test. Significant GO terms in enrichment were visualized using R packages.

Time-dependent differential expression analysis (TDDE)

We applied a simple and novel technique to rank DE genes by directly comparing the amount of changes of their TPM value under different conditions in terms of geometric calculation over time. For each gene, we compared the p10 and 7m changes of its TPM values between control and *Jarid2*$^{\alpha MHC}$ hearts. To quantify the degree of changes, we calculated an angle between two 2-dimensional vectors: one vector for *Jarid2*$^{\alpha MHC}$ and the other vector for the control. Y value of the starting point in the vectors was obtained from TPM value at p10 and y value of the ending point is from TPM value at 7m. The difference between x values of the two points in a vector was adopted from the maximum difference of y values. We calculated an outer product of the two vectors to obtain the angle which indicates the degree of change. To detect significant genes, we fit the angle data into Gaussian distribution and filter angles with p value < 0.05. The significant genes were visualized by heat map using TPM values.

Statistical analysis

Data represent the average of 3 to 5 replicates and standard error of the mean (SEM). The replicate numbers are indicated in the text. Significance was determined by the student's *t*-test, and differences are considered significant with a *p*-value of ≤0.05 (*) and very significant; *p*≤0.01 (**).

Acknowledgements: We thank Dr. Timothy A Hacker for providing echocardiography.

References

1 Ziaeian B, Fonarow GC: Epidemiology and aetiology of heart failure. Nat Rev Cardiol 2016;13:368-378.

2 McNally EM, Golbus JR, Puckelwartz MJ: Genetic mutations and mechanisms in dilated cardiomyopathy. J Clin Invest 2013;123:19-26.

3 Hall DD, Ponce JM, Chen B, Spitler KM, Alexia A, Oudit GY, Song LS, Grueter CE: Ectopic expression of Cdk8 induces eccentric hypertrophy and heart failure. JCI Insight 2017;2

4 van Berlo JH, Maillet M, Molkentin JD: Signaling effectors underlying pathologic growth and remodeling of the heart. J Clin Invest 2013;123:37-45.

5 Ujfalusi Z, Vera CD, Mijailovich SM, Svicevic M, Yu EC, Kawana M, Ruppel KM, Spudich JA, Geeves MA, Leinwand LA: Dilated cardiomyopathy myosin mutants have reduced force-generating capacity. J Biol Chem 2018;293:9017-9029.

6 Camacho P, Fan H, Liu Z, He JQ: Small mammalian animal models of heart disease. Am J Cardiovasc Dis 2016;6:70-80.

7 Bang ML: Animal Models of Congenital Cardiomyopathies Associated With Mutations in Z-Line Proteins. J Cell Physiol 2017;232:38-52.

8 McNally EM, Mestroni L: Dilated Cardiomyopathy: Genetic Determinants and Mechanisms. Circ Res 2017;121:731-748.

9 Taegtmeyer H, Sen S, Vela D: Return to the fetal gene program: a suggested metabolic link to gene expression in the heart. Ann N Y Acad Sci 2010;1188:191-198.

10 Naqvi N, Li M, Calvert JW, Tejada T, Lambert JP, Wu J, Kesteven SH, Holman SR, Matsuda T, Lovelock JD, Howard WW, Iismaa SE, Chan AY, Crawford BH, Wagner MB, Martin DI, Lefer DJ, Graham RM, Husain A: A proliferative burst during preadolescence establishes the final cardiomyocyte number. Cell 2014;157:795-807.

11 Morton SU, Brodsky D: Fetal Physiology and the Transition to Extrauterine Life. Clin Perinatol 2016;43:395-407.

12 Tzahor E, Poss KD: Cardiac regeneration strategies: Staying young at heart. Science 2017;356:1035-1039.

13 Harvey RP, Wystub-Lis K, del Monte-Nieto G, Graham RM, Tzahor E: Cardiac

Regeneration Therapies - Targeting Neuregulin 1 Signalling. Heart Lung Circ 2016;25:4-7.

14 D'Uva G, Aharonov A, Lauriola M, Kain D, Yahalom-Ronen Y, Carvalho S, Weisinger K, Bassat E, Rajchman D, Yifa O, Lysenko M, Konfino T, Hegesh J, Brenner O, Neeman M, Yarden Y, Leor J, Sarig R, Harvey RP, Tzahor E: ERBB2 triggers mammalian heart regeneration by promoting cardiomyocyte dedifferentiation and proliferation. Nat Cell Biol 2015;17:627-638.

15 Mercurio V, Pirozzi F, Lazzarini E, Marone G, Rizzo P, Agnetti G, Tocchetti CG, Ghigo A, Ameri P: Models of Heart Failure Based on the Cardiotoxicity of Anticancer Drugs. J Card Fail 2016;22:449-458.

16 Jung J, Mysliwiec MR, Lee Y: Roles of JUMONJI in mouse embryonic development. Dev Dyn 2005;232:21-32.

17 Mysliwiec MR, Bresnick EH, Lee Y: Endothelial Jarid2/Jumonji is required for normal cardiac development and proper Notch1 expression. J Biol Chem 2011;286:17193-17204.

18 Cho E, Mysliwiec MR, Carlson CD, Ansari AZ, Schwartz RJ, Lee Y: Cardiac-specific developmental and epigenetic functions of Jarid2 during embryonic development. J Biol Chem 2018

19 Landeira D, Fisher AG: Inactive yet indispensable: the tale of Jarid2. Trends Cell Biol 2011;21:74-80.

20 Mysliwiec MR, Carlson CD, Tietjen J, Hung H, Ansari AZ, Lee Y: Jarid2 (Jumonji, AT rich interactive domain 2) regulates NOTCH1 expression via histone modification in the developing heart. J Biol Chem 2012;287:1235-1241.

21 Bovill E, Westaby S, Reji S, Sayeed R, Crisp A, Shaw T: Induction by left ventricular overload and left ventricular failure of the human Jumonji gene (JARID2) encoding a protein that regulates transcription and reexpression of a protective fetal program. J Thorac Cardiovasc Surg 2008;136:709-716.

22 Seok HY, Chen J, Kataoka M, Huang ZP, Ding J, Yan J, Hu X, Wang DZ: Loss of MicroRNA-155 protects the heart from pathological cardiac hypertrophy. Circ Res 2014;114:1585-1595.

23 Lee Y, Song AJ, Baker R, Micales B, Conway SJ, Lyons GE: Jumonji, a nuclear protein that is necessary for normal heart development. Circ Res 2000;86:932-938.

24 Moses KA, DeMayo F, Braun RM, Reecy JL, Schwartz RJ: Embryonic expression of an Nkx2-5/Cre gene using ROSA26 reporter mice. Genesis 2001;31:176-180.

25 Mysliwiec MR, Chen J, Powers PA, Bartley CR, Schneider MD, Lee Y: Generation of a conditional null allele of jumonji. Genesis 2006;44:407-411.

26 Costa-Silva J, Domingues D, Lopes FM: RNA-Seq differential expression analysis: An extended review and a software tool. PLoS One 2017;12:e0190152.

27 Baker AH, Péault B: A Gli(1)ttering Role for Perivascular Stem Cells in Blood Vessel Remodeling. Cell Stem Cell 2016;19:563-565.

28 Kramann R, Schneider RK, DiRocco DP, Machado F, Fleig S, Bondzie PA, Henderson JM, Ebert BL, Humphreys BD: Perivascular Gli1+ progenitors are key contributors to injury-induced organ fibrosis. Cell Stem Cell 2015;16:51-66.

29 Zhao J, Liem RK: α-Internexin and Peripherin: Expression, Assembly, Functions, and Roles in Disease. Methods Enzymol 2016;568:477-507.

30 Vogel P, Hansen G, Fontenot G, Read R: Tubulin tyrosine ligase-like 1 deficiency results in chronic rhinosinusitis and abnormal development of spermatid flagella in mice. Vet Pathol 2010;47:703-712.

31 Somekawa S, Imagawa K, Hayashi H, Sakabe M, Ioka T, Sato GE, Inada K, Iwamoto T, Mori T, Uemura S, Nakagawa O, Saito Y: Tmem100, an ALK1 receptor signaling-dependent gene essential for arterial endothelium differentiation and vascular morphogenesis. Proc Natl Acad Sci U S A 2012;109:12064-12069.

32 Mizuta K, Sakabe M, Hashimoto A, Ioka T, Sakai C, Okumura K, Hattammaru M, Fujita M, Araki M, Somekawa S, Saito Y, Nakagawa O: Impairment of endothelial-mesenchymal transformation during atrioventricular cushion formation in Tmem100 null embryos. Dev Dyn 2015;244:31-42.

33 Talukder MA, Kalyanasundaram A, Zhao X, Zuo L, Bhupathy P, Babu GJ, Cardounel AJ, Periasamy M, Zweier JL: Expression of SERCA isoform with faster Ca2+ transport properties improves postischemic cardiac function and Ca2+ handling and decreases myocardial infarction. Am J Physiol Heart Circ Physiol 2007;293:H2418-2428.

34 Rosenthal F, Feijs KL, Frugier E, Bonalli M, Forst AH, Imhof R, Winkler HC, Fischer D, Caflisch A, Hassa PO, Lüscher B, Hottiger MO: Macrodomain-containing proteins are new mono-ADP-ribosylhydrolases. Nat Struct Mol Biol 2013;20:502-507.

35 Smith SJ, Towers N, Saldanha JW, Shang CA, Mahmood SR, Taylor WR, Mohun TJ: The cardiac-restricted protein ADP-ribosylhydrolase-like 1 is essential for heart chamber outgrowth and acts on muscle actin filament assembly. Dev Biol 2016;416:373-388.

36 Zeqiraj E, Tang X, Hunter RW, García-Rocha M, Judd A, Deak M, von Wilamowitz-Moellendorff A, Kurinov I, Guinovart JJ, Tyers M, Sakamoto K, Sicheri F: Structural basis for the recruitment of glycogen synthase by glycogenin. Proc Natl Acad Sci U S A 2014;111:E2831-2840.

37 Laforêt P, Malfatti E, Vissing J: Update on new muscle glycogenosis. Curr Opin Neurol 2017;30:449-456.

38 Lubelwana Hafver T, Wanichawan P, Manfra O, de Souza GA, Lunde M, Martinsen M, Louch WE, Sejersted OM, Carlson CR: Mapping the in vitro interactome of cardiac sodium (Na. Proteomics 2017;17

39 Fahrenbach JP, Stoller D, Kim G, Aggarwal N, Yerokun B, Earley JU, Hadhazy M, Shi NQ, Makielski JC, McNally EM: Abcc9 is required for the transition to oxidative metabolism in the newborn heart. FASEB J 2014;28:2804-2815.

40 Mohammed Abdul KS, Jovanović S, Du Q, Sukhodub A, Jovanović A: A link between ATP and SUR2A: A novel mechanism explaining cardioprotection at high altitude. Int J Cardiol 2015;189:73-76.

41 Gorsi B, Whelan S, Stringer SE: Dynamic expression patterns of 6-O endosulfatases during zebrafish development suggest a subfunctionalisation event for sulf2. Dev Dyn 2010;239:3312-3323.

42 Dupays L, Kotecha S, Angst B, Mohun TJ: Tbx2 misexpression impairs deployment of second heart field derived progenitor cells to the arterial pole of the embryonic heart. Dev Biol 2009;333:121-131.

43 Qu X, Jia H, Garrity DM, Tompkins K, Batts L, Appel B, Zhong TP, Baldwin HS: Ndrg4 is required for normal myocyte proliferation during early cardiac development in zebrafish. Dev Biol 2008;317:486-496.

44 Ling SSM, Chen YT, Wang J, Richards AM, Liew OW: Ankyrin Repeat Domain 1 Protein: A Functionally Pleiotropic Protein with Cardiac Biomarker Potential. Int J Mol Sci 2017;18

45 Kim TG, Chen J, Sadoshima J, Lee Y: Jumonji represses atrial natriuretic factor gene expression by inhibiting transcriptional activities of cardiac transcription factors. Mol Cell Biol 2004;24:10151-10160.

46 Goldbergova MP, Parenica J, Jarkovsky J, Kala P, Poloczek M, Manousek J, Kluz K, Kubkova L, Littnerova S, Tesak M, Toman O, Pavek N, Cermakova Z, Tomandl J, Vasku A, Spinar J: The association between levels of tissue inhibitor of metalloproteinase-1 with acute heart failure and left ventricular dysfunction in patients with ST elevation myocardial infarction treated by primary percutaneous

coronary intervention. Genet Test Mol Biomarkers 2012;16:1172-1178.

47 Porayette P, Fruitman D, Lauzon JL, Le Goff C, Cormier-Daire V, Sanders SP, Pinto-Rojas A, Perez-Atayde AR: Novel mutations in geleophysic dysplasia type 1. Pediatr Dev Pathol 2014;17:209-216.

48 Elahi MM, Matata BM: Gender differences in the expression of genes involved during cardiac development in offspring from dams on high fat diet. Mol Biol Rep 2014;41:7209-7216.

49 Wang F, Hou J, Han B, Nie Y, Cong X, Hu S, Chen X: Developmental changes in lysophospholipid receptor expression in rodent heart from near-term fetus to adult. Mol Biol Rep 2012;39:9075-9084.

50 Kumar D, Mains RE, Eipper BA: 60 YEARS OF POMC: From POMC and α-MSH to PAM, molecular oxygen, copper, and vitamin C. J Mol Endocrinol 2016;56:T63-76.

51 O'Donnell PJ, Driscoll WJ, Bäck N, Muth E, Mueller GP: Peptidylglycine-alpha-amidating monooxygenase and pro-atrial natriuretic peptide constitute the major membrane-associated proteins of rat atrial secretory granules. J Mol Cell Cardiol 2003;35:915-922.

52 Young P, Nie J, Wang X, McGlade CJ, Rich MM, Feng G: LNX1 is a perisynaptic Schwann cell specific E3 ubiquitin ligase that interacts with ErbB2. Mol Cell Neurosci 2005;30:238-248.

53 Mao X, Gu X, Lu W: GSG1L regulates the strength of AMPA receptor-mediated synaptic transmission but not AMPA receptor kinetics in hippocampal dentate granule neurons. J Neurophysiol 2017;117:28-35.

54 Maurer SF, Fromme T, Grossman LI, Hüttemann M, Klingenspor M: The brown and brite adipocyte marker Cox7a1 is not required for non-shivering thermogenesis in mice. Sci Rep 2015;5:17704.

55 Huang D, Liu B, Huang K: Enoyl coenzyme A hydratase 1 protects against high-fat-diet-induced hepatic steatosis and insulin resistance. Biochem Biophys Res Commun 2018;499:403-409.

56 Yin Z, Ren J, Guo W: Sarcomeric protein isoform transitions in cardiac muscle: a journey to heart failure. Biochim Biophys Acta 2015;1852:47-52.

57 Pérez-Serra A, Toro R, Sarquella-Brugada G, de Gonzalo-Calvo D, Cesar S, Carro E, Llorente-Cortes V, Iglesias A, Brugada J, Brugada R, Campuzano O: Genetic basis of dilated cardiomyopathy. Int J Cardiol 2016;224:461-472.

58 Amzulescu MS, Rousseau MF, Ahn SA, Boileau L, de Meester de Ravenstein C, Vancraeynest D, Pasquet A, Vanoverschelde JL, Pouleur AC, Gerber BL: Prognostic Impact of Hypertrabeculation and Noncompaction Phenotype in Dilated Cardiomyopathy: A CMR Study. JACC Cardiovasc Imaging 2015;8:934-946.

59 Louzao-Martinez L, Vink A, Harakalova M, Asselbergs FW, Verhaar MC, Cheng C: Characteristic adaptations of the extracellular matrix in dilated cardiomyopathy. Int J Cardiol 2016;220:634-646.

60 Li L, Zhao Q, Kong W: Extracellular matrix remodeling and cardiac fibrosis. Matrix Biol 2018;68-69:490-506.

61 Ghosh AK, Murphy SB, Kishore R, Vaughan DE: Global gene expression profiling in PAI-1 knockout murine heart and kidney: molecular basis of cardiac-selective fibrosis. PLoS One 2013;8:e63825.

62 Major JL, Dewan A, Salih M, Leddy JJ, Tuana BS: E2F6 Impairs Glycolysis and Activates BDH1 Expression Prior to Dilated Cardiomyopathy. PLoS One 2017;12:e0170066.

63 Burke MA, Chang S, Wakimoto H, Gorham JM, Conner DA, Christodoulou DC, Parfenov MG, DePalma SR, Eminaga S, Konno T, Seidman JG, Seidman CE: Molecular profiling of dilated cardiomyopathy that progresses to heart failure. JCI Insight 2016;1

64 Rupert CE, Coulombe KL: The roles of neuregulin-1 in cardiac development, homeostasis, and disease. Biomark Insights 2015;10:1-9.

65 Bersell K, Arab S, Haring B, Kühn B: Neuregulin1/ErbB4 signaling induces cardiomyocyte proliferation and repair of heart injury. Cell 2009;138:257-270.

66 Song Y, Xu J, Li Y, Jia C, Ma X, Zhang L, Xie X, Zhang Y, Gao X, Zhu D: Cardiac ankyrin repeat protein attenuates cardiac hypertrophy by inhibition of ERK1/2 and TGF-β signaling pathways. PLoS One 2012;7:e50436.

67 Chen C, Shen L, Cao S, Li X, Xuan W, Zhang J, Huang X, Bin J, Xu D, Li G, Kitakaze M, Liao Y: Cytosolic CARP promotes angiotensin II- or pressure overload-induced cardiomyocyte hypertrophy through calcineurin accumulation. PLoS One 2014;9:e104040.

68 Zhong L, Chiusa M, Cadar AG, Lin A, Samaras S, Davidson JM, Lim CC: Targeted inhibition of ANKRD1 disrupts sarcomeric ERK-GATA4 signal transduction and abrogates phenylephrine-induced cardiomyocyte hypertrophy. Cardiovasc Res 2015;106:261-271.

69 Mende U, Kagen A, Cohen A, Aramburu J, Schoen FJ, Neer EJ: Transient cardiac expression of constitutively active Galphaq leads to hypertrophy and dilated cardiomyopathy by calcineurin-dependent and independent pathways. Proc Natl Acad Sci U S A 1998;95:13893-13898.

70 Hou N, Wen Y, Yuan X, Xu H, Wang X, Li F, Ye B: Activation of Yap1/Taz signaling in ischemic heart disease and dilated cardiomyopathy. Exp Mol Pathol 2017;103:267-275.

71 Brody MJ, Hacker TA, Patel JR, Feng L, Sadoshima J, Tevosian SG, Balijepalli RC, Moss RL, Lee Y: Ablation of the cardiac-specific gene leucine-rich repeat containing 10 (lrrc10) results in dilated cardiomyopathy. PloS one 2012;7:e51621.

72 Brody MJ, Cho E, Mysliwiec MR, Kim TG, Carlson CD, Lee KH, Lee Y: Lrrc10 is a novel cardiac-specific target gene of Nkx2-5 and GATA4. Journal of molecular and cellular cardiology 2013;62:237-246.

73 Nevil M, Bondra ER, Schulz KN, Kaplan T, Harrison MM: Stable Binding of the Conserved Transcription Factor Grainy Head to its Target Genes Throughout Drosophila melanogaster Development. Genetics 2017;205:605-620.

74 Langmead B, Trapnell C, Pop M, Salzberg SL: Ultrafast and memory-efficient alignment of short DNA sequences to the human genome. Genome Biol 2009;10:R25.

75 Li B, Dewey CN: RSEM: accurate transcript quantification from RNA-Seq data with or without a reference genome. BMC Bioinformatics 2011;12:323.

Chapter 4

Summary and Future directions

Summary

Jarid2 is a critical factor in heart development. *Jarid2* deficient mice develop cardiac defects in embryonic and adult hearts. *Jarid2* KO mice are embryonic or early lethal just after birth depending on genetic background [1, 2]. During embryonic stages, *Jarid2* KO mice develop cardiac defects mimicking human congenital cardiac defects. *Jarid2* deficient mice in the endocardial and endothelial cells recapitulate cardiac defects observed in *Jarid2* KO mice [3]. In chapter 2 of this thesis, I set out to determine the function of Jarid2 in the early-cardiac cells. *Jarid2* deficient mice in the early myocardium died within a day after birth. The mice revealed VSD, thin myocardium and hypertrabeculation with partial penetrance. However, the *Jarid2* deficient mice in the differentiated cardiomyocytes exhibited neither embryonic cardiac defects nor postnatal death. These suggest an essential function of Jarid2 in the early myocardium, and a dispensable role in the differentiated cardiomyocyte. Interestingly, the mutant mice with deleted *Jarid2* in the differentiated cardiomyocytes developed dilated cardiomyopathy and suffered premature death in chapter 3. The adult mutant mice displayed loss of cardiac functions and thin ventricular walls. To determine the precise mechanisms, RNA-seq was performed in postnatal hearts and adult hearts. The deposition of collagen and extracellular matrix protein related genes were increased, while metabolic related genes were decreased in the adult-mutant hearts. In the *Jarid2* deficient hearts, fetal genes and DCM-related genes were up regulated in the neonatal hearts, and mature sarcomere and contractile associated genes were down regulated in the adult hearts. These findings

imply that Jarid2 is necessary to regulate mature forms of cardiomyocytes in the postnatal heart.

Jarid2 is an enzymatically inactive member of the histone demethylase, Jmj family [4]. However, Jarid2 interacts with other histone modifying enzymes and suppresses gene expression [5-8]. In chapter 2 of this thesis, Jarid2 interacted with PRC2 and inhibited expression of Isl1 in the developing heart. This study suggests that absence of *Jarid2* in the early myocardium induces abnormal cardiac gene expression, such as neuronal genes.

In summary, this thesis demonstrates the roles of Jarid2 in the myocardium. This is the first study proving the mechanism of Jarid2 and PRC2 in the heart and is also a novel study addressing the role of Jarid2 in the postnatal heart.

Future directions

In this thesis, I demonstrate that Jarid2 has essential functions in the myocardium during embryonic and postnatal stages. However, the critical pathways by which Jarid2 inhibits the target gene expression, and which targets in the myocardium directly influence the phenotypic defects in the heart remain to be elucidated.

In chapter 2, Jarid2 regulated Isl1 expression by interacting with PRC2 complexes. However, it is still a question whether the physiological defects observed in *Jarid2*^{Nkx} hearts are related with the increased Isl1 expression. I proposed a dysregulated conduction system gene expression in *Jarid2*^{Nkx} hearts. However, further studies are needed to determine whether Isl1 expression is increased in the conduction cells of *Jarid2*^{Nkx} hearts. Additionally, the regulations of Bmp10 and Fn1 expression are still remained to be solved. I performed additional Chip assays on the Bmp10 promoter region, but Jarid2 accumulation was not determined, suggesting that Bmp10 is not a direct target of Jarid2. It is possible that Isl1 activates Bmp10 expression because Isl1 expresses in the cardiac progenitor cells [9]. Another possible mechanism is from the increased cardiac jelly. Extracellular matrix components bind to many growth factors and move the signals between the cells [10]. The increased cardiac jelly may induce Bmp10 expression by binding to growth factors. Although increased Bmp10 expression is correlated with the phenotype of hypertrabeculation in the *Jarid2*^{Nkx} heart, it is not sufficient due to an unchanged cell proliferation rate. Therefore, other mechanisms, such as increased cardiac jelly may be involved in the hypertrabeculation phenotype of *Jarid2*^{Nkx} hearts.

Generally, cardiac jelly should be degraded by matrix metalloproteinases to terminate excessive trabeculation [11]. However, *Jarid2*^{Nkx} hearts displayed remaining cardiac jelly when it was diminished in controls. Fn1 is generated by cardiomyocyte and endothelial cells [10]. It needs to be further investigated whether deletion of *Jarid2* in the endocardium induces Fn1 expression.

To determine the function of Jarid2 in the postnatal heart, RNA-seq analysis was performed at p10 in chapter 3. *Jarid2* deficient hearts exhibited increases in fetal gene expression and heart failure-related gene expression. However, it is unknown how Jarid2 inhibits the expression of these genes in the myocardium. We have Jarid2 occupied promoters by ChIP-chip analysis on embryonic hearts [8]. I overlapped the dysregulated gene at p10 with embryonic ChIP-chip data, but only a small number of genes were overlapped because of the different conditions between fetal and neonatal stages. ChIP-seq analysis on p10 hearts would be required to determine direct targets of Jarid2 in the postnatal stage.

Additionally, Nrg1-ErbB4 signaling pathways and *Ankrd1* expression were dysregulated in *Jarid2* deficient hearts, but further studies are required to explain how Jarid2 regulates Nrg1, ErbB4 and Ankrd1 expression levels. Ankrd1 is a downstream target of Nkx2.5 in the cardiomyocytes [12]. Therefore, it is plausible that Jarid2 represses Ankrd1 via regulation of Nkx2.5 transcriptional activity. It needs further experiments whether Ankrd1 expression is regulated by Jarid2, and the Nkx2.5 accumulates on the *Ankrd1* promoter, and this accumulation is interrupted by Jarid2. It is possible that ErbB4 is a direct target of Jarid2. Cleaved intracellular domain of ErbB4 moves to the nucleus and interacts with hypoxia-inducible factor 1α (HIF-1α) [13]. HIF-1α related signaling is

activated during the fetal stage, suggesting that ErbB4 and HIF-1α interacting signals can induce fetal genes in the *Jarid2*$^{\alpha MHC}$ hearts.

It is a critical new finding that *Jarid2*$^{\alpha MHC}$ mice develop dilated cardiomyopathy without a compensative hypertrophic phenotype. Therefore, future studies will attempt to determine precise mechanisms of Jarid2 to prevent DCM development in the myocardium.

References

1 Jung J, Kim TG, Lyons GE, Kim HR, Lee Y: Jumonji regulates cardiomyocyte proliferation via interaction with retinoblastoma protein. J Biol Chem 2005;280:30916-30923.

2 Takeuchi T, Kojima M, Nakajima K, Kondo S: jumonji gene is essential for the neurulation and cardiac development of mouse embryos with a C3H/He background. Mech Dev 1999;86:29-38.

3 Mysliwiec MR, Bresnick EH, Lee Y: Endothelial Jarid2/Jumonji is required for normal cardiac development and proper Notch1 expression. J Biol Chem 2011;286:17193-17204.

4 Johansson C, Tumber A, Che K, Cain P, Nowak R, Gileadi C, Oppermann U: The roles of Jumonji-type oxygenases in human disease. Epigenomics 2014;6:89-120.

5 Peng JC, Valouev A, Swigut T, Zhang J, Zhao Y, Sidow A, Wysocka J: Jarid2/Jumonji coordinates control of PRC2 enzymatic activity and target gene occupancy in pluripotent cells. Cell 2009;139:1290-1302.

6 Pasini D, Cloos PA, Walfridsson J, Olsson L, Bukowski JP, Johansen JV, Bak M, Tommerup N, Rappsilber J, Helin K: JARID2 regulates binding of the Polycomb repressive complex 2 to target genes in ES cells. Nature 2010;464:306-310.

7 Shirato H, Ogawa S, Nakajima K, Inagawa M, Kojima M, Tachibana M, Shinkai Y, Takeuchi T: A jumonji (Jarid2) protein complex represses cyclin D1 expression by methylation of histone H3-K9. J Biol Chem 2009;284:733-739.

8 Mysliwiec MR, Carlson CD, Tietjen J, Hung H, Ansari AZ, Lee Y: Jarid2 (Jumonji, AT rich interactive domain 2) regulates NOTCH1 expression via histone modification in the developing heart. J Biol Chem 2012;287:1235-1241.

9 Zhuang S, Zhang Q, Zhuang T, Evans SM, Liang X, Sun Y: Expression of Isl1 during mouse development. Gene Expr Patterns 2013;13:407-412.

10 Lockhart M, Wirrig E, Phelps A, Wessels A: Extracellular matrix and heart development. Birth Defects Res A Clin Mol Teratol 2011;91:535-550.

11 Stankunas K, Hang CT, Tsun ZY, Chen H, Lee NV, Wu JI, Shang C, Bayle JH, Shou W, Iruela-Arispe ML, Chang CP: Endocardial Brg1 represses ADAMTS1 to maintain the microenvironment for myocardial morphogenesis. Dev Cell 2008;14:298-311.

12 Ling SSM, Chen YT, Wang J, Richards AM, Liew OW: Ankyrin Repeat Domain 1 Protein: A Functionally Pleiotropic Protein with Cardiac Biomarker Potential. Int J

Mol Sci 2017;18

13 Paatero I, Jokilammi A, Heikkinen PT, Iljin K, Kallioniemi OP, Jones FE, Jaakkola PM, Elenius K: Interaction with ErbB4 promotes hypoxia-inducible factor-1α signaling. J Biol Chem 2012;287:9659-9671.

Appendix1

Supplemental Figures

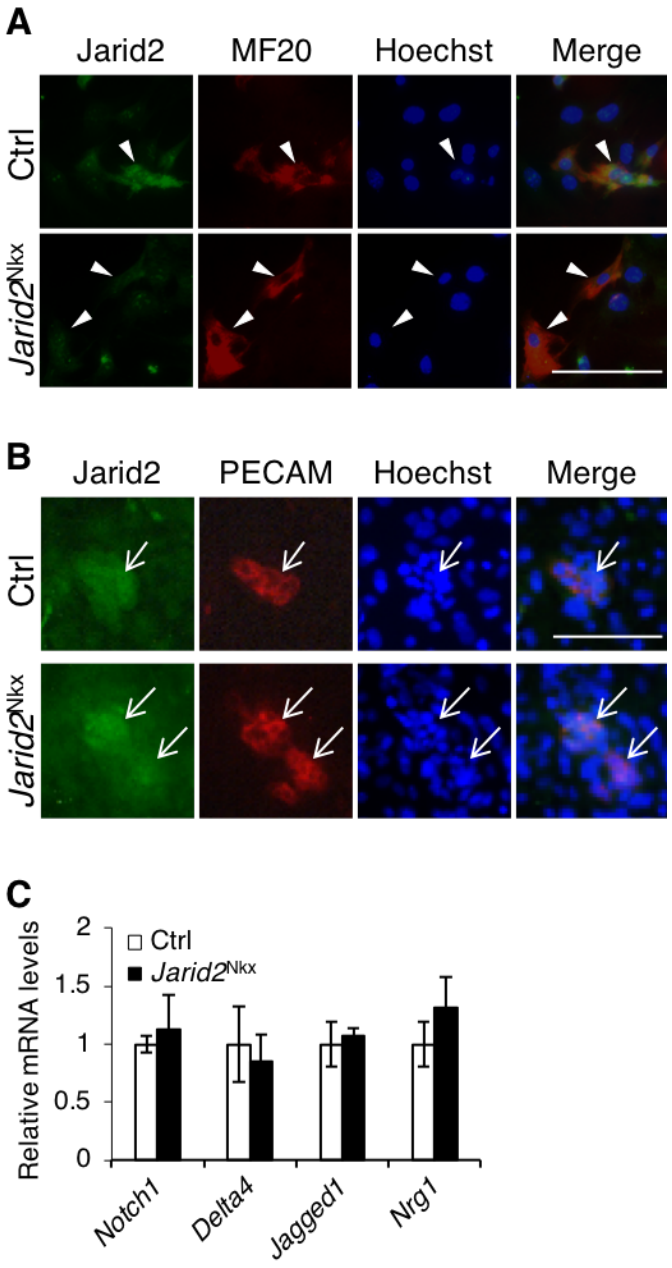

Figure A1-1. Immunostaining was performed on cultured heart cells from control or *Jarid2*^{Nkx} hearts using Jarid2 (Green) and MF20 (Red, A) or PECAM (Red, B) antibodies. Arrowheads indicated myocardial cells (A), while arrows indicate endocardial/endothelial cells (B). Scale bar, 50μm. C, qRT-PCR was performed on control or *Jarid2*^{Nkx} hearts at E13.5. The expression levels were normalized to the control. n=3.

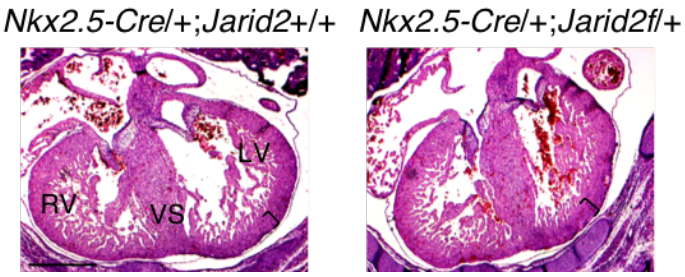

Figure A1-2. H&E staining was performed on *Nkx2.5-Cre* (*Nkx2.5-Cre/+;Jarid2+/+*) or heterozygous mutant (*Nkx2.5-Cre/+;Jarid2f/+*) embryos at E15.5. The bracket indicates a thickness of the compact layer. RV, right ventricle; VS, ventricular septum; LV, left ventricle. Scale bar, 500 μm.

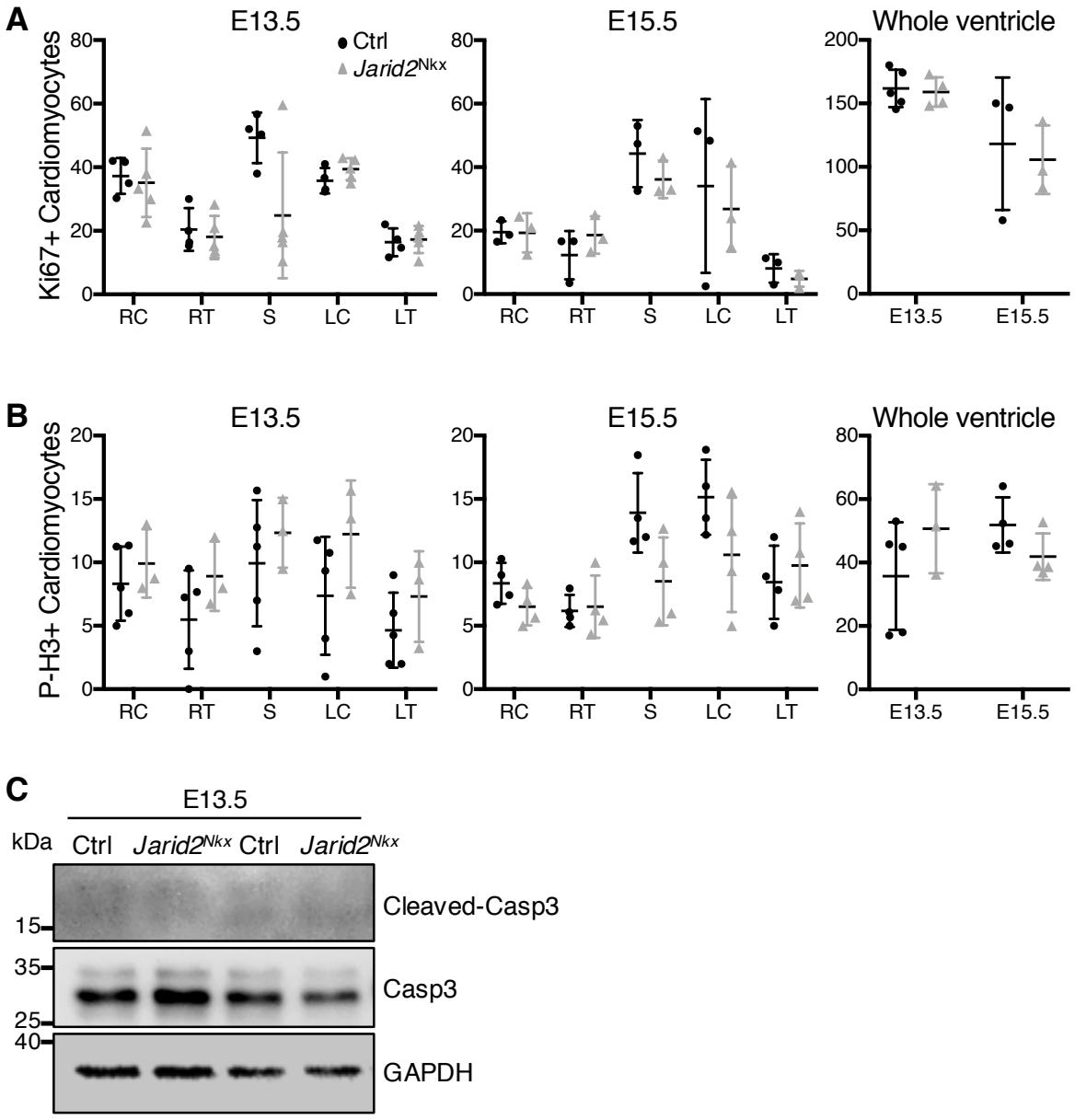

Figure A1-3. Cell proliferation rates were determined on control or *Jarid2*^{Nkx} hearts. Co-immunostaining was performed using Ki67 and MF20 (A) or P-H3 and MF20 (B) antibodies. Scatter plots show the number of the positive cells per section at E13.5 and E15.5. Three sections per heart from three or four embryos were immunoassayed. Mean

± S.D. RC, right compact layer; RT, right trabecular layer; LC, left compact layer; LT, left trabecular layer; S, ventricular septum. C, Cleaved-Caspase 3 and Caspase 3 expression levels were determined by Western blotting on E13.5 hearts. The representative Western blot is shown. GAPDH is a loading control.

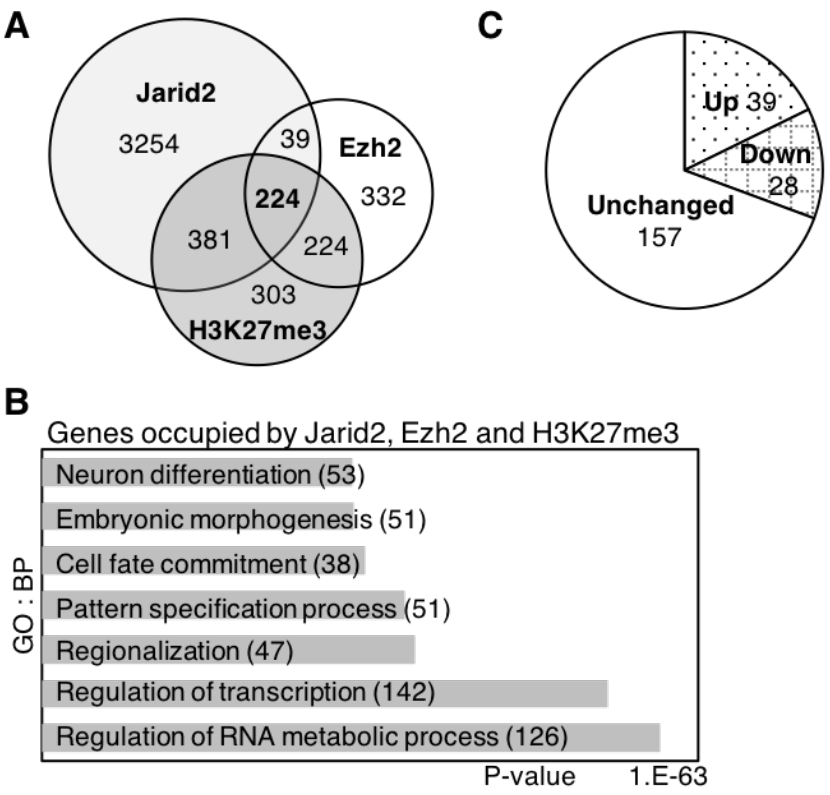

Figure A1-4. Gene expression profile analyses by Jarid2, H3K27me3 or Ezh2. A, Venn diagram demonstrates the overlap of genome-wide occupancy of Jarid2 and H3K27me3 by ChIP-chip with published Ezh2 ChIP-seq data. The published Ezh2 potential targets were determined using E12.5 hearts [1]. B, Highly significant BPs for the 224 genes in (A) were determined by GO/DAVID. C, The 224 overlapping genes were overlaid with the Jaird2 microarray data. The pie chart shows the number of dysregulated genes in *Jarid2* KO.

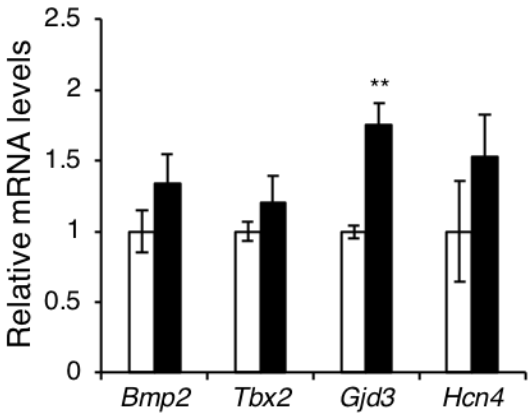

Figure A1-5. Expression of conduction system (nodal lineage) markers was examined by qRT-PCR on E13.5 control or *Jarid2*^{Nkx} hearts. The expression levels were normalized to the control, n=4.

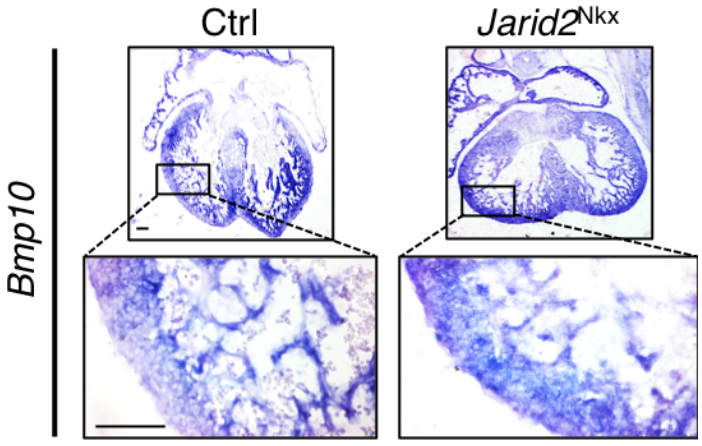

Figure A1-6. Section *in Situ* hybridization was performed using DIG-labeled *Bmp10* riboprobes on control or *Jarid2*^{Nkx} embryos at E13.5. *Bmp10* expression was detected in the trabecular layer in the control heart but expanded deep into the compact layer in *Jarid2*^{Nkx} heart. The boxed region of upper pictures is magnified. Scale bar, 150 μm.

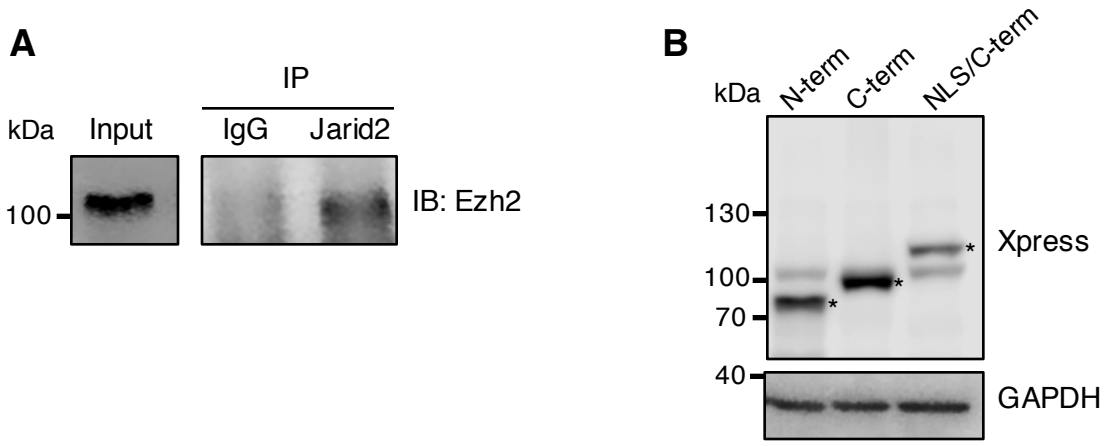

Figure A1-7. A, Co-immunoprecipitation was performed on E15.5 control hearts to determine a physical interaction between Jarid2 and Ezh2. Immunoprecipitation (IP) was performed with IgG or Jarid2 antibody, followed by immunoblotting (IB) with Ezh2 antibody. B, Jarid2 mutants were transfected into 10T1/2 cells, and the transfection was confirmed by Western blotting. Xpress antibody was used for detecting Jarid2 mutants (stars) because each mutant was inserted in an Xpress-tagged plasmid [2]. GAPDH is a loading control.

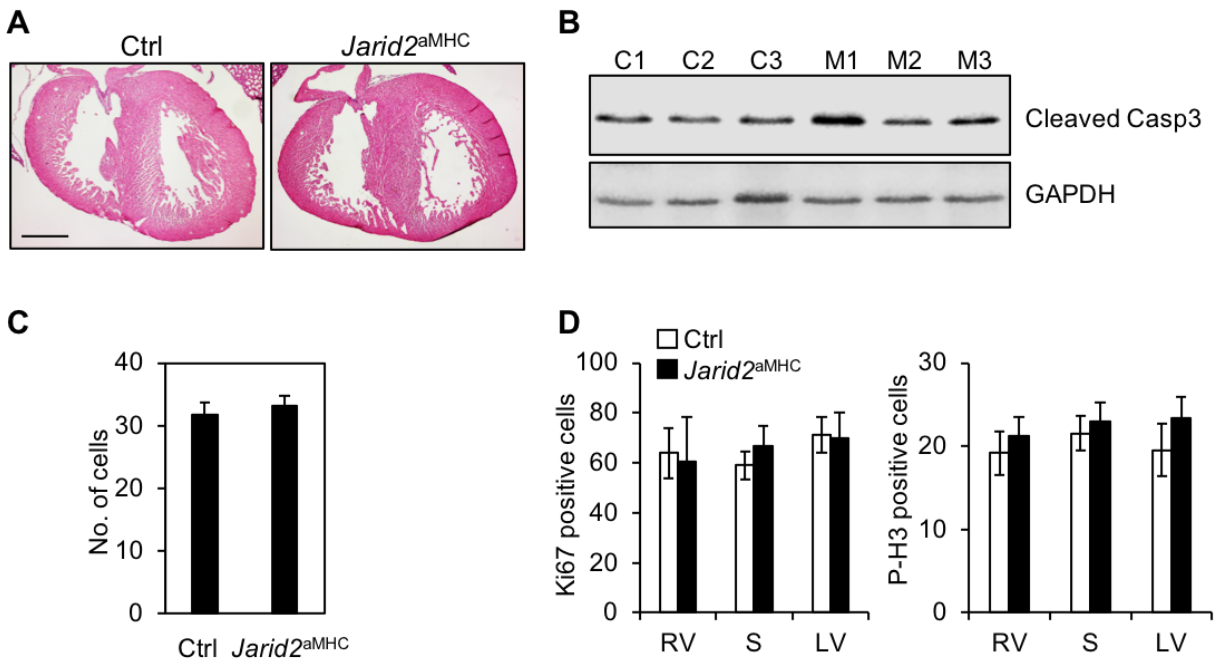

Figure A1-8. A, H&E staining was performed on e18.5 hearts to determine developmental defects. Scale bar, 500um. B, Cleaved caspase 3 expression was determined by Western blotting on 7m hearts on control (C) and *Jarid2*$^{\alpha MHC}$ (M) hearts. GAPDH was used as a loading control. n=3. C, WGA staining was performed on 7m hearts, and the number of cardiomyocytes were counted. n=3. D, Proliferation rate of cardiomyocytes was measured on p10 control or *Jarid2*$^{\alpha MHC}$ heart. Co-immunostaining was performed using MF-20 and Ki67 or phospho-H3 antibodies and double-positive cells were counted. R, right ventricle; L, left ventricle; S, septum. n=3.

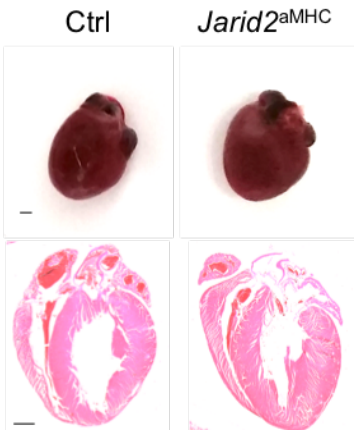

Figure A1-9. Whole heart images and H&E staining analysis were compared between control and *Jarid2*$^{\alpha MHC}$ hearts at 3m of ages. Scale bar, 1mm.

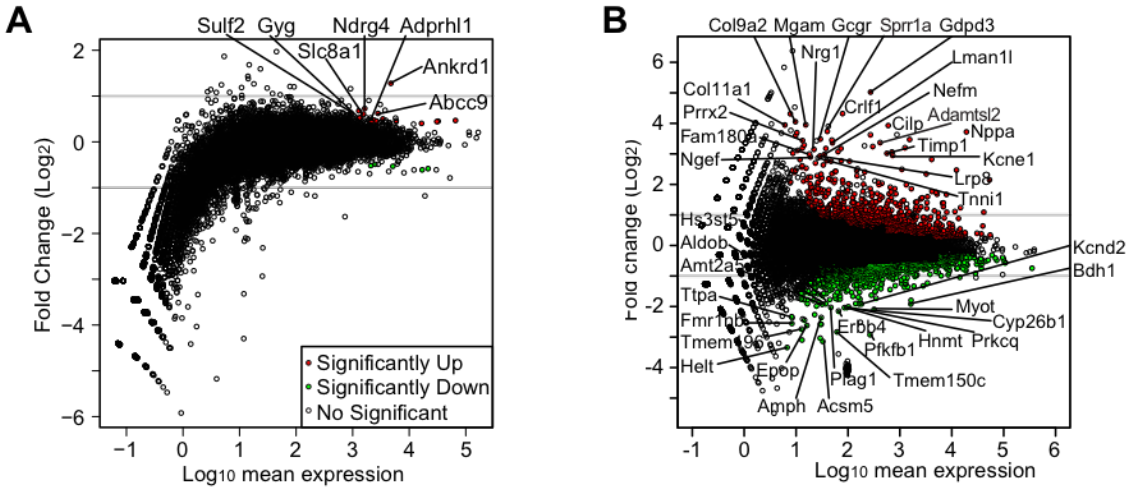

Figure A1-10. A, MA plot showed differentially expressed genes at p10 by DESeq2. 20 genes were statistically significant (adj *p*-value<0.05). B, MA plot showed differentially expressed genes at 7m by DESeq2. 2336 genes were statistically significant (adj *p*-value<0.05).

Appendix2

Supplemental Tables

Table A2-1. Cardiac phenotypic defects observed in *Jarid2*^{Nkx} mice.

	Type of abnormality	VSD	Hypertraveculation	Thin myocardium
Stages	***Jarid2*^{Nkx}**			
E15.5	1	x	x	x
	2	x	x	x
	3		x	x
	4	x	x	x
E17	1	x	x	x
	2	x		
	3	x	x	x
E19	1	x	x	
	2	x	x	x
	3	x		x
	4	x	x	

Table A2-2. 39 up-regulated genes in *Jarid2* KO hearts among overlapped genes occupied by Jarid2, Ezh2 and H3K27me3.

Gene symbol	*p* value	*Jarid2* KO	Gene name
ISL1	*1.46*E-*21*	3.20	ISL1_transcription_factor,_LIM/homeodomain
DNAJC22	*8.13*E-*16*	2.54	DnaJ_(Hsp40)_homolog,_subfamily_C,_member_22
DUOX2	*1.84*E-*37*	2.26	Dual_oxidase_2
HOXB3	*1.68*E-*24*	2.24	Homeo_box_B3
EVX2	*2.08*E-*20*	2.24	Even_skipped_homeotic_gene_2_homolog
PRDM6	*1.84*E-*28*	2.23	PR_domain_containing_6
NPAS3	*2.6*E-*27*	2.21	Neuronal_PAS_domain_protein_3
SYT6	*5.89*E-*15*	2.18	Synaptotagmin_VI
SP5	*5.35*E-*34*	2.13	Trans-acting_transcription_factor_5
NEUROD2	*9.42*E-*110*	2.03	Neurogenic_differentiation_2
LEF1	*1.56*E-*26*	1.98	Lymphoid_enhancer_binding_factor_1
SFMBT2	*4.59*E-*18*	1.84	Scm-like_with_four_mbt_domains_2
CLDN3	*1.37*E-*15*	1.81	Claudin_3
SALL1	*2.8*E-*51*	1.74	Sal-like_1_(Drosophila)
GCGR	*4.45*E-*21*	1.71	Glucagon_receptor
BARHL2	*7.16*E-*53*	1.68	BarH-like_2_(Drosophila)
PDLIM2	*2.87*E-*16*	1.68	PDZ_and_LIM_domain_2
NFATC1	*3.3*E-*18*	1.68	Nuclear_factor_of_activated_T-cells,_cytoplasmic,_calcineurin-dependent_1
TNFAIP2	*7.09*E-*14*	1.67	Tumor_necrosis_factor,_alpha-induced_protein_2
DRD4	*1.48*E-*15*	1.65	Dopamine_receptor_4
ASCL2	*4.33*E-*21*	1.59	Achaete-scute_complex_homolog_2_(Drosophila)
EMX1	*6.43*E-*89*	1.58	Empty_spiracles_homolog_1_(Drosophila)
COL2A1	*5.62*E-*17*	1.55	Collagen,_type_II,_alpha_1
TAL1	*1.89*E-*34*	1.54	T-cell_acute_lymphocytic_leukemia_1
PRDM8	*7.34*E-*19*	1.54	PR_domain_containing_8
TNFRSF25	*3.36*E-*55*	1.51	Tumor_necrosis_factor_receptor_superfamily,_member_25
GP1BB	*1.14*E-*24*	1.50	Glycoprotein_Ib,_beta_polypeptide
1700019N12RIK	*3.18*E-*28*	1.49	RIKEN_cDNA_1700019N12_gene
TCFAP2A	*1.07*E-*66*	1.47	Transcription_factor_AP-2,_alpha
SALL3	*9.01*E-*66*	1.47	Sal-like_3_(Drosophila)
HOXA4	*7.79*E-*52*	1.45	Homeo_box_A4
LHX1	*1.55*E-*59*	1.39	LIM_homeobox_protein_1
COMP	*1.08*E-*17*	1.37	Cartilage_oligomeric_matrix_protein

NKX2-3	*1.5*E-*147*	1.31	NK2_transcription_factor_related,_locus_3_ (Drosophila)
JPH3	*4.71*E-*14*	1.26	Junctophilin_3
CLSTN1	*1.25*E-*36*	1.24	Calsyntenin_1
CLDN7	*1.74*E-*14*	1.24	Claudin_7
POU4F1	*4.69*E-*17*	1.22	POU_domain,_class_4,_transcription_factor_1
NGFR	*4.27*E-*34*	1.21	Nerve_growth_factor_receptor (TNFR_superfamily,_member_16)

Table A2-3. 28 down-regulated genes in *Jarid2* KO hearts among overlapped genes occupied by Jarid2, Ezh2 and H3K27me3.

Gene symbol	*p* value	*Jarid2* KO	Gene name
CRABP1	5.83E-14	-8.67	Cellular_retinoic_acid_binding_protein_I
PAX6	4.23E-46	-3.84	Paired_box_gene_6
OLIG2	2.17E-36	-2.70	Oligodendrocyte_transcription_factor_2
SLC6A7	4.73E-21	-2.46	Solute_carrier_family_6_(neurotransmitter_transporter,_L-proline),_member_7
GNAS	1.59E-14	-1.90	GNAS_(guanine_nucleotide_binding_protein,alpha_stimulating)_complex_locus
CLDN5	1.51E-18	-1.90	Claudin_5
PIGZ	1.86E-28	-1.84	Phosphatidylinositol_glycan_anchor_biosynthesis,_class_Z
EBF2	2.5E-19	-1.82	Early_B-cell_factor_2
MSX1	2.25E-55	-1.82	Homeobox,_msh-like_1
HOXD8	2.38E-15	-1.72	Homeo_box_D8
ELAVL3	2.13E-36	-1.57	ELAV_(embryonic_lethal,_abnormal_vision,_Drosophila)-like_3_(Hu_antigen_C)
GM1337	2.78E-14	-1.53	Predicted_gene_1337
POU3F2	2.61E-20	-1.48	POU_domain,_class_3,_transcription_factor_2
HOXB7	8.27E-30	-1.45	Homeo_box_B7
HAND1	3E-16	-1.40	Heart_and_neural_crest_derivatives_expressed_transcript_1
WNT1	9.65E-46	-1.40	Wingless-related_MMTV_integration_site_1
DPF1	3.06E-14	-1.40	D4,_zinc_and_double_PHD_fingers_family_1
KCNC4	1.17E-37	-1.37	Potassium_voltage_gated_channel,_Shaw-related_subfamily,_member_4
FBXO2	1.07E-22	-1.34	F-box_protein_2
HOXA7	4.38E-56	-1.33	Homeo_box_A7
NFIX	1.63E-28	-1.31	Nuclear_factor_I/X
AQP5	3.55E-20	-1.31	Aquaporin_5
LBX2	1.08E-15	-1.31	Ladybird_homeobox_homolog_2(Drosophila)
HOXD4	9.8E-15	-1.30	Homeo_box_D4
EPHB1	3.07E-22	-1.26	Eph_receptor_B1
PPL	8.1E-39	-1.22	Periplakin
ESRRB	4.28E-21	-1.22	Estrogen_related_receptor,_beta

*NKX*2-5	5.13E-16	-1.22	NK2_transcription_factor_related,_locus_5_ (Drosophila)
*1700001O22RIK**	3.29E-15	-2.01	RIKEN cDNA 1700001O22 gene
*2010001M09RIK**	1.65E-18	-1.31	RIKEN cDNA 2010001M09 gene
*ATP5D**	6.81E-15	-1.67	ATP synthase, H+ transporting, mitochondrial F1 complex, delta subunit
*CEBPA**	2.09E-21	-2.99	CCAAT/enhancer binding protein (C/EBP), alpha
*ESRRA**	7.66E-66	-1.23	Estrogen related receptor, alpha
*FXYD1**	1.13E-79	-1.40	FXYD domain-containing ion transport regulator 1
*HOXB6**	2.78E-22	-2.50	Homeo box B6
*IGF2**	5.01E-14	-1.42	Insulin-like growth factor 2

Stars indicate the genes were occupied by only Jarid2 and Ezh2.

Table A2-4. Mendelian ratios of postnatal *Jarid2*$^{\alpha MHC}$ mice.

Age	No. of litters	No. of live mice	Genotype of live mice			
			+/+;f/f	***+/+;f/+***	***Cre/+;f/+***	***Cre/+;f/f***
p21	26	171	38 (22.2%)	42 (24.6%)	46 (26.9%)	45 (26.3%)

Mice were examined to determine a Mendelian ratio at postnatal day (p) 10.

Table A2-5. 72 DE genes at p10 by DESeq2 or EBSeq.

Gene Symbol	FC(Log_2) -DESeq	FC -EBSeq	Name
Krt75	-5.17	0.05	Keratin 75
Arhgap36	-1.60	0.29	Rho GTPase activating protein 36
Myl1	-1.63	0.29	Myosin, light polypeptide 1
Wnk4	-1.04	0.51	WNK lysine deficient protein kinase 4
Tmem100	-0.81	0.52	Transmembrane protein 100
Enkur	-0.74	0.56	Enkurin, TRPC channel interacting protein
Gli1	-0.67	0.62	GLI-Kruppel family member GLI1
Vsig2	-0.70	0.63	V-set and immunoglobulin domain containing 2
Hba-a2	-0.61	0.65	Hemoglobin alpha, adult chain 2
Lgals4	-0.76	0.65	Lectin, galactose binding, soluble 4
Tgfb1	-0.53	0.66	Transforming growth factor, beta 1
Hba-a1	-0.58	0.66	Hemoglobin alpha, adult chain 1
Prph	-0.64	0.67	Peripherin
Dapk1	-0.63	0.69	Death associated protein kinase 1
Kctd17	-0.52	0.69	Potassium channel tetramerisation domain containing 17
Tbx2	-0.49	0.69	T-box 2
Rplp2	-0.52	0.72	Ribosomal protein, large P2
Egfl7	-0.49	0.74	EGF-like domain 7
Mdh1	0.40	1.30	Malate dehydrogenase 1, NAD (soluble)
Ctnna1	0.44	1.32	Catenin (cadherin associated protein), alpha 1
Pam	0.45	1.32	Peptidylglycine alpha-amidating monooxygenase
Tmod1	0.48	1.34	Tropomodulin 1
Pln	0.45	1.37	Phospholamban
Actc1	0.47	1.39	Actin, alpha, cardiac muscle 1
Myl12a	0.50	1.41	Myosin, light chain 12A, regulatory, non-sarcomeric
Ktn1	0.53	1.42	Kinectin 1
Rmnd5a	0.48	1.43	Required for meiotic nuclear division 5 homolog A
Tmem230	0.43	1.43	Transmembrane protein 230
Ank	0.54	1.44	Progressive ankylosis
Gyg	0.49	1.44	Glycogenin
Adprhl1	0.46	1.44	ADP-ribosylhydrolase like 1
Ttll1	0.53	1.44	Tubulin tyrosine ligase-like 1
Abcc9	0.62	1.46	ATP-binding cassette, sub-family C (CFTR/ MRP), member 9
Pank3	0.73	1.47	Pantothenate kinase 3
Cpox	0.52	1.48	Coproporphyrinogen oxidase
Eif4e3	0.46	1.48	Eukaryotic translation initiation factor 4E member 3
Slc8a1	0.61	1.49	Solute carrier family 8 (sodium/calcium

			exchanger), member 1
Ccnd2	0.60	1.50	Cyclin D2
Ampd3	0.46	1.50	Adenosine monophosphate deaminase 3
Prkaa2	0.61	1.52	Protein kinase, AMP-activated, alpha 2 catalytic subunit
Sulf2	0.63	1.53	Sulfatase 2
Lrrc3b	0.72	1.56	Leucine rich repeat containing 3B
Ndrg4	0.73	1.57	N-myc downstream regulated gene 4
Atp11a	0.51	1.58	ATPase, class VI, type 11A
Gsg1l	0.67	1.59	GSG1-like
Pip5k1b	0.60	1.60	Phosphatidylinositol-4-phosphate 5-kinase, type 1 beta
Pakap	0.61	1.60	Paralemmin A kinase anchor protein
Gbe1	0.74	1.61	Glucan (1,4-alpha-), branching enzyme 1
Bcap29	0.68	1.61	B cell receptor associated protein 29
Zdbf2	0.89	1.62	Zinc finger, DBF-type containing 2
Suclg2	0.56	1.63	Succinate-Coenzyme A ligase, GDP-forming, beta subunit
Cdh2	0.68	1.63	Cadherin 2
Mark1	0.60	1.65	MAP/microtubule affinity regulating kinase 1
Aqp4	0.84	1.68	Aquaporin 4
Bves	0.63	1.68	Blood vessel epicardial substance
Tmem182	0.92	1.71	Transmembrane protein 182
Ntn1	0.83	1.76	Netrin 1
Wif1	0.75	1.78	Wnt inhibitory factor 1
Lnx1	0.63	1.78	Ligand of numb-protein X 1
Lrig1	0.84	1.78	Leucine-rich repeats and immunoglobulin-like domains 1
Rabgap1l	0.66	1.78	RAB GTPase activating protein 1-like
Lpar3	1.06	1.85	Lysophosphatidic acid receptor 3
Zfp770	0.83	1.88	Zinc finger protein 770
Atp2a1	1.21	1.96	ATPase, Ca++ transporting, cardiac muscle, fast twitch 1
Pirt	0.77	1.99	Phosphoinositide-interacting regulator of transient receptor potential channels
Tspyl4	1.03	2.03	TSPY-like 4
Ankrd1	1.28	2.49	Ankyrin repeat domain 1 (cardiac muscle)
Irx2	1.97	3.04	Iroquois related homeobox 2 (Drosophila)
C530008M17Rik	1.18	3.19	RIKEN cDNA C530008M17 gene
Esrrg	1.20	3.26	Estrogen-related receptor gamma
Il23a	1.19	3.30	Interleukin 23, alpha subunit p19
Irx1	1.59	4.30	Iroquois related homeobox 1 (Drosophila)

FC, fold change.

Table A2-6. P10 DE genes were overlapped with ChIP-chip data sets

Gene Symbol	FC	Jarid2	H3K27m3	H3K9m3	Name
Tmem100	-0.81	2.75E-19			Transmembrane protein 100
Lgals4	-0.76	1.16E-17			Lectin, galactose binding, soluble 4
Vsig2	-0.70	3.9E-27			V-set and immunoglobulin domain containing 2
Gli1	-0.67	1.37E-39	1.04E-79		GLI-Kruppel family member GLI1
Prph	-0.64	9.31E-30	8.77E-62	2.99E-22	Peripherin
Tgfb1	-0.53	1.03E-23			Transforming growth factor, beta 1
Egfl7	-0.49	1.6E-35			EGF-like domain 7
Ctnna1	0.44	4.27E-16			Catenin (cadherin associated protein), alpha 1
Ampd3	0.46	7.86E-31			Adenosine monophosphate deaminase 3
Adprhl1	0.46	2.91E-22			ADP-ribosylhydrolase like 1
Ttll1	0.53	3.47E-36	4.96E-18	4.66E-14	Tubulin tyrosine ligase-like 1
Pank3	0.73	2.74E-35			Pantothenate kinase 3
Tmem182	0.92	1.59E-15			Transmembrane protein 182
Il23a	1.19	9.45E-22			Interleukin 23, alpha subunit p19
Atp2a1	1.21	5.95E-40			ATPase, Ca++ transporting, cardiac muscle, fast twitch 1

Table A2-7. Primers for qRT-PCR

Gene name	Forward	Reverse
Jarid2	gatgacagcgatgggatcc	catttaccgccttcaggct
18S	cgccgctagaggtgaaattct	cgaaactccgactttcgttct
Fn1	agagagtgcccctactaca	cgatattggtgaatcgcaga
Crtl1	cccccgtctactt gtgga	ctga gccaaatgctgtagg
Vcan	cagaagctaggcgtggccag	catcaggctcaccacttgaaac
Col2a1	gctggtgaagaaggcaaacgag	ccatcttgacctgggaatccac
Vtn	ccattcagagcgtctatttcttctc	tccactcgccgggttcta
Adamts1	catgcaagaagatgtcaggaatagt	catgatacccaggtcttgtactagtga
Notch1	gccttcgtgctcctgttctt	agcaccatctgaggcattct
Delta4	tgtgtgattgccacagaggtataa	atgtcccatacaggatgcaatg
Jagged1	tcagaggcgtcctctgaaaaa	agcaacagacccaagccact
Nrg1	tgtcacccagactcctagtcaca	tgctgttctctaccgatgacgt
Erbb2	gtacagtgaggatcccacattacct	agactgaggccgaacctctg
Erbb4	caatgcatgacaagcccaaa	cgggacacaaaagggttctct
Pax6	ccctcaccaacacgtacag	tcataactccgcccattcac
Sall3	aaagaacgcagagaccctca	gtgtccttcagctccgagtc
Emx1	agcgacgttccccaggacgggctgc	tgcgtctcggagaggctgaggctgc
Barhl2	agctgctagccgaggccggg	tgctgtccatgctccccagca
Neurod2	gctactccaagacgcagaagct	cacagagtctgcacgtaggaca
Pou4f2	gatgcggagagcttgtcttcca	cttactctgggagacgatgtcc
Isl1	ccttgcaaagcgacatagatca	gagcctggtcctccttctgaa
Nkx2.5	gccatccgtctcggcttt	ccaagtgctctcctgctttcc
Nfatc1	gccacaggcctcgtatcagt	tgagccctgtggtgagacttg
Msx1	aggactcctcaagctgccagaa	cggttggtcttgtgcttgcgta
Lef1	actgtcaggcgacacttccatg	gtgctcctgtttgacctgaggt
Sall1	gcttgcactatctgtggaagagc	ctgggaacttgacaggattgcc
Bmp10	tgctaacatcatccggagctt	ccattaaaagtgactggttgagaaaac
Igfbp2	atggccggtacaaccttaagc	cgcgctgtccgttcaga
Igf1	aaggagaaggaaaggaagtacatttg	tttcctgcacttcctctacttgtg
Bmp2	cgcagcttccatcacgaa	cccactcatctctggaagttcct
Tbx2	tcatcgctgtcactgcctacca	cggcttacagtgctcctcatac
Gjd3	tgatcttccgcatcctggtgct	atcgtagcaggtctggcgacag
Hcn4	gattatccacccctacagtgac	accacattgaagacgatccag
Nppa	gtggactaggctgcaacagctt	acacaccacaagggcttagga
Nppb	acaagatagaccggatcgga	acccaggcagagtcagaaac
Myh7	atgtgccggaccttggaa	cctcgggttagctgagagatca
Myh6	gctggctggaaaagaacaag	tcttgcctcctttgccttta

Acta1	aggacctgtatgccaacaac	acatctgctggaaggtggac
Tnni1	atgccggaagttgagaggaaa	tccgagaggtaacgcacctt
Tnni3	caaaagtcaccaagaacatca	tgccacggaggtcatagatct
Acta2	tctcttccagccatctttcattg	tatcacacttcatgatgctgttataggt
Actc1	agatcatgtttgagaccttcaatgtg	acaccatcgccagaatcca
Ankrd1	tcacggctgccaacatgat	tctgaactccccaggaaggaa
Tpm1	gaccacgctctcaacgatatga	gacatccagcttgacgaagga
Myl2	atgctgaccacacaagcagaga	ggtaatgatgtggaccaaattcttataa
Pln	cgatcaccgaagccaaggt	aaggcaaaagtagggagacaagttt
Nrg1	tgtcacccagactcctagtcaca	tgctgttctctaccgatgacgt
ErbB4	caatgcatgacaagcccaaa	cgggacacaaaagggttctct

References for Appendices

1 He A, Ma Q, Cao J, von Gise A, Zhou P, Xie H, Zhang B, Hsing M, Christodoulou DC, Cahan P, Daley GQ, Kong SW, Orkin SH, Seidman CE, Seidman JG, Pu WT: Polycomb repressive complex 2 regulates normal development of the mouse heart. Circ Res 2012;110:406-415.

2 Kim TG, Kraus JC, Chen J, Lee Y: JUMONJI, a critical factor for cardiac development, functions as a transcriptional repressor. J Biol Chem 2003;278:42247-42255.